Tran-SET

Transportation Consortium of South-Central States

Solving Emerging Transportation Resiliency, Sustainability, and Economic Challenges through the Use of Innovative Materials and Construction Methods: From Research to Implementation

Evaluation of Asphalt Mixtures Resistance to Cement-Treated Base (CTB) Reflective Cracking in the Laboratory

Project No. 19BLSU02

Lead University: Louisiana State University

Collaborative Universities: Bradley University

Final Report

November 2020

Disclaimer

The contents of this report reflect the views of the authors, who are responsible for the facts and the accuracy of the information presented herein. This document is disseminated in the interest of information exchange. The report is funded, partially or entirely, by a grant from the U.S. Department of Transportation's University Transportation Centers Program. However, the U.S. Government assumes no liability for the contents or use thereof.

Acknowledgements

The authors would like to acknowledge the support by the Transportation Consortium of South-Central States (Tran-SET) and Louisiana Transportation Research Center (LTRC) for supporting us to do testing.

TECHNICAL DOCUMENTATION PAGE

1. Project No.	2. Government Accession No.	3. Recipient's Catalog No.
19BLSU02		

4. Title and Subtitle	5. Report Date
Evaluation of Asphalt Mixtures' Resistance to Cement-Treated Base (CTB) Reflective Cracking in the Laboratory	Nov. 2020
	6. Performing Organization Code
7. Author(s) PI: Husam Sadek https://orcid.org/0000-0002-3151-5643 Co-PI: Marwa Hassan https://orcid.org/0000-0001-8087-8232 Co-PI: Charles Berryman https://orcid.org/0000-0003-0779-9372 Conslt: Mohammad Hossain https://orcid.org/0000-0003-4997-786X GRA: Ipshit Idris https://orcid.org/0000-0003-3459-7311	**8. Performing Organization Report No.**
9. Performing Organization Name and Address Transportation Consortium of South-Central States (Tran-SET) University Transportation Center for Region 6 3319 Patrick F. Taylor Hall, Louisiana State University, Baton Rouge, LA 70803	**10. Work Unit No. (TRAIS)**
	11. Contract or Grant No. 69A3551747106
12. Sponsoring Agency Name and Address United States of America Department of Transportation Research and Innovative Technology Administration	**13. Type of Report and Period Covered** Final Research Report Aug. 2019 – Nov. 2020
	14. Sponsoring Agency Code

15. Supplementary Notes

Report uploaded and accessible at Tran-SET's website (http://transet.lsu.edu/).

16. Abstract

The primary objective of this project is to propose a laboratory setup to test and evaluate an asphalt mixture layer on top of a simulated Cement-Treated Base (CTB) layer against reflective cracking. An in-depth literature review on the experimental studies that were conducted throughout the world to investigate the resistance of asphalt mixtures to reflective cracking was conducted. Texas Transportation Institute (TTI) Overlay Tester (OT) was found to be the most appropriate equipment to study thermally-induced reflective cracking in the laboratory, and thereby was selected to be modified and used to assess the performance of asphalt mixtures on top of a pre-cracked CTB layer. Four different asphalt mixtures and two types of stabilized bases were successfully prepared in this study. The reflective cracking performance of the laboratory-produced asphalt mixtures was evaluated using both the modified and conventional OT setup at two different test temperatures. The attempt to modify the conventional OT setup for better mimicking field reflective cracking was unsuccessful because of the inability to establish a bonding between the top and bottom layers of the composite OT specimens. The repeatability of the collected data was acceptable since COVs were below 30%. Results of the conventional OT testing showed that decreasing the test temperature from room to low temperature resulted in the asphalt mixtures to change their behavior from "soft crack-resistant" mixtures to "tough crack resistant" mixtures. On the other hand, no observable effect of changing binder type and RAP content was found when the specimens were tested in conventional OT setup.

17. Key Words	18. Distribution Statement
Reflective cracking, Cement-Treated Base, Cement-Treated Soil, Asphalt mixture, Overlay Tester	No restrictions. This document is available through the National Technical Information Service, Springfield, VA 22161.

19. Security Classif. (of this report)	20. Security Classif. (of this page)	21. No. of Pages	22. Price
Unclassified	Unclassified	106	

Form DOT F 1700.7 (8-72) **Reproduction of completed page authorized.**

SI* (MODERN METRIC) CONVERSION FACTORS

APPROXIMATE CONVERSIONS TO SI UNITS

Symbol	When You Know	Multiply By	To Find	Symbol
		LENGTH		
in	inches	25.4	millimeters	mm
ft	feet	0.305	meters	m
yd	yards	0.914	meters	m
mi	miles	1.61	kilometers	km
		AREA		
in^2	square inches	645.2	square millimeters	mm^2
ft^2	square feet	0.093	square meters	m^2
yd^2	square yard	0.836	square meters	m^2
ac	acres	0.405	hectares	ha
mi^2	square miles	2.59	square kilometers	km^2
		VOLUME		
fl oz	fluid ounces	29.57	milliliters	mL
gal	gallons	3.785	liters	L
ft^3	cubic feet	0.028	cubic meters	m^3
yd^3	cubic yards	0.765	cubic meters	m^3
		NOTE: volumes greater than 1000 L shall be shown in m^3		
		MASS		
oz	ounces	28.35	grams	g
lb	pounds	0.454	kilograms	kg
T	short tons (2000 lb)	0.907	megagrams (or "metric ton")	Mg (or "t")
		TEMPERATURE (exact degrees)		
°F	Fahrenheit	5 (F-32)/9 or (F-32)/1.8	Celsius	°C
		ILLUMINATION		
fc	foot-candles	10.76	lux	lx
fl	foot-Lamberts	3.426	$candela/m^2$	cd/m^2
		FORCE and PRESSURE or STRESS		
lbf	poundforce	4.45	newtons	N
lbf/in^2	poundforce per square inch	6.89	kilopascals	kPa

APPROXIMATE CONVERSIONS FROM SI UNITS

Symbol	When You Know	Multiply By	To Find	Symbol
		LENGTH		
mm	millimeters	0.039	inches	in
m	meters	3.28	feet	ft
m	meters	1.09	yards	yd
km	kilometers	0.621	miles	mi
		AREA		
mm^2	square millimeters	0.0016	square inches	in^2
m	square meters	10.764	square feet	ft^2
m	square meters	1.195	square yards	yd^2
ha	hectares	2.47	acres	ac
km	square kilometers	0.386	square miles	mi^2
		VOLUME		
mL	milliliters	0.034	fluid ounces	fl oz
L	liters	0.264	gallons	gal
m	cubic meters	35.314	cubic feet	ft^3
m	cubic meters	1.307	cubic yards	yd^3
		MASS		
g	grams	0.035	ounces	oz
kg	kilograms	2.202	pounds	lb
Mg (or "t")	megagrams (or "metric ton")	1.103	short tons (2000 lb)	T
		TEMPERATURE (exact degrees)		
C	Celsius	1.8C+32	Fahrenheit	°F
		ILLUMINATION		
lx	lux	0.0929	foot-candles	fc
cd/m^2	$candela/m^2$	0.2919	foot-Lamberts	fl
		FORCE and PRESSURE or STRESS		
N	newtons	0.225	poundforce	lbf
kPa	kilopascals	0.145	poundforce per square inch	lbf/in^2

TABLE OF CONTENTS

LIST OF FIGURES

LIST OF TABLES

ACRONYMS, ABBREVIATIONS, AND SYMBOLS

AASHTO	American Association of State Highway and Transportation Official
ABR	Asphalt-Binder Replacement
ALF	Accelerated Loading Facility
AMPT	Asphalt Mixture Performance Tester
BRRC	Belgian Road Research Center
CCPR	Corrected Crack Progression rate
CPR	Crack Progression Rate
CRI	Crack Resistance Index
CSB	Cement-Stabilized Base
CTB	Cement-Treated Base
ENTPE	The École Nationale des Travaux Publics de l'État - National School of Public Works of the State, France.
ESAL	Equivalent Single Axle Load
Evotherm®	Chemical additive
FHWA	Federal Highway Administration
Gc	Critical Fracture Energy
G_{mb}	Bulk Specific Gravity of the Mixture
G_{mm}	Maximum Specific Gravity of the Mixture
HIPR	Hot-In-Place Recycling
HMA	Hot-Mix Asphalt
HWTT	Hamburg Wheel Tracking Tester
ISAC	Interlayer Stress-Absorbing Composite
LaDOTD	Louisiana Department of Transportation and Development
LL	Liquid Limit
MEFISTO	MEsskammer für FlugzeitInStrumente und Time-Of-Flight
N_{OT}	Number of OT cycles to failure
OMC	Optimum Moisture Content
OT	Overlay Tester
OTE	Overlay Testing Equipment

PCC	Portland Cement Concrete
PI	Plasticity Index
PL	Plastic Limit
RAP	Reclaimed Asphalt Pavement
RAS	Recycled Asphalt Shingles
RCD	Reflective Cracking Device
SAMI	Stress-Absorbing Membrane Interlayer
SAMI	Stress-Absorption Membrane Interlayer
Sasobit®	Organic additive
SBS	Styrene-Butadiene-Styrene
SCR	Heater Scarification
SD	Standard Deviation
SGC	Superpave Gyratory Compactor
Superpave	Superior Performing Asphalt Pavement
TTI	Texas Transportation Institute
UGR-FACT	University of Granada – Fatigue Asphalt Cracking Test
WMA	Warm-Mix Asphalt
WRC	Wheel Reflective Cracking

EXECUTIVE SUMMARY

Reflective cracking is one of the major forms of deterioration in flexible pavements constructed over old pavements with discontinuities in their surface. Although narrow reflective cracks do not negatively affect pavement performance wide reflective cracks with a crack width greater than 6 mm can lead to many performance-related problems which include high tensile stress at the bottom of the HMA overlay, increased roughness of the riding surface, water infiltration into the pavement layers. Additionally, poor interlocking between aggregate particles and localized degradation of the pavement along the crack can also occur. Reflective cracks might also develop other branch cracks, which can gradually lead to fatigue cracking. The resistance of asphalt mixtures to reflective cracking has not gained proper attention as compared to asphalt mixtures' resistance to classical fatigue cracking or thermal cracking.

Reflective Cracking is a prime concern during the selection of HMA overlays with stabilized bases like Cement-Treated Base (CTB) or Cement-Stabilized Base (CSB). Stabilized base, a popular composite base material, is a mixture of soil, cement, and water constructed to a high density. It has an inherent tendency to generate shrinkage cracks. Traffic loading and seasonal temperature variation cause vertical and horizontal movements within these cracks which propagate upward and cause reflective cracking in the surface course. Previous studies showed that it is the seasonal temperature variation that plays a more critical role in causing reflective cracking in the field as compared to traffic loading.

The primary objective of this project is to propose a laboratory setup to test and evaluate an asphalt mixture layer on top of a simulated CTB or CSB layer against reflective cracking. Therefore, to attain this goal an in-depth literature review on reflective cracking, CTB, and the experimental studies that were conducted throughout the world to investigate the resistance of asphalt mixtures to reflective cracking has been conducted (Task 1). It was found that the Texas Transportation Institute (TTI) Overlay Tester (OT) most closely simulates thermally-induced reflective cracking in the laboratory. Its performance-based test results, rapid testing time, commercial availability, lower equipment cost, high sensitivity to asphalt mixture design parameters, and the availability of standard test procedure proved its efficiency to evaluate the reflective cracking performance of asphalt mixtures on top of a pre-cracked CTB/CSB layer and thereby selected for this project (Task 2). Four different asphalt mixtures (prepared with two different asphalt binders and two different RAP contents) and two types of stabilized bases with two different compressive strengths (150 psi for CTB and 350 psi for CSB) were successfully prepared (Task 3). The reflective cracking performance of the laboratory-produced asphalt mixtures was evaluated using both the modified and conventional OT setup at room temperature and low temperature based on the number of cycles to failure (N_{OT}), Critical Fracture Energy (G_c), and Crack Progression Rate (CPR) (Task 4). Finally, a final report was prepared that includes problem description, objectives, methodology, analysis of data, results, and conclusion (Task 5).

The attempt to modify the conventional OT setup for better mimicking field reflective cracking was unsuccessful. The glue used to attach the HMA layer with the underlying CTB/CSB layer was very strong which prevented the crack to propagate to the HMA layer. When the prime coat was used as a substitute for epoxy glue, the prime coat was unable to generate any bond between the top and bottom layers. As a result, the HMA layer slipped when the composite OT specimen was mounted in the vertical OT setup.

Results of the conventional OT testing showed that decreasing the test temperature from room temperature to low temperature caused an increase in the Critical Fracture Energy (G_c) while a decrease in Crack Progression Rate (CPR). Therefore, a reduction of test temperature from room to low temperature resulted in the asphalt mixtures to change their behavior from "soft crack-resistant" mixtures to "tough crack resistant" mixtures. Although, the specimens prepared with unmodified and softer asphalt binder exhibited higher Gc values in most cases, no trend was observed in CPR values due to the change in binder type. Similar conclusion was made when the effect of RAP content on the reflective cracking performance was evaluated. The specimens prepared with 20% Reclaimed Asphalt Pavement (RAP) or no RAP sometimes behaved as tough crack-resistant while sometimes showed soft crack-resistant behavior. Further research is necessary to understand the true effect of changing binder type and RAP content on the reflective cracking performance of asphalt mixture specimens.

1. INTRODUCTION

Cement-Treated Base (CTB) is a composite material that is widely used as a base for pavement structures to enhance the strength and durability of the surface course without increasing the total thickness of the pavement layer. CTB is an engineered material designed to prevent damages in pavements due to wetting-drying or freezing-thawing cycles. The use of CTB under hot-mix asphalt (HMA) overlays reduces deflections and tensile strain in the HMA surface under the wheel load. It also facilitates drainage, which is a major requirement to keep the pavement structure in good service conditions.

CTB is prone to the development of reflective cracking, which is one of the major forms of deterioration in pavements constructed with HMA overlays (*1*). CTB is susceptible to the development of shrinkage cracks due to drying shrinkage. These shrinkage cracks in the CTB deteriorate under traffic load and temperature variations, propagate upward and eventually reflect through the pavement surface. Narrow reflective cracks having a width of less than 3 mm are cosmetic in nature and do not negatively influence the functional performance of the pavement structure (*2*, *3*). However, reflective cracks with a crack width greater than 6 mm can lead to many performance-related problems, including inadequate load transfer across the joints, high tensile stress at the HMA bottom, and increased roughness of the riding surface (*4*, *5*). Wide reflective cracks promote water infiltration into the pavement layers, enervate the underlying base, subbase, or subgrade layer, and promote stripping of HMA from the aggregate (*6*–*8*). Additionally, poor interlocking between aggregate particles and localized degradation of the pavement along the crack can also occur (*2*, *3*). Reflective cracks might also develop other branch cracks, which can gradually lead to fatigue cracking (*9*). All these detrimental effects of the reflective cracking result in performance problems of the pavement structures.

The issue of reflective cracking has not received proper attention as compared to classical fatigue studies. It is important to obtain a profound understanding of the reflective cracking mechanism since it affects the functional performance of the pavement. Reflective cracking is a major concern during the selection of asphalt mixture surface courses for flexible or rigid pavements with stabilized bases, or even when the current pavement structure has severe cracks in its surface. Moreover, it is crucial to evaluate asphalt mixtures against reflective cracking when they are placed over a pre-cracked base so that long-term structural and functional performance of the overlaid pavements can be ensured. The mechanism of reflective cracking causes the propagation of CTB shrinkage cracks to the surface course (*10*).

Significant efforts have been made to control reflective cracking in the surface course which includes increasing the thickness of the HMA overlay (*7*), introducing “micro-cracking” and stress-relief interlayers, i.e., Stress-Absorbing Membrane Interlayer (SAMI) and geosynthetic fabrics (*3*).

Yet, limited studies have been conducted to evaluate the performance of asphalt mixtures constructed over a pre-cracked CTB. Several laboratory test setups were developed throughout the years, and many studies were conducted by researchers to evaluate the performance of asphalt mixtures against reflective cracking. While some test setups study the effects of traffic and temperature separately, some other test setups study the effects of traffic and temperature variations simultaneously through the application of vertical loads and horizontal opening displacement. However, the ability of these setups to accurately simulate the complex field reflective cracking mechanism is a matter of debate. Besides, there is a lack of standardized test

procedures to evaluate the reflective cracking performance of asphalt mixtures. The most commonly used Tex-248-F uses Overlay Tester (OT) which might not fully mimic the reflective cracking occurring in the field since the cracked CTB layer is not considered here beneath the HMA specimen and it might be the reason for high variability in the OT results.

In this research project, the available laboratory test setups that are used nationally and internationally to evaluate the resistance of asphalt mixtures to reflective cracking were conceptually assessed and evaluated. Through an extensive literature review, a total of seventeen reflective cracking testing devices were found and evaluated. The best three among the available devices were chosen and ranked based on various factors, i.e., commercial availability, ease of use, variability and repeatability of the test results, and field validation. The device that has been ranked first was considered and the efficiency of the considered setup was evaluated as a true representative of field reflective cracking, as well as its ability to accurately differentiate between the performances of various HMA mixtures. Some potential modifications have been proposed to be incorporated into the considered test setup so that it can simulate field reflective cracking more closely. Finally, the performance of various asphalt mixtures against reflective cracking was assessed using the considered test setup before and after the incorporation of proposed modifications.

In this report, the findings from the comprehensive literature review are summarized. Besides, the methodologies followed to prepare CTB/CSB and HMA mixtures, the testing procedure, and analysis results are all documented in detail. Finally, the project findings, conclusion, and recommendations are stated.

2. OBJECTIVES

The primary goal of this study is to propose a laboratory setup to test and evaluate an asphalt mixture layer on top of a simulated Cement-Treated Base (CTB) layer against reflective cracking. To achieve this goal, the following objectives are set for the project:

- Assess the available laboratory test setups used for evaluating asphalt mixtures against reflective cracking and identify their limitations;
- Select a laboratory test setup to evaluate the effect of CTB reflective cracking on asphalt mixture layer on top of it; and
- Evaluate the performance of different asphalt mixtures against reflective cracking using a selected laboratory test setup.

The accomplishment of the project objectives in the research phase the following tasks have been achieved:

- **Task 1:** Conducting an in-depth literature review on reflective cracking, CTB, and the experimental studies that were conducted throughout the world to investigate the resistance of asphalt mixtures to reflective cracking;
- **Task 2:** Based on the findings of Task 1, identifying the testing device among the available ones that most closely simulate the actual mechanism of reflective cracking, and assessing its efficiency to evaluate the reflective cracking performance of asphalt mixtures on top of a CTB layer;
- **Task 3:** Preparing four different asphalt mixtures and two types of soil-cement bases for testing using the selected test setup;
- **Task 4:** Evaluating the reflective cracking resistance for laboratory-produced asphalt mixtures on top of a CTB layer using the considered laboratory test setup at room temperature and low temperature; and
- **Task 5:** Preparation and submission of the final report that includes problem description, objectives, methodology, analysis of data, results, and conclusion.

3. LITERATURE REVIEW

In this chapter, an in-depth literature review has been conducted regarding the advantages and challenges of using the CTB layer in asphalt pavements, the mechanisms causing reflective cracking, and popular techniques to significantly reduce the occurrence of it. Available laboratory testing procedures and setups being used worldwide to simulate the effects of reflective cracking on asphalt mixtures have also been explored, and a total of seventeen reflective cracking testing devices and setups are critically evaluated. Among those seventeen devices, the best three are chosen and ranked based on various factors as described in detail in the following sections. The effectiveness of the test setup that has been ranked first has been further evaluated to identify it as the most reliable cracking test setup to determine the resistance to reflective cracking. Finally, the limitations of the selected setup have been identified, and some modifications are proposed so that it can simulate the complex reflective cracking phenomenon occurring in the field more closely.

3.1. Reflective cracking

Reflective cracking is a special type of cracking when a crack originated in the base course, or subgrade layer is propagated to the surface course of the pavement (*11*). Reflective cracking occurs in the HMA overlay when it is placed on an existing pavement having discontinuities in its surface in the form of shrinkage cracks (*12–18*). Traffic loading and temperature gradient cause vertical and horizontal movements of these cracks, which result in progressive crack propagation through the surface course (*2*). These surface cracks demonstrate the same pattern as the cracks in the base (*3*, *11*). Reflective cracks are frequent in both flexible and rigid pavements constructed with stabilized bases (*19*). The propagation of reflective cracks is influenced by the thickness and characteristics of the HMA overlay and the quality of the existing subgrade (*20*). Reflective cracks typically extend towards the surface slowly (1 inch/year) and become visible at the surface by three years in service depends on the thickness of the surface layer (*21*).

(a) (b)

Figure 1. Types of reflective cracking, (a) double (b) single (*22*).

Reflective cracking in pavements can be categorized into two types: traditional single and double reflective cracking. The type of reflective cracking is related to the level of horizontal crack/joint movement as well as the magnitude of vertical deflection between crack edges/joints due to traffic and environmental effect (*22*). Previous studies showed that double reflective cracking (Figure 1a) typically occurs in thin HMA overlays constructed over Portland Cement Concrete (PCC) base (*22*, *23*). The debonding between the interface of HMA and PCC near the joint as well as excessive vertical joint deflection result in double reflective cracking (i.e., 40-60 mm from each side of the joint centerline) (*24*). More details about the double reflective cracking can be found elsewhere

(*23*, *25*, *26*). However, double reflective cracking is more common in semi-rigid pavements and can rarely found in flexible pavements as compared to traditional single reflective cracking (*22*).

The scope of this study is limited to the evaluation of traditional bottom-up reflective cracking (Figure 1b) located directly above the crack rather than double reflective cracking on each side of the crack. Therefore, the remaining part of this report will focus on more frequent and complex traditional single reflective cracking.

3.2. Cement-Treated Base (CTB)

Cement-Treated Base (CTB), also known as soil-cement, is a very popular composite material that is used worldwide as a base for highways, roads, streets, parking lots, and airports for providing strength to the surface course. It is a thorough mixture of pulverized soil materials such as native soils with or without manufactured aggregates with Portland cement and water compacted to a high density (*27*, *28*). When the cement hydrates after compaction and curing, the mixture forms a hard, durable, frost-resistant paving material. A wearing course of asphalt mixture or Portland Cement Concrete (PCC) is applied over the CTB to complete the pavement structure (*10*, *27*).

According to the Louisiana DOTD Specification, there are two types of soil-cement bases based on their compressive strength (i.e., 150+ psi and 300+ psi). Therefore, a soil-cement base having a compressive strength of a minimum 150 psi (1 MPa) will be referred to as Cement-Treated Base (CTB) while a soil-cement base having a minimum compressive strength of 300 psi (2 MPa) will be referred to as Cement-Stabilized Base (CSB) for the remaining part of the report.

The process of CTB construction follows a definitive procedure, and it begins with roadway preparation. Before construction, the roadway should be prepared first by checking the crown and grade, correcting any weak subgrade portion, prewetting by adding moisture, and scarifying or pulverizing the soil material. The mixing of cement, aggregate, soil, and water can be conducted either using a mixed-in-place method or using a central mixing plant. Immediately after mixing, the soil-cement mixture is compacted to maximum density, finished to a smooth, rut, ridge, or crack free surface using tamping rollers, vibratory-steel-wheel rollers, or pneumatic-tire rollers. Although compacted and finished CTB contains enough moisture for cement hydration, a moisture-retaining cover, i.e., bituminous material, wet straw, or sand, is placed on the completed CTB to retain the moisture and allow cement hydration (*27*, *28*). However, minimum cement content and optimum moisture content is to be determined before the beginning of construction (*27*). In Louisiana, the minimum cement content is obtained from DOTD TR 432 (*29*) and optimum moisture content and density values are obtained from the moisture-density test, DOTD TR 418 (*30*).

3.3. Advantages and challenges of using CTB layer in asphalt pavements

Using CTB instead of conventional granular unbound bases under the surface provides a variety of tangible benefits. Soil-cement materials provide additional strength and support without increasing the total thickness of the pavement layers (*31*). CTB is an engineered material designed to prevent damages due to wetting-drying or freezing-thawing cycles. Using CTB as a base material makes the pavement structure durable and long-lasting as it becomes less susceptible to climatic effects (*28*). Since CTB provides a much stiffer base than an unbound granular base, it minimizes pavement deflections under wheel loading (Figure 2). As a result, strains are lower in

the asphalt surface which helps to retard the onset of surface distressing mechanisms and thereby extends pavement service life (*28*, *31*).

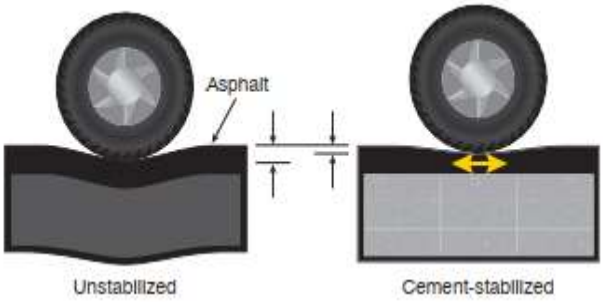

Figure 2. CTB reduces deflections and tensile strain in the HMA surface under wheel load (*28*).

Additionally, less thickness is required for CTB than that of conventional unbound granular bases carrying the same traffic because the loads are distributed over a wider area (*31*) (Figure 3). The application of in-situ soils and manufactured aggregates can help to reduce the necessity to haul in costly granular aggregates (*28*).

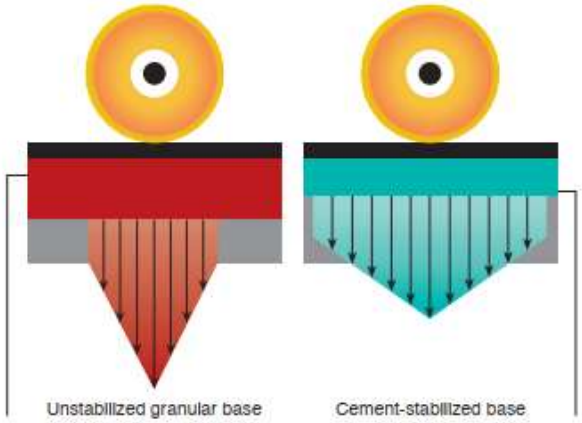

Figure 3. Wheel loads are distributed over a larger area in CTB (*28*).

The ingression of moisture from rain or the infiltration of moisture through high water tables or capillary action in un-stabilized bases of flexible pavements causes softening of HMA, reduces strength and modulus. However, because of cement's ability to reduce the moisture permeability, pavements constructed with CTB form a base that works as a moisture barrier and prevents moisture from entering the base or underlying layers even when the pavement is saturated (Figure 4). This ability to prevent moisture intrusion significantly reduces the potential for pumping of subgrade soils when CTB is used in pavements as a base material (*28*).

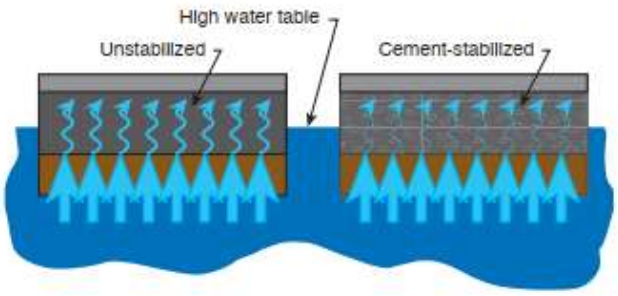

Figure 4. CTB prevents moisture infiltration (*28*).

Due to the rapid construction process of CTB, there is little disruption to traffic (*28*). Rutting and shoving are minimized in a CTB pavement in all layers except the asphalt surface. Like Portland cement, CTB attains strength with age, and this reserve strength can withstand greater traffic load and volume throughout its service life (*28*). Also, CTB is an effective treatment that can be applied to the soil to improve its strength, to increase the bearing capacity, the number of equivalent standard axle load (ESAL), to reduce water vulnerability, and thus to extend the service life of the pavement structure (*31*). Additionally, depending on project needs, CTB increases the construction speed and in some cases reduces the overall time of the project (*31*)**.**

Apart from the aforementioned benefits and advantages, the main challenge of using CTB as a base course in flexible pavements is the formation of shrinkage cracks in its surface which is the main type of discontinuity in CTB. Rather than being a result of a structural deficiency, shrinkage is the natural characteristic of CTB. Shrinkage cracks are developed on the surface of CTB which can reflect through the asphalt surface and the surface cracks tend to follow the same pattern as the cracks in the base (*32*).

Factors that contribute to shrinkage cracking and crack spacing in CTB include material compaction and moisture levels, soil type, curing, and effects of rapid moisture loss and cement content (*2*, *32*). When moisture is excess to attain maximum density, the material undergoes more drying which increases the potential for shrinkage cracking (*2*). Due to larger surface areas and higher moisture content for compaction and higher cement content for adequate durability, cement-stabilized fine-grained material develops higher total shrinkage than granular soils (*32*). Right after the placement of CTB, there is a loss of moisture due to evaporation which leads to inadequate cement hydration and quick-drying and shrinking of CTB (*2*). Although increasing cement will decrease total shrinkage, an excessive amount of cement is not always beneficial. Higher cement content results in greater consumption of water during hydration and thus increase drying shrinkage. Furthermore, higher cement content results in excessive strength that causes larger crack spacing (*32*).

3.4. Mechanism of CTB Reflective Cracking

Drying shrinkage is one of the main sources of CTB reflective cracking (*2*) and the mechanism of CTB reflective cracking causes the propagation of subsurface shrinkage cracks to the surface course (*3*). Traffic and environmental loading separately or combinedly contribute to the formation and propagation of reflective cracking (*2*, *8*). Additionally, expansive subgrade soils and subgrade moisture gradient might also induce vertical and horizontal movements in cracks (*11*, *33*). The mechanism of reflective cracking is explained in detail below.

When an existing pre-cracked pavement or base is fully bonded with an HMA overlay and is subjected to cyclic temperature decrease, it performs an opening action on the overlay at crack locations. Temperature decrease and subsequent contraction and curling of existing pavement induce horizontal movement in cracks and joints. It causes the cracks to open up and gives rise to tensile stresses (Mode I cracking) at the bottom of the HMA overlay (Figure 5a) (*8*, *34*, *35*). Moreover, the drop in temperature increases asphalt mixture stiffness, making it more prone to reflective cracking (*33*, *34*).

Traffic loading and the associated vertical movements play a role in the second step of the crack propagation phase (*2*). When a wheel load moves over a crack, it can create three stress pulses, two maximum shear stresses, and one maximum bending (*36*). The first stress pulse is due to the differential vertical movement between the crack edge when wheel load approaches towards the crack. The most loaded side of the crack moves downward while the unloaded side moves upward inducing shear stresses (Mode II cracking) between the crack edge (Figure 5b). The second stress pulse is the bending or flexural stress induced in the crack when the wheel comes over the crack (Figure 5c). The third stress pulse is the opposite situation to the first stress pulse, which again induces shear stresses (Mode II cracking) between the crack edges (Figure 5d) (*8*, *11*, *33*, *34*). When one of the aforementioned stresses or the combination of the stresses, namely, tensile, shear, or bending, goes beyond the tensile strength of the overlay, reflective cracking will occur (*11*, *37*).

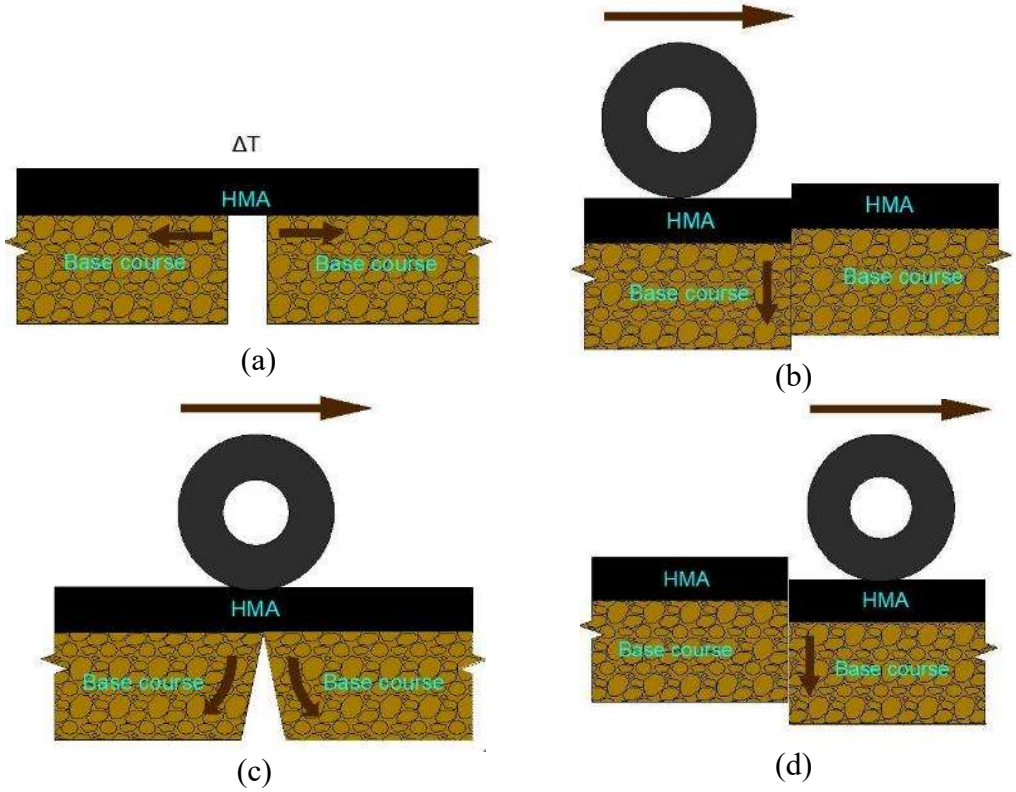

Figure 5. Mechanisms of reflective cracking, (a) increased tensile stress at HMA bottom, (b) shear stress between the crack edge, (c) bending stress between the crack edge, and (d) shear stress between the crack edge.

3.5. Techniques to mitigate reflective cracking

Various mitigation techniques are used to control reflective cracking in CTB both in the construction phase and in the rehabilitation phase of any existing pavement structure. In the

construction phase, the use of correct construction techniques can effectively retard the onset of reflective cracking in pavement structures. The use of proper construction techniques includes the use of appropriate cement and moisture contents, compacting the CTB at moisture content less than the optimum, proper mixing and compaction, and curing (*2*, *18*). The CTB surface must be kept moist before the placement of a permanent moisture barrier, such as a curing compound, a bituminous emulsion prime coat, or a chip seal. Besides, completing stabilization within two hours of cement mixing is necessary to prevent the hydration of cement before final compaction (*2*). When the final paving of the HMA surface is delayed for 14 to 28 days, it allows more time for any shrinkage cracks to develop. Placing the surface after most of the shrinkage has occurred can result in fewer and thinner cracks in the HMA layer as the HMA will tend to bridge the already-formed cracks (*2*). Construction of CTB with excessive clay is detrimental since clay contains more water and compacted with a higher moisture content which means more potential to shrinkage cracking. Blending with granular and/or sandy materials can help to reduce the clay percentage and thus can control reflective cracking (*18*). Using additives during CTB construction is beneficial because these additives possess certain properties that can delay the formation of CTB cracks in its early life. Various admixtures are available that can minimize the potential of shrinkage cracking in CTB. Admixtures like shrinkage-compensating cement, gypsum, water reducers, fly ash and blast-furnace slag can reduce water demand, aid in the mixing process, extend mixing time, and provide a filler material that can effectively reduce the need for excess cement (*2*, *18*).

Apart from the reflective cracking mitigation techniques in the construction phase mentioned earlier, HMA mixtures itself can be modified or reinforced during construction to prevent reflective cracking. Modification of the HMA involves using polymer-modified asphalt, rubberized asphalt, stone matrix asphalt, sulfur asphalt, or carbon black as HMA overlay. Additionally, steel-reinforcing nettings, geotextile, or geogrids are used for HMA overlay reinforcement (*38*).

During the service life of pavements, narrow reflective cracks in the asphalt surface may cause no performance problems. However, if the existing HMA pavement supports high traffic volume and develops cracks wider than 6 mm, it needs to be rehabilitated. In the rehabilitation phase, minor reflective cracks can be sealed with standard bituminous sealing compounds such as chip seal (*18*, *38*). If cracks in a stabilized pavement are poorly deteriorated, more extensive repair procedures including the milling and replacing of the wearing surface, heater scarification (SCR), hot-in-place recycling (HIPR), cold-in-place recycling, and full-depth reclamation can be used (*38*).

Two other popular techniques are also available that can significantly reduce the occurrence of reflective cracking in the rehabilitation phase, such as applying a stress relief layer and microcracking. When cracks appear in the base course, they generate stress concentrations in the HMA surface which can lead to reflective cracks in the HMA. When a flexible material is inserted between the base and surface layers it helps to release the stress. Unbound granular layer, chip seal, Stress-Absorbing Membrane Interlayer (SAMI), geosynthetic fabrics, soft asphalt interlayer, rubber modified asphalt interlayer, strata reflective crack relief system, Interlayer Stress Absorbing Composite (ISAC), and bond breaker are all such kinds of stress-relief interlayers (*2*, *32*, *38*). However, when compared to other reflective cracking mitigation techniques it can be more expensive because the placement of interlayers requires an appropriately trained field crew (*2*). Figure 6 illustrates the use of chip seal, geotextile, and unbound granular layer as stress-relieving interlayers to control reflective cracking.

Another method is “microcracking” or “pre-cracking” which is a relatively new approach and can be effectively used to reduce crack width. Through the application of several passes of a vibrating roller after one to two days of final compaction, hundreds of tiny micro-cracks are developed instead of single transverse cracks on the CTB surface. These microcracks release shrinkage stress in its early life and create a crack pattern that resists the development of wide shrinkage cracks and therefore, reduces the chance of reflective cracking in pavements constructed with CTB (*2*, *32*, *39*). The structural capacity of the pavement will not deteriorate due to the presence of these hairline cracks rather the microcracks will eventually heal and the cement-stabilized material will regain its strength over time (*32*). Excessively high cement contents can give rise to crack severity in terms of crack width, crack length, or both if microcracking is not applied. Microcracking reduces the severity of shrinkage cracks in the base, regardless of cement content, and in some cases also significantly reduces total crack length (*40*).

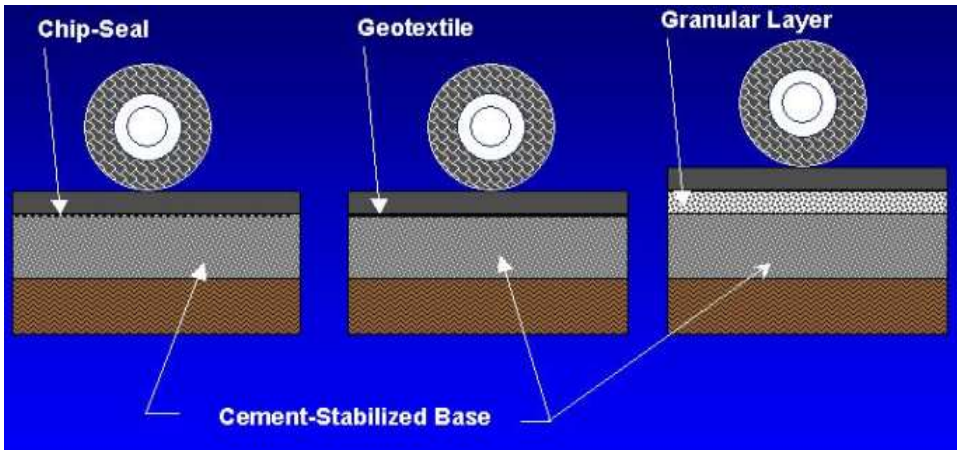

Figure 6. Three approaches to stress relief to reduce reflective cracking (*32*).

3.6. Available laboratory test setups to simulate reflective cracking

Several laboratory test setups were developed and advanced by researchers at different times and locations based on their understanding of reflecting cracking mechanisms. Some researchers focused on the effect of traffic loading and considered it the leading cause of reflective cracking to develop the laboratory test setup. Other researchers considered the variation in temperature as the primary cause for reflective cracking.

In Louisiana, the most popular testing setup that is frequently used to study low temperature cracking in the laboratory is Semi-Circular Bend test from the Louisiana Transportation Research Center (SCB-LTRC) due to its relatively lower variability (COV < 20%), easy data interpretation, good correlation with low-temperature cracking validated at MnRoad, and availability of the standard test method (*41*). However, the focus of this study is thermally-induced, bottom-up reflective cracking due to cyclic horizontal movement between the cracks rather than low temperature cracking or fracture. In a comprehensive study, Zhou et al. evaluated four different testing devices, namely Overlay Tester (OT), Disk-shaped Compact Tension (DCT) test, SCB-LTRC, and SCB test at room temperature from Illinois (SCB-IL), to identify the most reliable cracking test that can routinely evaluate asphalt mixtures (*42*). A number of limitations were identified from SCB-LTRC. SCB-LTRC was found to be insensitive to asphalt binder content and demonstrated an unexpected increase in cracking resistance when adding Recycled Asphalt Shingles (RAS) to the mixtures. Due to these limitations, SCB-LTRC was put out of consideration

to be used in evaluating the reflective cracking performance of asphalt mixtures and more concentration was put on nationally and internationally used reflective cracking testing devices.

The test setups obtained from an extensive review of existing literature can be differentiated based on the effect they attempt to mimic, i.e., daily and seasonal temperature variation and/or traffic loading. Various researchers presumed that temperature change is more significant for reflective cracking than that of traffic (*43–45*). However, it is essential to simulate both effects for capturing the complex field reflective cracking phenomenon in the laboratory.

The temperature variation induces horizontal movement between cracks while traffic loading induces differential vertical movements. Some tests that study reflective cracking simulate these two effects separately, while others mimic both effects simultaneously through the application of vertical loads and horizontal opening displacement. Based on the effects the test setups simulate, the laboratory reflective cracking setups can be classified into three major groups, i.e., Group A, B, and C. Groups A and B represent the setups that only simulate temperature variation and traffic load associated reflective cracking, respectively. Group C consists of setups that mimic the combined effect of temperature change and traffic loading. More details are provided in the following sub-sections.

Group A - Testing setups that simulate the effect of temperature variation only

The testing setups in Group A simulate the effect of daily or seasonal temperature variation while not considering the effect of traffic loading. All these setups are uniaxial tension test setups and work in a similar principle. That is, for all the setups the major components consist of a fixed part and a movable part over which the beam or slab specimens are mounted. The movable part produces horizontal cyclic tensile force to the specimen, which causes the cracks to open and close. ENTPE's Fissurometer (*46*), University of Illinois' testing equipment for Interlayer Stress-Absorbing Composite system (*47*), Texas Transportation Institute (TTI) Overlay Tester (*22*), Iraqi Overlay Testing Equipment (OTE) (*11*), Technical University of Vienna's mechanical compression testing machine for wedge splitting (*48*), Aeronautical Technological Institute, and Brazil's bending or shear testing device (*49*) fall within this category.

Group B - Testing setups that simulate the effect of traffic loading only

Group B includes setups that duplicate the effect of traffic loading only. This group can be further classified into two sub-groups: the setups that apply a wheel load moving back and forth over the specimen, and the setups that apply only a vertical point load in predetermined locations, static and/or cyclic, on the specimens. The vertical load, either by wheel or point load, typically induce shear stress and/or flexural stress between the crack edges and enables differential vertical movements between the two sides of the crack. Hamburg Wheel Tracking Tester (*50*) is in the first subgroup of Group B setups while Florida Atlantic University, USA's testing device for geogrid system (*51*), BRRC test device (*52*), and Cracow University of Technology, Poland's bending or shear testing device (*53*) lie within the second subgroup of Group B setups.

Group C - Testing setups that simulate the combined effect of temperature variation and traffic loading

Group C consists of laboratory testing setups that simulate the effect of temperature variation and traffic loading simultaneously. This group can be further classified into two sub-groups based on the type of vertical load they apply. The first sub-group produces vertical forces in the form of a

reciprocating wheel, while the second sub-group applies cyclic vertical point loads with various frequencies, load amplitudes, and testing temperatures. For both subgroups, horizontal cyclic tensile forces are applied to the specimen which simulates the effect of temperature variation. These two types of force induce tensile, shear, and bending stresses simultaneously into the specimen. Wheel Reflective Cracking device (*54*) and Accelerated Simulative Wheel Tracking device (*55*) are in the first sub-group, while Universal Testing Machine (*56*), Reflective Cracking Device (RCD) (*57*), Laboratory of Public Roads, France's shrinkage-bending test device (*58*), MEFISTO test device (*59*), and UGR-FACT test device (*60*) are included in the second sub-group.

Table 1 illustrates a comprehensive summary of various aspects of a total of the seventeen available testing setups that attempt to simulate the mechanisms of reflective cracking in the laboratory.

Table 1. Available Laboratory Test Setups to Simulate Reflective Cracking.

Group	Testing Device	Developer/User	Purpose	Specimen Type, Material & Geometry	Testing Condition	Data Acquisition/Parameter of interest	Failure Criteria
A	Fissurometer (*46*)	GERLAND and ENTPE, France	Classify different anti-reflective cracking methods (i.e., sand asphalt, geotextiles, thick coat, and crack bridging) based on their resistance to reflective cracking	- Slab specimen - HMA surface & cracked concrete base	- Cyclic uniaxial load - Opening & closing speed of the moving part = 2.7 mm/hr - Opening amplitude of moving part = 0.3 mm - Wearing course thickness = 6 cm - Test temperature = 5°C	- $(K_F)n$: tension modulus weakening after the fatigue of n cycles - $(K_{US})n$: the ratio of ultrasonic transmission between after n cycles and one cycle	Breaking of specimen
	Testing equipment for ISAC system (*47*)	University of Illinois, USA	Assess the performance of the ISAC layer to mitigate reflective cracking	- Beam specimens - HMA Overlay (2.5 in.), ISAC layer & jointed PCC base (90 x 6 x 5 in.)	- Cyclic uniaxial load - Frequency = 0.0016 in./min - Test temperature = -1.1°C	- Strain in HMA overlay as a function of load cycles - Number of cycles to failure	Cracking in HMA overlay
	TTI Overlay Tester (*22*)	Texas Transportation Institute	Measure the reflective cracking susceptibility of asphalt concrete	- Beam specimens - Asphalt concrete (6 x 3 x variable height in.)	- Opening displacement = 0 - 0.079 in. - Loading rate = 0.307 in./min - Cycle time = 10 sec/cycle - 10 min /cycle - One-phase/two-phase loading - Test temperature = 0-25°C	- Critical Fracture Energy - Crack Resistance Index - Reflection Cracking Life	- 93% reduction of the maximum load, or - 1000 loading cycles
	Iraqi Overlay Testing Equipment (OTE) (*11*)	Iraq Institute of Technology	Simulate the mechanism of reflective cracking in laboratory	- Beam specimens - HMA overlay & asphalt concrete base (15 x 3 x various heights in.) - 5 mm crack in the base	- Opening displacement = 0 - 20 mm - Loading rate = 1.25 mm/min - Cycle time = 1 sec/cycle - 60 min/cycle - One-phase loading - Test temperature = 0 - 25°C	- Strain in HMA as a function of load cycles - Number of cycles to failure	Cracking in the HMA overlay

Table 1. Available Laboratory Test Setups to Simulate Reflective Cracking (continued).

Group	Testing Device	Developer/User	Purpose	Specimen Type, Material & Geometry	Testing Condition	Data Acquisition/Parameter of interest	Failure Criteria
A	Mechanical compression testing machine for wedge splitting (*48*)	Technical University of Vienna, Austria	Characterize the fracture behavior of Asphalt concrete material	- Cubic, rectangular, or cylindrical specimen - Asphalt concrete - A rectangular groove at the surface - A starter notch at the bottom of the groove	- Loading rate = 0.05 in./min - Test temperatures = 8, 3, -0.5, -10 and -21° C	- Horizontal splitting force vs crack opening - Maximum splitting force vs test temperature - Specific fracture energy vs test temperature	Splitting of specimen
	Bending or shear testing device (*49*)	Aeronautical Technological Institute, ATI, Brazil	Evaluate the effectiveness of polyester geogrid as an interlayer reinforcement	- Beam specimen - Two layers of asphalt concrete, one uncracked and one with 0.11, 0.24, or 0.35 in. cracks (18 x 6 x 3 in.) - Polyester geogrid on crack tip	- Sinusoidal loading - Frequency = 20 Hz	- *FEG*: Factor of the effectiveness of geogrid - Number of load cycles to failure	First visible crack on the surface
B	Testing device for the geogrid system (*51*)	Florida Atlantic University, USA	- Assess how the placement configuration of the stiff geogrid affects the reflective crack propagation - Quantify the effectiveness of geogrids	- Beam specimen - Asphalt concrete (18 x 6 x 3 in.) - Geogrid (at the bottom or sandwiched in asphalt concrete) - Plywood base with 0.39 in. joint	- Monotonically increased static load - *Cyclic load*: Sinusoidal waveform, amplitude = 222, 444, 888, 1110 and 1332 N and frequency = 2 Hz	- *FEF*: Fabric Effectiveness Factor - Z: Embedment factor	- *Cif* = First visible crack - *Cmf* = When crack propagates halfway depth of the specimen - *Ctf* = When a crack appears at the top of the specimen
	Hamburg Wheel Tracking Tester (*50*)	Hamburg, Germany	Measure the effectiveness of stress-absorbing interlayers (i.e., SBS-modified interlayer, fiberglass-polyester, paving mat interlayer, SAMI)	- Beam specimen - Asphalt cement surface (1.6 in.), interlayer & cement concrete base (11.4 x 2.8 x 1.6 in.) - 0.2 in. crack in the base	- Repetitive dynamic wheel load - Frequency = 52 cycles/min - Test temperature = 15°C	Number of wheel passes to failure	The occurrence of cracks at the bottom of the surface layer

Table 1. Available Laboratory Test Setups to Simulate Reflective Cracking (continued).

Group	Testing Device	Developer/User	Purpose	Specimen Type, Material & Geometry	Testing Condition	Data Acquisition/Parameter of interest	Failure Criteria
B	BRRC test device (*52*)	Belgian Road Research Centre, Belgium	Evaluate the performance of anti-reflective cracking interfaces (i.e., SAMI, geogrid, geocomposite, steel reinforcing netting)	- Beam specimen - Asphalt cement surface (2.36 in.), interlayer & cement concrete base (24 x 5.5 x 2.75 in.) - 4 mm crack in the base	- Cyclic vertical load - Magnitude = 12 kN - Frequency = 1 Hz - 0.5s loading, 0.5s unloading - Test temperature = 15°C	- The slope of the quasi-linear portion of "vertical stamp position vs time" curve - Testing time corresponding to the point of inflection	Cracks at asphalt cement bottom
	Bending or shear testing device (*53*)	Cracow University of Technology, Poland	- Study the character of co-action of the geotextile and asphalt layers - Check the adhesion of the entire structure	- Beam specimen - Asphalt concrete surface (2 in.), geotextile & asphalt concrete base (12 x 3 x 3 in.)	- *Bending under static load*: Loading rate = 0.47 in/mm and test temperature = 20°C - *Bending under dynamic load*: Loading amplitude = 2 kN, frequency = 5 Hz and test temperature = 20°C - Shearing: Loading rate = 0.039 in/min and test temperature = 30°C	- *Bending under static load:* Bending strength, moment of crack, and maximum force - *Bending under dynamic load:* Number of cycles to failure - Shearing: Maximum shear force and maximum shear stress	Cracking of the asphalt mixture
C	Wheel Reflective Cracking device (*54*)	Road Laboratory, Technical University of Madrid, Spain	Examine geosynthetics in anti-reflection pavement cracking systems	- Beam specimen - Asphalt concrete surface (2 in.), geosynthetics & asphalt concrete base (12 x 3 x 0.4 in.)	- Moving wheel load - Frequency = 43 passes/min - Crack opening speed: 0.024 in./h - Maximum deflection: 0.018 in. - Test temperature = 5°C ± 1°C	- Reflective cracking strength - Number of wheel passes times the rate of loading	Maximum relative vertical movement of 0.2 mm between the crack edges

Table 1. Available Laboratory Test Setups to Simulate Reflective Cracking (continued).

Group	Testing Device	Developer/User	Purpose	Specimen Type, Material, and Geometry	Testing Condition	Data Acquisition/Parameter of interest	Failure Criteria
C	Universal Testing Machine (*56*)	University of Cantabria, Spain	Evaluate the behavior of Geosynthetics as anti-cracking systems	- Beam specimen - Asphalt concrete surface (2 in.), geosynthetics & asphalt concrete base (2 in.) - 45 mm crack in the base	*First part:* - One high frequency sinusoidal load - Frequency = 10 Hz - Cycle time = 0.1 sec - Low-frequency triangular loads - Frequency = 0.033, 0.005, and 0.002 Hz - Cycle time = 30, 200 and 500 sec - Load magnitude = 12 kN *Second part:* - Superposition of low and high-frequency load - Load magnitude = 11 and 2.5 kN - Frequency = 0.005 and 10 Hz - Cycle times = 200 and 0.1 sec	- Load vs displacement - Number of load cycles to failure	Crack opening of 0.5 mm
	Reflective Cracking Device (*57*, *61*)	University of Portugal	Simulate the reflective cracking phenomenon	- Beam specimens - Asphalt concrete (1.57, 1.97, and 2.36 in.)	- Horizontal actuator to produce horizontal displacement - Vertical actuator to produce vertical displacement - Frequency = 10 Hz - Test temperature = 20°C	- Reflective cracking fatigue life vs vertical crack activity after the overlay - Reflective cracking fatigue life vs coefficient of stiffness reduction at the failure point - Reflective cracking fatigue life vs overlay thickness	50% of the initial stiffness value
	Shrinkage-bending test device (*58*)	Laboratory of Public Roads, France	Assess the efficiency of anti-cracking systems	- Beam specimens - Asphalt concrete overlay (2.36 in.) & rich sand base (0.79 in.)	- Horizontal crack opening speed = 0.024 in/hr - Cyclic vertical loading and frequency = 1 Hz -Test temperature = 5°C	- Crack initiation time and length - Crack propagation time and length -Time of specimen breaking	-

Table 1. Available Laboratory Test Setups to Simulate Reflective Cracking (continued).

Group	Testing Device	Developer/User	Purpose	Specimen Type, Material, and Geometry	Testing Condition	Data Acquisition/Parameter of interest	Failure Criteria
C	Accelerated simulative wheel tracking device (*55*)	University College of Dublin	Evaluate the resistance to reflective cracking of various asphalt concrete mixtures	- Slab specimens - Asphalt concrete - 5.5 in x 11 in x 2 in (Bottom-up cracking) or 5.5 x 10.2 x 2 in. (Top-down cracking)	- Moving wheel load - Frequency = 42 passes/min - Load magnitude: 520 N (Bottom-up cracking) or 412 N (Top-down cracking) - Test temperature = 25°C	- Top-down number of wheel pass to failure - Bottom-up number of wheel pass to failure	The instant when a crack progresses through the full depth of the specimen
	MEFISTO test device (*59*)	Regional Laboratory of Pont et Chausse, France	Simulate the reflective cracking phenomenon	- Beam specimens - Asphalt concrete (26 x 2 x 2 in.)	- Static horizontal load - Sinusoidal cyclic vertical load and frequency = 10 Hz	- Number of repetitions versus vertical force or dissipated energy - Number of repetitions versus crack length	-
	The UGR-FACT test device (*60*)	University of Granada, Spain	Evaluate the mechanical performance of bituminous mixes under fatigue cracking	- Beam specimens - Asphalt concrete (7.87 x 2.36 x 2.36 in.)	- Stress-controlled, vertical cyclic loading in versed sine - Load amplitude = 0.5 – 2 kN - Frequency = 5 Hz - Test temperature = 20°C	- N_f: Failure cycle - ω: Total dissipated energy	- When the macro-crack propagates throughout the entire specimen Or - 2,000,000 loading cycles

Based on the in-depth review of the literature and the comprehensive summary of various aspects of the seventeen available setups shown in Table 1, the research team selected the most appropriate setup from each group. From Group A, the TTI Overlay Tester (OT) setup was selected. From Group B, the Hamburg Wheel Tracking Tester (HWTT) setup was selected, while from Group C the Wheel Reflective Cracking (WRC) setup was selected. These three testing setups were ranked from 3 (least appropriate) to 1 (most appropriate).

The HWTT setup was ranked in third place because it most closely mimics the nature of traffic loading observed in the field among the setups in Group B. Also, HWTT can induce bending and shear stresses simultaneously, and accurately differentiate the reflective cracking resistance of various asphalt mixtures reinforced with stress-absorbing interlayers. Besides, it is a well-known device and commercially available. The WRC apparatus was ranked in second place since it is the only setup among Group C that simulates all the chief failure mechanisms causing reflective cracking in the field. The WRC setup can accurately evaluate the resistance to reflective cracking of various reinforced asphalt mixture specimens, and the consistency of the laboratory test results with field test results. Finally, TTI Overlay Tester (OT) setup was ranked in the first place because of its universal acceptance as an effective tool to study reflective cracking in the laboratory, rapid testing time, reasonable reproducibility of the test results, field validation, availability of standard test methods, and so on. More details about each setup are provided in the following sub-sections which include the background, major components, specimen preparation, and testing. Additionally, test specific comments are provided based on their advantages and limitations.

3.6.1. Test Setup 3: Hamburg Wheel Tracking Tester (HWTT)

Hamburg Wheel Tracking Tester (HWTT) originally developed by the city of Hamburg, Germany in the 1970s, is normally used to measure the combined effects of rutting and moisture damage in asphalt concrete. It is done by rolling a steel wheel across the surface of asphalt concrete cylindrical specimens or slab immersed in hot water (Figure 7). Besides, being used for this purpose, it was also used to study the traffic load associated reflective cracking.

Figure 7. Hamburg Wheel Tracking Tester (HWTT) device.

Researchers of the School of Transportation at Southeast University, China used an HWTT device to evaluate and rank the effectiveness of four stress-absorbing interlayers that slow down the occurrence of reflective cracking in asphalt overlay. The SBS-modified asphalt-sand concrete interlayer, asphalt-rubber sand concrete interlayer, fiberglass-polyester paving mat interlayer, and SAMI were used in that study for comparison. A control specimen, which does not contain any

stress-absorbing interlayer was tested using HWTT (Figure 8a), while the other specimens contain one of the four interlayers. The specimen structure excluding the control specimens consists of a base layer of cement concrete, a stress-absorbing interlayer, and a surface layer of asphalt cement on the top. At first, a 290 × 290 × 40 mm cement concrete slab was prepared, and a tack coat of emulsified asphalt binder was brushed. Then, an interlayer was placed above the base followed by laying off a loose mixture of short-term aged HMA. The asphalt concrete laid was then compacted using a vibratory roller compactor and a uniform thickness of 40 mm was produced. When the compacted HMA cools down, the concrete slab was turned upside down and a cut of 5 mm width was made that represents a crack in the base. Finally, the entire specimen was divided and cut into four equal 290 × 70 × 80 mm specimens (Figure 8b). The specimen was placed within the HWTT apparatus over a rubber pad that simulates the effect of the subgrade.

The HWTT consists of a steel wheel that moves back and forth and applies a repetitive dynamic wheel load over the specimen. The test was run at a loading rate of 52 passes/min with a load pressure of 0.7 MPa at a temperature of 15°C. The number of passes to failure is recorded manually which is used to quantify the ability of interlayers to retard reflective cracking. The endpoint of the test or the failure criteria is defined as the appearance of cracks at the bottom of the HMA surface layer. However, no crack appeared within the specimen even after a hundred thousand passes of the wheel. Therefore, to accelerate damage accumulation the setup of the specimen placement was modified. Two supports were added at both edges of the specimen to make it a simply-supported one-way slab over which a load area of 50 × 20 mm moves back and forth repetitively as illustrated in Figure 8c.

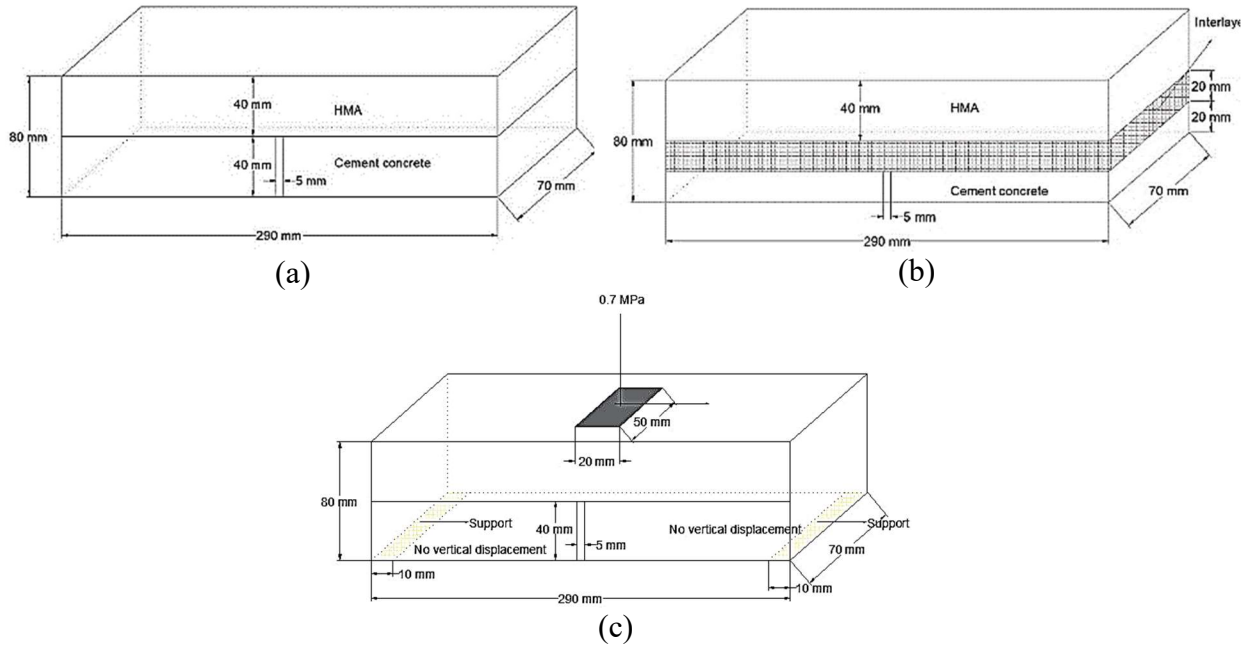

Figure 8. HWTT test specimens, (a) without an interlayer, (b) with interlayer, and (c) simply-supported one-way slab (*50*).

The quality of the test results using the HWTT setup was also assessed by Yu, Cao, and Yang (*62*). HWTT was used to differentiate the performances of four different interlayer materials including SBS-modified asphalt-sand concrete, asphalt-rubber sand concrete, fiberglass-polyester mat, and SAMI. The performances of the interlayers in retarding reflective cracking were compared based on the number of loading cycles to failure. It was found that an interlayer could prolong pavement

life significantly. The SAMI-Rubber interlayer demonstrated a higher number of load cycles to failure and thereby, exhibited better performance than other interlayers. The practicality of HWTT to mimic traffic load-associated reflective cracking was perceived as reasonable due to its better load-bearing capacity compared to other fatigue tests.

Rather than using only the number of cycles to failure, Yu, Lu, and Yang (*50*) investigated the HWTT test quality based on the ratio between the standard deviation from mean loading cycles to failure and mean loading cycles to failure (e.g., SD/mean). It was assumed that a smaller SD/mean ratio indicated more stability of the test results. The test results exhibited stability with a lower SD/mean ratio for asphalt-rubber sand concrete interlayer. It was found that anti-reflective cracking measures could withstand a higher number of loading cycles before failure and significantly prolong the fatigue life of specimens. The asphalt-rubber sand concrete interlayer was ranked first since it exhibited the lowest SD/mean ratio as compared to the other three stress-absorbing interlayers and therefore, exhibited the best reflective cracking performance (*50*). The adoption of HWTT was found to be reasonable due to the use of a dynamic wheel load.

According to these two studies, the HWTT device with the used setup can simulate the effect of traffic loading only, which is considered less critical to producing reflective cracking by various researchers. It produces flexural stresses and a lesser extent of shear stresses between the crack edges and cannot generate tensile stresses due to the cyclic temperature variation which is the most important mechanism causing reflective cracking in the field. The variability and sensitivity of the HWTT device results for reflective cracking resistance evaluation are unknown due to its limited use by other researchers. Besides, no field test has been conducted to validate its results. Comparisons between different anti-reflective cracking measures are based on one specimen of each configuration that is sawed into four equal pieces, and thus, the sample size is limited. The specimen dimensions are 290 mm × 70 mm × 40 mm in which may lead to a scale effect concern as compared with real pavement structure. The load condition is not consistent with practical situations. The failure is observed by eyes, which causes human subjectivity of the test results. No standard test method is available to evaluate reflective cracking resistance of asphalt mixtures or anti-reflective cracking systems using HWTT. Due to these limitations, the HWTT device is not a widely used setup to study the reflective cracking mechanism in the laboratory.

3.6.2. Test Setup 2: Wheel Reflective Cracking (WRC)

Wheel Reflective Cracking (WRC) is a test setup that can simultaneously produce tensile, flexural, and shear stresses involved in the mechanism of reflective cracking in asphalt overlays with a cracked base layer beneath it. This setup was originally adapted from the traditional wheel tracking test device and was further developed by the Road Laboratory of the Technical University of Madrid, Spain to examine geosynthetics in anti-reflection pavement cracking systems (*34*). The schematic of the WRC setup and its laboratory view is shown in Figure 9.

The WRC testing setup simulates all the failure mechanisms causing reflective cracking. The effect of a one-time temperature drop is simulated by conducting the test at 5°C ± 1°C. There are two chassis, a fixed plate, a sliding plate, and a micromotor attached to the sliding plate as shown in Figure 9a. The plates have a 10 mm gap between them to represent a crack. The wheel moves reciprocally over the chassis which enables half of the specimen to move while the other half remains stationary and simulates consequent opening-up of the cracks due to temperature variation. Application of flexural stress and shear stress is achieved by a rubber mat supported central rocker. Flexural stress is induced when the rocker bends vertically due to the passage of

the wheel over the chassis in the back-and-forth direction and produces maximum vertical deformation when the wheel is on the center of the WRC setup. On the other hand, shear stress is generated by the rocker when the relative vertical movement between the crack edges occurs. When the load is directly above the crack there is a deflection but no relative vertical movement. Asymmetrical loading with respect to the center of the crack produces downward movement in the loaded portion while upward movement in the unloaded portion.

The procedure of preparing specimens in this test is similar to the traditional wheel tracking test. Like a wheel tracking test, the specimens are cut from 305 × 305 × 60 mm specimens. The first stage of specimen preparation procedure includes placement of a 10 mm asphalt concrete base in the 305 × 305 mm mold (Figure 10a), application of asphalt tack coat over the base, and subsequent placement of geotextile (Figure 10b). After that laying and compacting the asphalt overlay is laid and compacted in a way that the total height of the specimen becomes 60 mm. Lastly, specimens are saw cut resulting in a shape of a prism (305 × 75 × 60 mm), where every specimen has an equal number of longitudinal geotextile filaments (Figure 10c). The control specimens are prepared without the use of geotextile. The prepared specimen is bonded with the fixed and sliding plate using epoxy which typically takes 12 hours to harden.

The WRC, with the specimen placed in it, is mounted on the wheel tracking device and the entire system is conditioned for 12 hours in a chilled chamber at 5°C ± 1°C. The test is then started by the application of the load with the moving wheel and the horizontal tractive displacement. The wheel moves back and forth at a rate of 43 passes/min, and the horizontal tractive displacement rate is 600 µm/h. Over the testing period, the number of load cycles, the accumulated horizontal strain, the vertical deflection, and the relative vertical movement between the crack edges is continuously measured. The failure criteria defined is the maximum relative vertical movement of 0.2 mm between the crack edges. The parameters of interest in this test are the time in minutes to reach the failure criterion, referred to as reflective cracking strength, or the number of wheel passes times the rate of loading. The longer the specimen takes to reach the failure criterion, the higher the strength it exhibits against reflective cracking and therefore, has better performance.

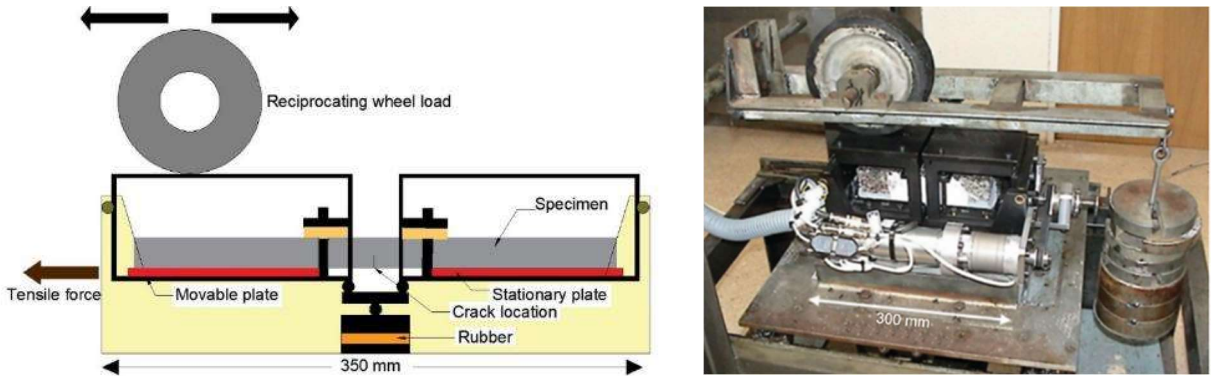

(a) (b)

Figure 9. Wheel Reflective Cracking (WRC) apparatus, (a) schematic (b) laboratory view (*34*).

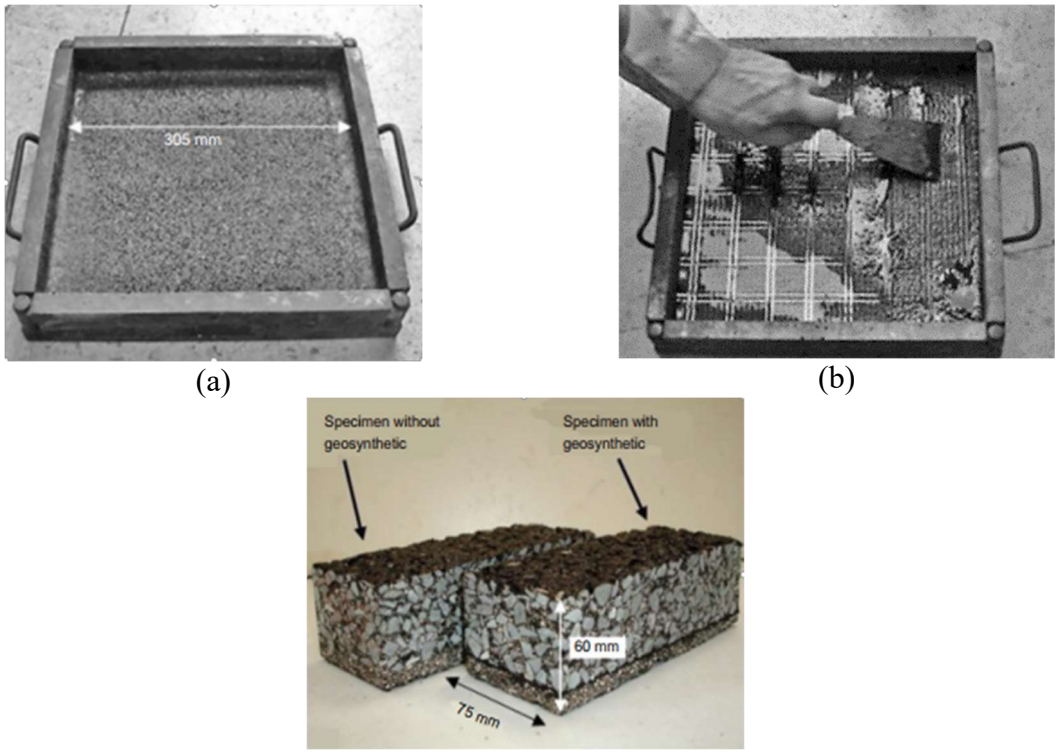

Figure 10. Order of specimen preparation, (a) laying off 10 mm asphalt base, (b) tack coat application followed by placement of geotextile, and (c) final specimen after compaction and sawing (*34*).

Prieto, Gallego, and Pérez (*34*) used the WRC setup to compare anti-reflective cracking systems in resisting reflective cracking. Three asphalt overlays were tested with three different geosynthetics having different resistance to reflective cracking and quantified their relative crack reflection strength. It was concluded that the WRC setup could quantitatively compare specimens with different resistance to crack reflection, and the specimens fabricated with the best martial exhibit best performance when tested in the WRC.

In another study, Gallego and Prieto (*33*) conducted a sensitivity and coherence study of the WRC test. Three different asphalt overlays were tested and evaluated their relative strength. One with geosynthetic and two without any geosynthetic assumed to have different resistance to reflective cracking. It was observed that the relative strength of each overlay aligned with the expected results obtained from the current Spanish experience in full-scale test sections. The overlay with geosynthetic exhibited approximately 1.5 times better resistance to reflective cracking in terms of average time to reach failure criteria as compared to the overlays with no geosynthetic.

According to these two studies, the WRC setup can simulate all the major mechanisms leading to reflective cracking. It was proved to be a reasonable tool that allows the researchers to quantitively differentiate between different asphalt overlays and anti-reflective geosynthetic products. It offers modification in testing temperature, maximum deflection, and cracks opening velocity to better match the local conditions in the field. The device can produce debonding and crack formation observed in failed overlay pavements in the field. However, it is a short-term test and not truly a performance-based test because it cannot represent all quantitative effects that cause long-term cracking during the pavement service life. Further study is warranted to correlate medium and long-term overlay performance to short-term WRC test results. The simulated base here is steel

plates which may not truly represent base courses in the field. The repeatability of the test result is questionable because the research effort regarding its variability is limited. Test results obtained from the WRC test setup to some extent are consistent with the results obtained in the field, but the field experimental studies are still limited to justify its use by other researchers. Moreover, it has a very long testing period. Around 12 hours of specimen preparation, 12 hours of specimen conditioning, and 4 to 10 hours of testing which can be a major drawback in adopting this setup for further research efforts. It has no standard test method to guide the researchers through specimen preparation, testing, data collection, and analysis.

3.6.3. Test Setup 1: Texas Transportation Institute (TTI) Overlay Tester (OT)

One of the major mechanisms that lead to the reflective cracking phenomenon is the daily and seasonal temperature change which produces contraction and expansion of cracks or joints in the base layer under the overlay (*11*). Researchers of Texas Transportation Institute (TTI) at Texas A&M University developed an Overlay Tester (OT) in the 1970s to simulate this mechanism in the laboratory (*22*). This apparatus can also be used to measure the fatigue cracking susceptibility of asphalt mixtures (*63*). TTI developed two OT testers, i.e., small and large OT. The small OT tests specimens with smaller dimensions (15 × 3 in. × variable height) while the large OT uses specimens of relatively larger dimensions (20 × 6 in. × variable height). Both OT setups were successfully used by various researchers to examine the effectiveness of several anti-reflective cracking products to slow down the occurrence of reflective cracking (*64–70*). However, these two OT setups require the use of long beam samples which is difficult to produce in the laboratory and also to obtain from the field (*22*). Therefore, TTI upgraded the small OT setup which uses smaller 6 in. diameter specimens to be mounted on two aluminum or steel base plates for testing (Figure 11). These 6 in. diameter specimens can easily be prepared in the laboratory using a Superpave Gyratory Compactor (SGC) sample or can be cored from the field.

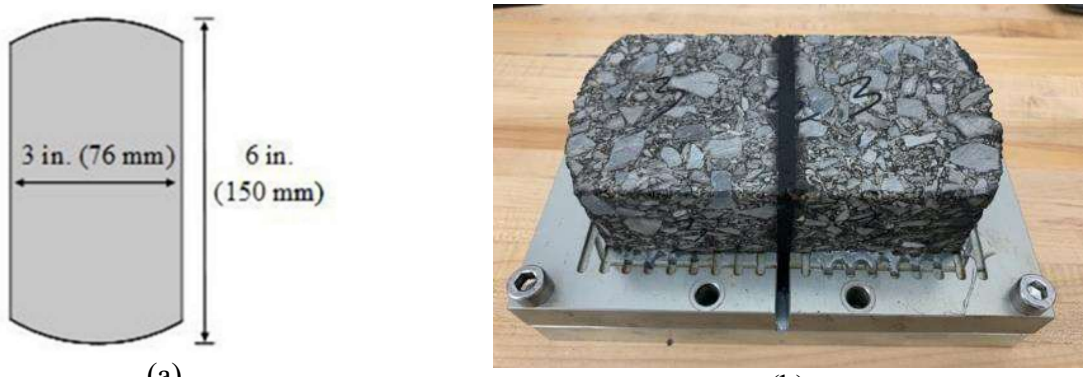

(a) (b)

Figure 11. Upgraded TTI OT specimen, (a) with a smaller size (6 in. diameter), and (b) mounted on the base plates before testing.

The OT base plates are placed 2 mm apart to represent a crack or joint in the base. The setup tests both laboratory-molded and field cores per Tex-248-F (*63*). The standard dimension of the prepared specimen is 6 × 3 × 1.5 ± 0.02 in. which is glued over the base plates using epoxy. The sequence of specimen preparation is illustrated in Figure 12.

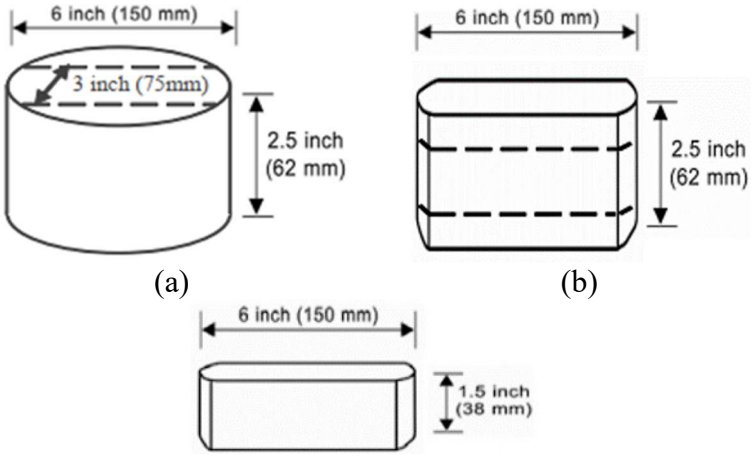

Figure 12. Order of specimen preparation, (a) laboratory molded or field cored specimen, (b) sawed specimen, and (c) final specimen (*63*).

Testing is typically conducted at room temperature (i.e., 25°C) where specimens are tested under displacement-controlled one-phase loading (Figure 13a). It has a standard maximum opening displacement of 0.63 mm (0.025 in.) which equal to the displacement occurred in rigid pavements having a 15 ft joint under 14°C change in temperature (*22*). The typical loading rate, 10 sec/cycle, does not imitate the loading rate in the field; rather, it was proposed for accelerated crack propagation (*71*). Throughout the testing period, the time, displacement, load, and the number of loading cycles to failure are measured and recorded. Figure 13b illustrates the first hysteresis loop for the first loading cycle during testing, and Figure 13c shows typical test results up to ten loading cycles. The failure criteria defined in Tex-248-F is a 93% reduction of the maximum load with the load measured from the first cycle. The typical parameters of interest in this test are Critical Fracture Energy (G_c), Crack Progression Rate (CPR) (*63*), and the Number of Cycles to Failure (N_{OT}) (*72*).

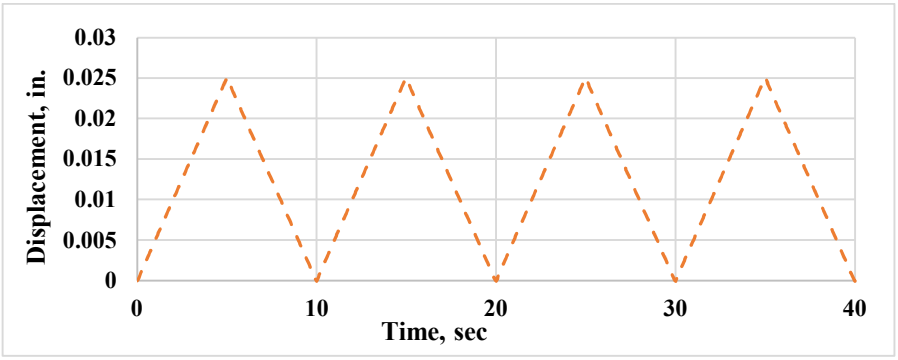

(a)

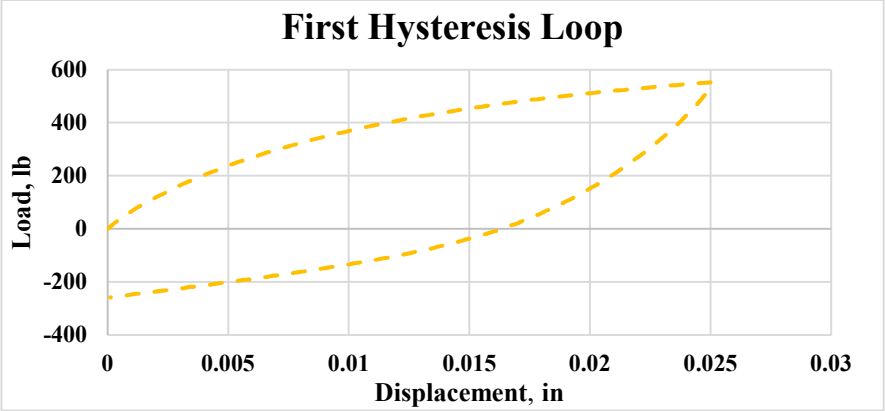

(b)

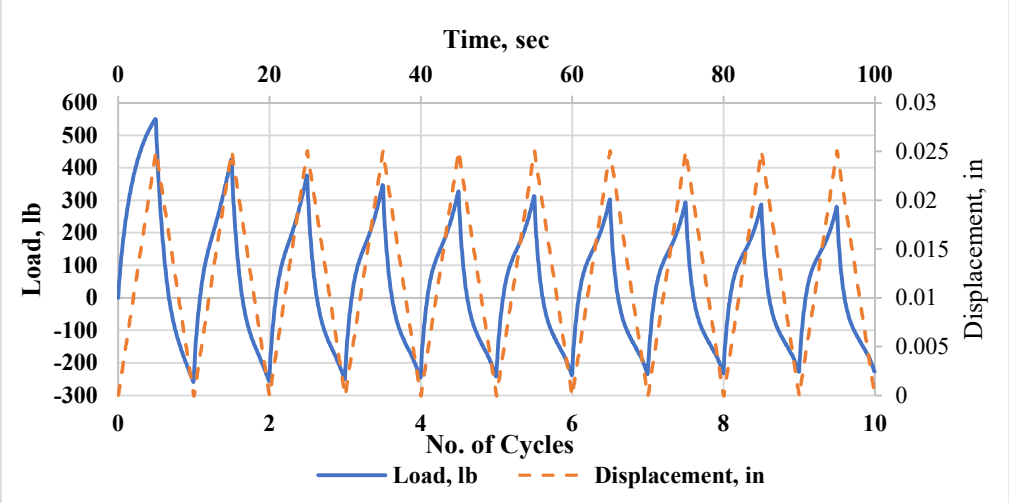

(c)

Figure 13. Loading and test result, (a) one-phase loading, (b) Hysteresis loop, and (c) typical test results.

Walubita et al. (*73*) used OT setup to determine the cracking-resistance and fracture performance of eight different geosynthetic interlayer materials. Specimens were prepared by placing geosynthetic interlayers at a depth of 1.5 in. (37.5 mm) from the top, and notching specimens to 0.74 in. (18.75 mm) height from the bottom. These specimens along with a control specimen with no geosynthetic interlayer were tested in OT setup using a monotonic tensile loading mode of 0.132 in./min (3.375 mm/min) at 0°C. Results showed that the incorporation of geosynthetic interlayers significantly enhanced the cracking and fracture performance (i.e., more than 20%) as compared to the control specimen. Additionally, the OT results in a monotonic tensile loading mode demonstrated good repeatability with a reasonably acceptable level of statistical variability in the test data.

Li et al. (*74*) used OT setup to compare and rank twenty-nine different asphalt mixtures (i.e., ranging from fine-graded mixtures to coarse-graded mixtures and Superpave mixtures) typically used in Texas based on their resistance to reflective cracking. Moreover, the suitability and variability of the test protocol in examining the cracking resistance of open- and coarse-graded HMA mixes were evaluated. Results showed that the fine- and dense-graded mixtures expectedly withstood a higher number of load cycles to failure with lower variability in terms of the coefficient

of variance. It implied that OT could effectively differentiate and rank mixtures with various resistance to reflective cracking.

Ozer et al. (*75*) assessed the impact of Recycled Asphalt Shingle (RAS) on mechanical properties of various asphalt mixtures at high asphalt binder replacement (ABR) through a series of mixture performance tests. In addition to the push-pull test, the fatigue behavior of the mixtures was evaluated using OT at intermediate temperature. Results of OT tests showed that the highest resistance to fatigue cracking was obtained for mixtures with softer asphalt binder (i.e., PG46-34) combined with the lowest percentage of RAS (i.e., 2.5%). Besides, the loading cycles to failure decreased with an increase in RAS content (i.e., from 2.5% to 5% and 7.5%) combined with the use of stiffer asphalt binder (i.e., PG58-28). The load applied initially was higher because the incorporation of higher percentages of RAS increased the stiffness of the mixtures.

Walubita et al. (*76*, *77*) attempted to optimize repeatability and lower the variability of Tex-248-F by evaluating the sensitivity of its critical steps. It was found that sample number, age, and drying method, glue quantity, air voids content, and temperature changes are some of the factors that can produce variability in the test results.

Chowdhury et al. (*78*) installed several end-to-end geosynthetic test pavements at three different locations in Texas, resulting in a total of 26 test sections, and monitored the performance of various geosynthetic products. Field specimens were collected and tested using small and large OT and found that the effectiveness of geosynthetic products in controlling reflective crack is questionable. Moreover, geosynthetics perform slightly better in early service life than that of control sections but become ineffective when the overlay becomes older.

Zhou and Scullion (*22*) evaluated the performance of six typically used asphalt overlay mixtures in Texas against reflective cracking. The results indicated that the aggregate type and absorption had a significant influence on the reflective cracking resistance. Moreover, the reflective cracking life was found to be reciprocally related to the high-temperature performance grade while proportionally related to asphalt content. The finer mixtures with higher asphalt contents exhibited better performance against reflective cracking.

Cleveland, Button, and Lytton (*79*) used the upgraded OT setup with a modification in specimen configuration to evaluate the relative effectiveness of eight commercially available geosynthetic materials in retarding reflective cracking in HMA overlays. Instead of using a monolithic asphalt concrete specimen, a geosynthetic material sandwiched between two layers of asphalt mixture at a height of 1 in. (25.4 mm) from specimen bottom was introduced. They concluded that while the effect of geosynthetics in mitigating reflective cracking in HMA overlays can range from highly successful to disastrous failures, generally the geosynthetics showed a higher number of cycles to failure in the OT.

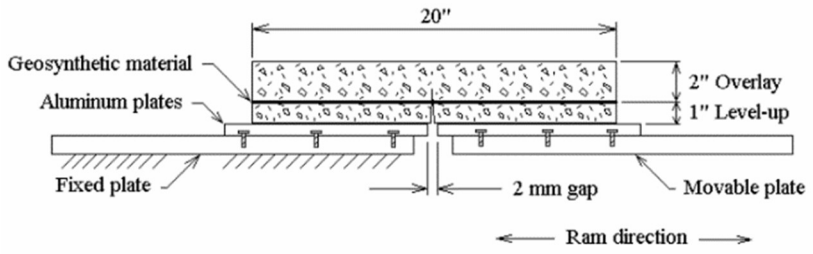

Figure 14. The modified specimen used in the OT setup (*79*).

Zhou and Scullion (*72*) investigated the variability and sensitivity of the upgraded OT. It was reported that the average number of cycles to failure was 140 with a standard deviation and coefficient of variation of 11.7% and 8.3%, respectively Typically, the coefficient of variation of HMA mixtures lies within 10-25% which confirmed that the OT is repeatable. The results of the sensitivity study showed that the device is sensitive to test temperature, opening displacement, air voids, asphalt performance grade, and asphalt content.

In the same study by Zhou and Scullion (*72*), the OT results were validated by comparing the reflective cracking life of field cores with known reflective cracking performance and beam fatigue test results. Field cores were obtained from different roads in Dallas, Abilene, Houston, and Waco districts in Texas to validate mixture performance against reflective cracking. Cores were also collected from MnRoads that were critical to low-temperature cracking. These cores were tested in OT and were confirmed that good mixtures that performed well with little to no reflective or low-temperature cracks in their service life also withstood a higher number of load cycles to failure (i.e., higher reflective cracking life when tested in OT and vice versa). OT results provided the same ranking as that of from beam fatigue test results confirming that this device can also be used to investigate the performance of asphalt mixtures against fatigue cracking.

In conclusion, the upgraded OT only simulates the effect of cyclic temperature variation, which is the prime factor causing reflective cracking. It is unable to mimic a one-time sudden temperature drop which increases the rigidity of asphalt mixtures and accelerates reflective cracking. Moreover, the upgraded OT setup cannot simulate the traffic load associated with reflective cracking and cannot produce flexural or shear stresses. Specimens are attached to the steel or aluminum plates which might not be a true representative of base course in the field. Despite these limitations, the upgraded OT setup is extensively used by the researchers because it has been proven to be a cost-effective and performance-related test that can be used to compare the resistance of different asphalt mixtures and anti-reflective cracking systems to reflective cracking. It is an accelerated damage accumulation test with a shorter testing period. Also, it has good repeatability of test results as well as a very good correlation with field performance, which is validated by various researchers in this field. This upgraded setup is fully computer-controlled, which eliminates the subjectivity of the operator. Furthermore, it has built-in programs to produce one-phase loading and two-phase loading representing different field loading conditions. It allows modification of test temperature, horizontal opening displacement, and cycle time to better match the local conditions in the field. Additionally, unlike other reflective cracking testing devices, it has a standard test procedure, Tex-248-F, to guide the researchers through specimen preparation, testing, data collection, and analysis. All these advantageous features surpass the limitations and make the upgraded OT the most practical and useful tool to study the resistance of asphalt mixtures against reflective cracking.

3.7. The effectiveness of the upgraded OT setup

Zhou et al. (*80*) suggested that various aspects of equipment should be critically examined to identify it as a reliable cracking (i.e., fatigue, reflective, thermal, or top-down) test setup. Various attributes were used to rank the candidate cracking tests, which included sensitivity to mixture design parameters, simplicity of the test in terms of specimen preparation, testing time, data analysis and interpretation, test variability, equipment availability and cost, and availability of test standard. In this section of the study, the effectiveness of the upgraded OT setup as a reliable

reflective cracking test has been evaluated based on the aspects suggested by Zhou et al. (*80*) and discussed in more detail in the following subsections.

3.7.1. The sensitivity of OT to asphalt mixture design parameters

The sensitivity of the OT test setup to asphalt mixture design parameters, such as mixture type, binder type, binder content, air voids, RAP/RAS content, and aggregates, has been thoroughly evaluated by researchers. Zhou and Scullion (*72*) noted that the OT results are sensitive to the key components of the HMA mixtures such as the grade of the asphalt binder, asphalt binder content, air voids, and aggregate properties. Zhou and Scullion (*22*) further evaluated the performance of six typically used asphalt overlay mixtures in Texas against reflective cracking using OT. It was observed that OT results were sensitive to asphalt binder content, the aggregate type, aggregate absorption, and the high-temperature performance grade.

Mogawer et al. (*81*) used the upgraded OT setup to assess the reflective cracking susceptibility of various thin-lift asphalt mixtures with high percentages of recycled materials with or without WMA technology. It was found that OT was sensitive to the mixture type. Asphalt mixtures without any WMA technology exhibited significantly lower reflective cracking resistance as compared to the control mixture. Although the incorporation of the WMA technology improved the reflective cracking resistance of the mixtures containing RAP, RAS, or both, these mixtures demonstrated different performance as the control mixture with the WMA technology. Porras et al. (*82*) used the upgraded OT setup to evaluate the reflective cracking performance of three field-produced WMA mixtures containing three different WMA technologies and compared it with a control HMA mixture. The reflective cracking life was found to be reciprocally related to mixture stiffness. The WMA mixture with Evotherm® (chemical additive) having the lowest stiffness showed higher resistance to reflective cracking than the WMA mixture with Sasobit® (organic additive) with the highest stiffness. Ozer et al. (*75*) used OT to examine the reflective cracking potential of various asphalt mixtures containing high RAS percentages. The value of the OT number of cycles to failure (N_{OT}) was found to be sensitive to the binder and mixture stiffness.

Li et al. (*74*) compared the reflective cracking potential of twenty-nine asphalt mixtures from six mixture types, including fine-graded, dense-graded, gap-graded, open-graded, and Superpave mix, and ranked them based on their resistance to reflective cracking. The OT results were found to be sensitive to the type of mixtures, asphalt binder content, air voids, and binder film thickness. Al-Qadi et al. (*83*) mentioned that N_{OT} is sensitive to binder performance grade, binder type, and its content, and OT was able to differentiate between asphalt mixtures qualitatively. Zhou et al. (*83*) produced five dense-graded mixtures to evaluate the sensitivity of OT to asphalt mixture design parameters as compared to a virgin mixture. Four mixtures were prepared by using binders having different stiffnesses combined with varying binder content and with the use of 20% RAP or 5% RAS. It was found that OT was sensitive to binder content. The addition of 0.5% more binder to the virgin mixture expectedly exhibited a significant enhancement in N_{OT}. The OT was found sensitive to the use of RAP and RAS, where the addition of either 20% RAP or 5% RAS decreased the reflective cracking resistance as compared to the control mixture without recycled materials. Moreover, the OT test setup was sensitive to binder stiffness as the use of a softer binder improved the reflective cracking resistance.

Most recently, Pan et al. (*84*) employed the upgraded OT setup to investigate the reflective cracking resistance of various unaged, aged, and rejuvenated asphalt mixtures and found that the peak load applied to the specimens were highly sensitive to the modulus of the mixtures. Long-

term aged mixtures had higher modulus, which resulted in a higher reduction in peak loads with loading cycles as compared to unaged and rejuvenated asphalt mixtures.

Overall, based on literature, it is understandable that the upgraded OT setup can differentiate between performances of asphalt mixtures due to the change in the characteristics and volumetric properties of asphalt mixtures, and is highly sensitive to the mixture design parameters. This high sensitivity is because of OT being a repeated loading test since repeated loading tests are typically more sensitive to test variables than that monotonic tests (*77*).

3.7.2. Variability and repeatability of OT testing data

Considerable efforts have been made by the researchers to understand the sources of high variability in OT results. Walubita et al. (*77*) noted that one of the key problems contributing to the reported high variability in the OT test results was primarily related to nonadherence to the OT test procedures. Walubita et al. (*76*) later attempted to optimize the repeatability and lower the variability of Tex-248-F (version 2007-2008) by evaluating the sensitivity of its critical steps. To minimize variability in N_{OT}, it was recommended that four or five replicate specimens should be tested instead of testing three specimens from which a set of best three replicates should be chosen based on the lowest coefficient of variation (COV). Oven drying of the OT specimens at a maximum temperature of 40 ± 3°C (104 ± 5°F) for a minimum of 12 hours to constant weight was proposed because the previous drying temperature, 60 ± 3°C (140 ± 5°F) deemed to be too high for some mixes. It was recommended by the same study that the allowable sitting time of the specimens after molding should be not more than 5 hours before testing. The glue quantity of 16.0 ± 0.5 g (0.035 lb.) per sample, as well as consistent gluing procedure, were specified. Moreover, the maximum allowable number of cycles for an OT specimen that does not reach a 93% load drop was reduced from 1,200 cycles to 1,000 cycles in the proposed modification. All these recommendations were included in 2014 version of Tex-248-F and subsequent versions to improve the consistency of the test results.

Garcia et al. (*85*) performed a thorough investigation of the key steps involved in OT protocol using various synthetic and HMA specimens to identify the possible sources of variability in the operational parameters. The reported source of variability included plate spacing, specimen sitting time, amount of glue, glue curing time, and the amount of torque required to attach the base plates to the machine. Garcia et al. (*86*) later proposed a modified gluing method that could provide an easy way of achieving both uniformity of the glued area and a gap-free of excess epoxy, which has been added in the 2017 version of Tex-248-F.

Garcia et al. (*87*) again proposed a novel methodology to assess the cracking resistance of the asphalt mixtures using OT and suggested two parameters, i.e., critical fracture energy (CFE) and crack progression rate (CPR) as cracking indicators to minimize variability in N_{OT}. In a recent study, Garcia et al. (*88*) implemented this methodology and used a large database of OT results from ten different asphalt mixtures to set the preliminary acceptance limits for the CFE and CPR parameters. The consistency and repeatability of CFE and CPR were better than the acceptable level of repeatability (i.e., COV< 20%) as compared to N_{OT}. As a result, these two new performance indices have been added in the most recent version of Tex-248-F in addition to N_{OT}. Most recently, Garcia et al. (*89*) compared the test results obtained from three commercially available OT devices and found that the reproducibility of the test results was reasonable. The variability of the results from each device was improved when CFE and CPR were used to analyze

the results instead of using N_{OT}. Overall, it was concluded that the OT results from various devices are repeatable and reproducible.

Even though those studies helped to improve the OT procedure, the variability of the results is still a concern to determine the reflective cracking resistance of various asphalt mixtures reliably.

3.7.3. The OT test simplicity, data analysis, and interpretation

Zhou et al. (*90*) noted that technician training requirements, time for preparing and testing specimens, and difficulty in data interpretation are some of the factors when considering the simplicity or complexity of a cracking test.

The preparation procedure of OT specimens is relatively simple as compared to other cracking tests (i.e., Beam Fatigue, Disk-shaped Compact Tension, or Semi-Circular Bending) since only four cuts are made to prepare the final specimen from an SGC compacted cylindrical specimen. Moderate specimen preparation time, along with an acceptable level of technician training, is required for OT specimen preparation and gluing specimens to the base plates. The specimen mounting is simple, and except for an external Linear Variable Differential Transformer (LVDT), no instrumentation is needed for testing. The test is rapid, which typically takes 30 minutes to 3 hours to complete. The data analysis is easy with built-in data analysis software. The interpretation of data is quick and simple since OT uses only index type parameters such as N_{OT}, CFE, and CPR as pass/fail criteria. Overall, OT is acceptably a simple and rapid test to measure reflective cracking performance in the laboratory.

3.7.4. The OT setup availability, cost, and standard test method

The OT is commercially available equipment which is designed and fully dedicated to simulating reflective cracking in the laboratory. The approximate cost of purchasing OT is $46,000, which is relatively lower than other commercially available cracking test devices. If AMPT is available in the laboratory, the OT fixture is around $5,000 and easy to setup.

Additionally, OT has a standard test procedure, Tex-248-F, to guide the researchers through specimen preparation, testing, data collection, and analysis. Because of these reasons, OT has either been adopted or being considered to be adopted as a reliable reflective cracking test by different state agencies, such as Texas, New Jersey, Montana, Nevada, Florida, and Ohio (*90*).

3.7.5. The OT lab-to-field correlation

The OT lab-to-field correlation has been investigated by researchers time-to-time. Zhou et al. (*71*) validated the OT results with the Federal Highway Administration (FHWA) Accelerated Loading Facility (ALF) fatigue test results on six lanes where loading was applied by a super single tire on the experimental pavement lanes. The ranking of fatigue cracking performance for asphalt mixtures by the FHWA-ALF test was similar to the ranking by the OT.

Zhou et al. (*90*) constructed eight test sections at the UT-Arlington Accelerated Pavement Testing facility to assess the cracking resistance of asphalt mixtures in terms of fatigue and reflective cracking. Cores were taken before APT testing, and OT specimens were prepared and tested. The OT showed the same rankings as APT test results in terms of both fatigue and reflection cracking.

Most recently, Cao et al. (*91*) collected asphalt mixtures containing RAP, RAS, and WMA technologies during the construction of FHWA-ALF lanes in McLean, Virginia, and correlated

between OT results and ALF fatigue performance. In addition to N_{OT} and CFE, a new parameter referred to as the Corrected Crack Progression rate (CCPR) was proposed considering the viscoelastic nature of asphalt mixtures. Although N_{OT} exhibited a very good correlation with the ALF performance despite high variability, the CFE parameter resulted in the poorest correlation with the ALF performance. However, the newly proposed CCPR parameter provided the best correlation with ALF fatigue performance.

In summary, it is clear based on the findings from previous experimental test results that OT results are valid for both fatigue and reflective cracking and has a strong lab-to-field correlation.

3.8. Potential modifications to improve the OT setup

Although the current OT setup has been extensively used by researchers to study thermally induced reflective cracking and measure the reflective cracking resistance of asphalt mixtures, it might not fully mimic reflective cracking in the field. The OT only measures the reflective cracking performance of asphalt mixtures, where the specimens are directly glued to steel base plates. The function of the base plates – and the glue – is to serve as a base course, which might not be a true representative of a cracked base course – and the prime coat – in the field. However, the reflective cracking mechanism suggests that the formation of reflective cracking is related to the presence of cracks on a real surface (i.e., base course) over which HMA overlays are placed. Cracks on the base course propagate upward due to temperature variation, and therefore, the absence of any representative base course makes the effectiveness of the current OT setup in simulating field reflective cracking questionable.

To address the above-mentioned issues and enhance the overall usefulness of the current OT setup, some potential modifications have been proposed here in this study. A 1.5 in. (38 mm) pre-notched (0.6 in. (15 mm) notch depth) CTB layer will be incorporated beneath the 1.5 in. layer of the HMA overlay. The 1.5 in. pre-notched CTB layer has been selected to match the thickness of the HMA layer. Additionally, the selected notch depth of 0.6 in. (15 mm) is similar to other fracture tests (e.g., Semi-circular bending test as per Illinois Test Procedure) and to initiate the crack at a predetermined location of the specimen. In this study, the CTB layer will be attached with a prime coat below the asphalt layer, and the composite specimen is to be glued to the steel base plates using epoxy. After conditioning at the target temperature for 1 hour, the specimen will be tested in OT using the same failure criterion, as suggested by the latest version of Tex-248-F. The schematic of the proposed modified OT setup is presented in Figure 15.

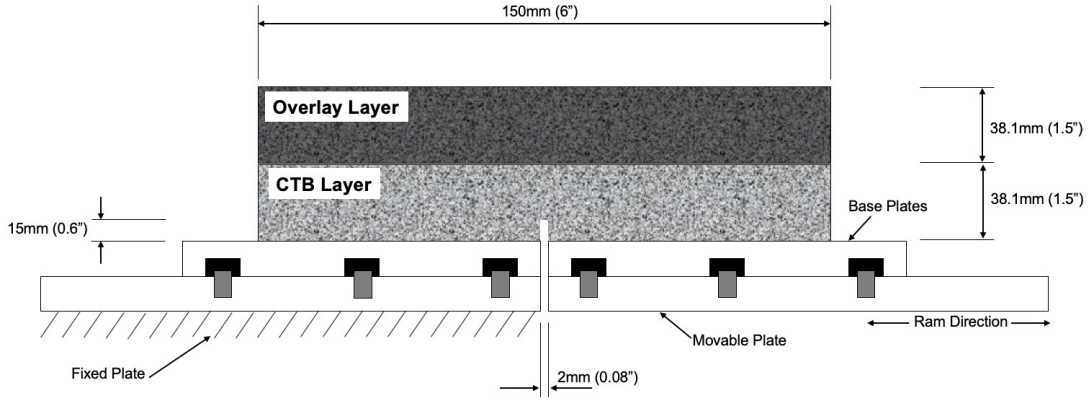

Figure 15. Potential modifications of OT setup.

3.9. Summary of findings

This chapter provides a comprehensive literature review of the available laboratory tests that attempted to study the reflective cracking phenomenon. A total of seventeen testing setups used worldwide to simulate reflective cracking were evaluated in this review with respect to their application, variability, sensitivity, and field validation. The best three testing devices among the available ones were chosen and thoroughly evaluated. Additionally, the effectiveness of the current OT setup was evaluated based on various aspects found in the literature such as the sensitivity of OT to asphalt mixture design parameters, variability and repeatability of the OT test data, test simplicity, equipment availability, and correlation to field performance. From this literature review the following insights have been obtained:

- Most of the available test setups that attempt to simulate reflective cracking evaluate the effectiveness of different HMA overlays or anti-reflective cracking products and their resistance to reflective cracking.
- No experimental study has been carried out only to evaluate the resistance of asphalt mixtures to reflective cracking where HMA overlay is constructed above a layer with cracks in its surface.
- The OT test is a rapid, performance-based tool that can differentiate between the performance of asphalt mixtures having various ranges of resistance to reflective cracking.
- The OT testing result is highly sensitive to the changes in the mixture characteristics and volumetric properties such as binder performance grade, binder content, air voids, aggregate characteristics, and mixture type.
- Although the OT requires reasonable specimen preparation time and a considerable level of training of the OT operator, it is a fairly simple test to adopt. The test is rapid, and the data analysis and interpretation are quite easy to perform.
- The cost of equipment is significantly lower as compared to other cracking test devices. An updated standard test procedure (i.e., Tex-248-F, version 2019) is also available to aid the operator from specimen preparation for testing.
- The major challenge with the current OT setup is the high variability of the test data. Researchers have identified various sources that can result in inconsistency and variability of the test results. Previous studies have provided recommendations time-to-time to minimize the high variability and improve the repeatability of the test result, which resulted in frequent updates in Tex-248-F. Therefore, complete adherence to the updated Tex-248-F from specimen preparation to testing can effectively improve the repeatability of the OT test data.
- Overall, the OT is the most suitable equipment to study the performance of asphalt mixtures against thermally induced reflective cracking in the laboratory.

4. METHODOLOGY

4.1. Preparation of CTB and CSB mixtures

4.1.1. Materials and properties

The constituent materials of the soil-cement base include soil, cement, and water. The recommended properties of the constituent materials to be used for the production of soil-cement base courses have been established in the 2016 Louisiana Standard Specifications for Roads and Bridges (*92*). Soil properties have been specified in Section 302 Class II Base Course and sub-section 302.02.1. Cement recommended properties have been provided in sub-sections 303.02, 1001.01, 1001.02, and 1001.05. Moreover, the properties of water are mentioned in sub-sections 303.02 and 1018.01 in Louisiana Specification. The design compressive strength criteria for soil materials treated and stabilized with cement are 150 psi (1 MPa) and 300 psi (2 MPa), respectively as determined in accordance with DOTD TR 432 (Method B or C).

According to Section 302, Class II Base Course and sub-section 302.02.1 of Louisiana Specification, soils for the soil-cement base course should consist of materials that can stabilize with cement in accordance with DOTD TR 432. The recommended soil types include A-1-a, A-1-b, A-2-4, A-2-6, A-4, and A-6 in accordance with DOTD TR 423 having a Liquid Limit (LL) of maximum 35%, a Plasticity Index (PI) of maximum 15%, and organic content of maximum 2%. The sand and silt content should be limited to a maximum of 79% and 60%, respectively in accordance with DOTD TR 407. Moreover, if an A-4 or A-6 soil is to be used for cement treatment, it should meet the durability requirements of DOTD TR 432.

The recommended cement types are Type I or II Portland cement, Type IP blended hydraulic cement, and Type IS ground granulated blast furnace slag cement according to sub-section 303.02. Portland cement should comply with AASHTO M 85 and Alkali content calculated as sodium oxide equivalent shall not exceed 0.60% by weight according to sub-section 1001.01. Portland blast-furnace slag cement shall contain a maximum of 50% ground granulated blast-furnace slag by weight. Pre-blending of Types I or II Portland cement, and ground granulated blast-furnace slag will be allowed if blended at an approved blending facility and mixed thoroughly to ensure a uniform blend. The ground granulated blast-furnace slag used in pre-blending shall be from the Approved Materials List and meet the requirements of subsection 1001.05 of Louisiana Specifications. Furnish soils or soil-aggregate combinations for cement stabilization or treatment should comply with the requirements of 302.02.1. If an A-4 or A-6 Soil Group material is used for cement treatment, it shall meet the durability requirements of DOTD TR 432.

Water shall be suitable for human consumption or shall comply with the properties shown in Table 2 when tested in accordance with AASHTO T 26 as mentioned in sub-section 1018.01.

Table 2. Water properties in accordance with AASHTO T 26.

Properties	Percent by Weight (Max.)
Alkali	0.1
Solids (Organic)	0.1
Solids (Inorganic)	0.4
Salt (NaCl)	0.5
Sugar, Oil, or Acid	0

Based on the recommendations provided by sub-section 302.02 of the Louisiana Specification, A-6 soil (with Group Index = 9), Clay Loam/Lean Clay, was collected for this research project in sandbags from a project site located in Ethal, LA as suggested by the East Baton Rouge District Engineer. Properties such as Atterberg limits (i.e., LL, PL, and PI) were first determined because PL is typically close to the optimum moisture content. Therefore, PL gives a good starting point to determine the moisture-density relationship for the mixture design of the soil-cement base. Moreover, organic content, sand content, and silt content were determined and compared with recommended values from Louisiana Specification. It was confirmed that the soil collected for the research project meets all the requirements set by Louisiana Specification. The recommended soil properties, the corresponding test standards, requirements, and measured properties of the collected soil are presented in Table 3.

Table 3. The recommended soil properties, corresponding test standards, requirements, and measured properties of the collected soil.

Properties	Standards	Requirements	Measured values
Liquid Limit (LL)	DOTD TR 428	≤35%	31%
Plasticity Index (PI)	DOTD TR 428	≤15%	17%
Organic content	DOTD TR 413	≤2%	2%
Sand	DOTD TR 407	≤79%	29%
Silt	DOTD TR 407	≤60%	46%

Type I Portland cement from Holcim complying with AASHTO M 85 and having a unit mass of 1500 kg/m^3 was selected for this project to produce both cement-stabilized base (CSB) and cement-treated base (CTB) materials. Alkali content calculated as sodium oxide equivalent was also below 0.60% by weight.

4.1.2. CTB/CSB mixture design

The mixture design of the soil-cement base materials involves two test procedures in accordance with Louisiana Specification. The first procedure is DOTD TR 418M Method A, B, C, or F (based on the % aggregate by dry mass retained on a 4.75 mm (No. 4) sieve of the soil) which is the Method of Test for Moisture Density Relationships. This procedure determines the relationship between the moisture content of the soil material and the resulting maximum dry density when it is compacted in the laboratory. The second procedure is DOTD TR432 Method A, B, or C (based on the % aggregate by dry mass retained on a 4.75 mm (No. 4) sieve of the soil) which is the Method of Test for Determining the Minimum Cement Content for incorporation into soils, soil-aggregate, or aggregate mixtures for stabilization or treatment. This method determines the minimum percentage of cement to be incorporated into soils or soil-aggregate mixtures that have met all other specification requirements for the materials to be stabilized or treated.

Determination of the moisture-density relationship

The moisture-density relationship of the collected soil was obtained using the Standard Proctor Test, and the optimum moisture and the corresponding maximum dry density was determined in accordance with DOTD TR 418M Method A. Method A was used because the soil selected contained less than 5% aggregate by dry mass retained on a 4.75 mm (No. 4) sieve. In this method, a 5 lb. (2,268 g) representative portion was obtained from a 30 lb. (13,608 g) dried soil sample, and approximately 10% water by the weight of dry soil (i.e., 226.8 g) was added to it to make slightly damped. After mixing thoroughly, the representative portion was passed through a 4.75

mm (No. 4) sieve, then kept covered and allowed to slake for 30 minutes. Test specimens were then compacted using a 5.50 ± 0.05 lb. (2.495 ± 0.023 kg) automatic rammer. The rammer had a 12.00 ± 0.06 in. (305 ± 2 mm) drop height with a striking face that is a 3.1416 in.^{2} (2,026.83 mm^2) in the sector face.

As shown in Figure 16, specimens were compacted in a 1/30 ft^3 (0.000944 m^3) cylindrical metal mold having an internal diameter of 4.00 ± 0.016 in. (101.60 ± 0.41 mm) and a height of 4.584 ± 0.005 in. (116.43 ± 0.13 mm). The mold also had a detachable collar which is 2.5 in. (64 mm) in height and could be fastened tightly to a base plate. The specimen was compacted in three layers with 25 blows per layer using the rammer. After compaction, the weight of the mold and the compacted specimen was recorded. Then, a representative portion of 1.1 lb. (500 g) was collected from the center of the compacted specimen and the moisture content was determined in accordance with DOTD TR 403 Method A-Rapid Drying. The method involved placing the wet 1.1 lb. representative portion on a hot plate and drying it to a constant weight (i.e., 0.1% weight loss between successive weightings no less than 5 minutes apart). The weight of the representative portion before and after drying was recorded and used to calculate the moisture content. In addition to the moisture content, dry and wet densities of the representative portion were also determined.

Figure 16. Compaction of soil with 5.5 lb. automatic rammer in 1/30 ft^3 cylindrical mold.

The remaining material from the mold was passed through a 4.75 mm (No. 4) sieve and recombined with the remaining representative portion. After that, water was added to the recombined representative portion to increase its moisture content by approximately 2% and mixed thoroughly. Then, the procedures of compaction, collection of the representative 1.1 lb. (500 g) wet portion from the compacted sample, drying, and the calculation of the moisture content, wet and dry densities are all repeated. The whole procedure is repeated until there is a substantial drop in the wet weight of the compacted material, or the material becomes too wet to compact. Then, dry densities were plotted against each moisture content as shown in Figure 17. The optimum moisture content (OMC) was determined which is the peak of the dry density versus moisture

content curve. It was found that the OMC is 14.4% and the corresponding maximum dry density is 112.3 lb./ft^3 (≅ 1,800 kg/m^3) as shown in Figure 17.

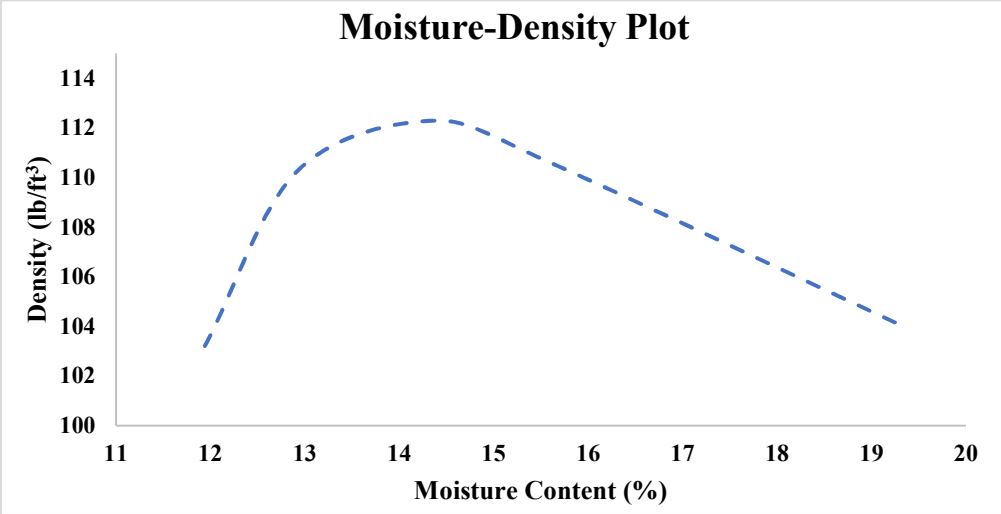

Figure 17. The moisture-density relationship is determined in accordance with DOTD TR 418M.

Determining the minimum Cement Factor by weight

The minimum cement content, also known as "Curve Cement Factor" or minimum Cement Factor by weight, for both 300+ psi CSB and 150+ psi CTB, was determined in accordance with DOTD TR 432 Method B. Method B was selected because the soil collected contained less than 5% aggregate by dry mass retained on a 4.75 mm (No. 4) sieve. A representative portion of the soil weighs 180 lb. (82 kg). The sample was prepared in accordance with DOTD TR 411M. The design moisture content was determined which is 1% above the optimum moisture content (i.e., 15,4%) as suggested in DOTD TR 432 Method B. The representative portion was then dried to a constant mass in accordance with DOTD TR 403 and TR 411M to eliminate the effects of hygroscopic moisture (i.e., moisture which an unprotected oven-dried soil absorbs from the air).

After drying the representative portion to a constant mass of 5 lb. (2.3 kg), the soil was placed in each of 20 different mixing pans to produce four sets of five specimens. Then, the quantity of water needed to bring each 5 lb. (2.3 kg) portion to the slacked moisture content (i.e., 5% below the design moisture content) was determined. The slake water was immediately added to each 5 lb. (2.3 kg) portion, mixed thoroughly, covered, and allowed to slake for 30 minutes. After that, 6%, 9%, 12%, and 15% cement by the mass of dry soil (i.e., 5 lb.) were added into the four sets of specimens. Then, the proper quantity of net water (i.e., the difference between slake water and design moisture content, 5%) was added to all the samples, mixed thoroughly, covered, and allowed to stand for 60 minutes. The beginning of molding test cylinders needs to be completed within 90 minutes of the addition of cement. Test specimens were then compacted using a 5.50 ± 0.05 lb. (2.495 ± 0.023 kg) automatic rammer (Figure 18a) with a 12.00 ± 0.06 in. (305 ± 2 mm) drop height and a striking face that is a 3.1416 in.^{2} (2026.83 mm^2) in the sector face. Specimens were compacted in a 1/30 ft^3 (0.000944 m^3) cylindrical metal mold having an internal diameter of 4.00 ± 0.016 in. (101.60 ± 0.41 mm) and a height of 4.584 ± 0.005 in. (116.43 ± 0.13 mm). The mold also had a detachable collar which was 2.5 in. (64 mm) in height and could be fastened tightly

to a base plate. The specimen was compacted in three layers with 25 blows per layer using the rammer.

After compaction, the specimens were ejected using a hydraulic jack as shown in Figure 18b. The specimens are then inverted on porous stone, protected from moisture loss (Figure 18c), and placed in the moist room for a curing period of 7 days. When the 7-days curing period is complete, the specimens were removed from the curing room and tested under compressive loading until failure (Figure 19). All four sets of test specimens were broken within 90 minutes from the time that the first cylinder is removed from the moist room. The failure load along with the type of break was noted and the average compressive strengths were determined.

(a) (b) (c)

Figure 18. Compaction, ejection, and protection of soil-cement specimens for curing.

Figure 19. Determination of compressive strength of the soil-cement specimen in accordance with DOTD TR 432.

The average compressive strength results were plotted against each corresponding cement content as shown in Figure 20. Finally, the cement contents (or Curve Cement Factors or minimum Cement Factors by Mass) for compressive strengths of 150 psi (1 MPa) and 300 psi (2 MPa) were determined. From the plot, it was found that a cement content of 2.86% by weight of soil is supposed to produce Cement-Treated Base (CTB) materials with a compressive strength of 150 psi. Moreover, 10% of cement content by weight is supposed to produce Cement-Stabilized Base (CSB) materials with a compressive strength of 300 psi. However, in-field practice the minimum cement content to produce CTB materials is 6% by weight of soil. Therefore, to follow the field practice, 6% cement content by weight was chosen for CTB in this project with a target minimum compressive strength of 200 ± 10 psi (1.38 ± 0.07 MPa). While 12% of cement content by weight was chosen for CSB with a target minimum compressive strength of 350 ± 10 psi (2.41 ± 0.07 MPa).

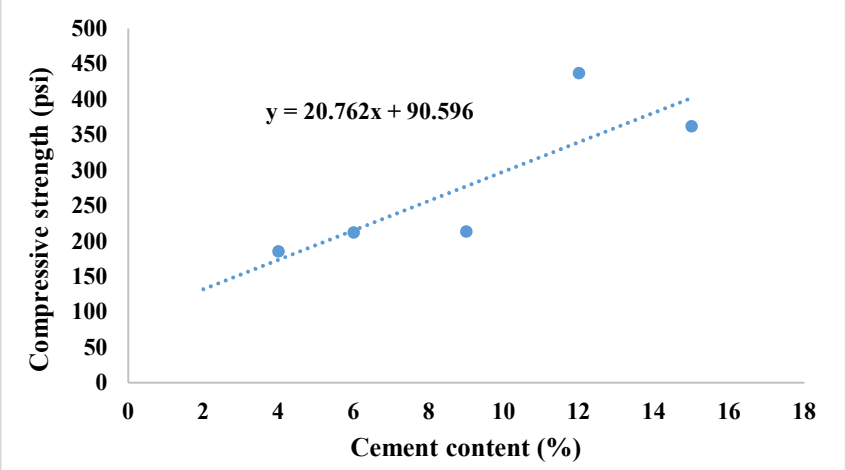

Figure 20. Determination of minimum cement content in accordance with DOTD TR 432.

As determined in the laboratory, the optimum moisture content of the collected soil was 14.4%. In-field, a moisture content that is slightly higher than the optimum moisture content is used to compensate for the hydration reaction between cement and water. Therefore, a design moisture content of 15.4% was used in this study. The final mixture design to produce CTB and CSB mixtures is shown in Table 4.

Table 4. Final mixture design to produce CTB and CSB mixtures.

Base type	% Soil by weight	Design Moisture Content by weight (%)	Minimum Cement Content by weight (%)	Target Minimum Compressive strength (psi)
Cement-Treated Base (CTB)	94	15.4	6	150 ± 10
Cement-Stabilized Base (CSB)	88	15.4	12	350 ± 10

4.2. Designing the OT mold for CTB/CSB specimen preparation

The specimens that were used during the determination of the moisture-density relationship and the minimum cement factor were cylindrical in shape. Specimens had a diameter of 4 in. (101.6 mm) and a height of 4.5 in. (114.3 mm). The mold that was used for the preparation and compaction of these specimens had a capacity of 1/30 ft^3. However, OT uses specimens with a different shape as compared to the specimens prepared during the determination of the moisture-

density relationship and the minimum cement factor. To incorporate CTB/CSB specimens under OT asphalt mixture specimens, the dimensions of CTB/CSB specimens need to be matched with the width (3 ± 0.02 in.) and length (6 in.) of the OT specimens (see Figure 21). Therefore, the research team developed a mold to prepare the CTB/CSB specimens with the intended shape and geometry as well as to facilitate proper compaction. The research team designed a SOLIDWORKS model of the mold, fabricated different components separately using a 3D printing facility at Louisiana State University (Figure 22a). Polylactic Acid (PLA), a commonly used thermoplastic material in the form of a 1.75 mm filament, that does not require the use of a heated print bed, was used for 3D printing.

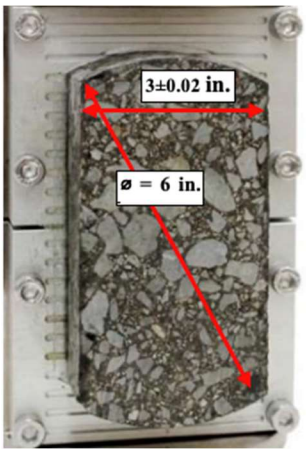

Figure 21. Top view and dimensions of the OT specimen.

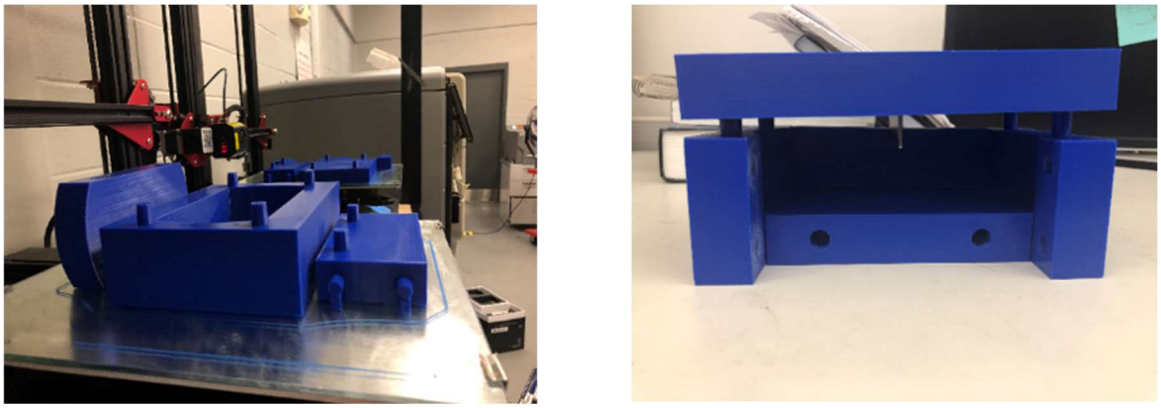

(a) (b)

Figure 22. (a) 3D printing of the mold, and (b) Printed mold.

The mold consisted of seven parts (one base, four side parts, one collar, and one top part where a steel plate embedded in the middle of the bottom surface). Two 3D printing trials have been conducted. In the first trial, the male and female parts had the same diameter of 0.4 in. (10.16 mm). As a result, male parts were not mating with the female parts (Figure 22b). So, sandpaper was used to reduce the diameter of the male parts. Although this reduced the diameter of the male parts, it became very difficult to detach different mold parts. Also, male parts showed a tendency to break during removal.

In the second trial, all the main parts have been changed to female parts (Figure 23a) and detachable pines having a diameter of 0.36 in. (9.144 mm) were designed and 3D printed (Figure 23b). The pines were supposed to work as hinges to facilitate the demolding of the specimen. The mold after assembling it with parts and pins is shown in Figure 23c. Additionally, clamps were used to hold different parts of the mold from all directions and provide sufficient strength to the mold to hold CTB/CSB specimens during and after compaction.

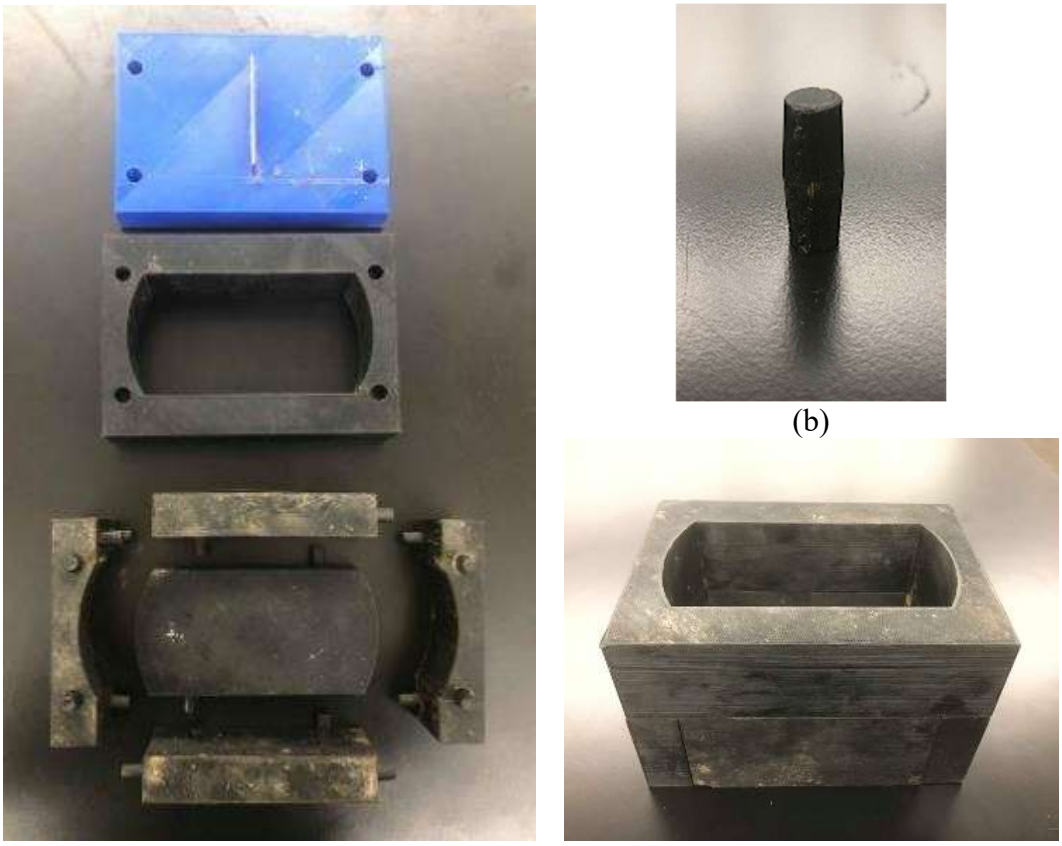

(a) (b) (c)

Figure 23. 3D-printed mold after the second trial, (a) 7 parts printed where all the parts are female, (b) detachable pin, and (c) mold assembled.

4.3. Preparation of CTB/CSB OT specimens

In this study, the research team conducted two trials for the preparation of CTB/CSB OT specimens using the 3D-printed mold. The details of the two trials are summarized in the following sub-sections.

4.3.1. First trial

In the first trial, the required quantities of soil, cement, and water were prepared. The required quantities were calculated from the maximum dry density (i.e., 112.3 lb./ft^3 (≅ 1,800 kg/m^3)) determined from DOTD TR 418 M. According to sub-section 302.12.01 of Louisiana Specification, the density requirements for soil-cement base course materials other than asphalt concrete should be a minimum of 95% of the maximum dry density per DOTD TR 418. Therefore, the target minimum density of compacted CTB material (including soil and cement) was 107.8 lb./ft^3 (96% of the maximum dry density). Using the volume of the 3D-printed mold (0.000424

m^3) and the relationship between density and weight, the target weight of the compacted CTB material (including soil and cement) was determined. The target weight of the compacted CTB material was found to be 1.61 lb. (731 g). Then, the weight of dry soil needed to produce 731 g of CTB material was calculated (i.e., 690 g) and the cement quantity was 41.4 g which is 6% by the weight of dry soil. Finally, the slake water and net water quantities were calculated (i.e., 76.1 g and 43.9 g, respectively).

The compaction was performed using a 5.50 ± 0.05 lb. (2.495 ± 0.023 kg) manual rammer with a drop height of 12.00 ± 0.06 in. (305 ± 2 mm). Due to the small height of the CTB/CSB specimens (i.e., 1.5 in.), the research team decided to compact the specimen in a single layer. The number of blows required was adjusted from 25 blows/layer to 34 blows/layer to match the compaction energy used during the determination of moisture density relationship or minimum cement content. The detailed calculation is presented in Table 5.

Table 5. Calculation of the required number of blows to prepare the CTB/CSB OT specimen.

Specimen Type	Number of blows per layer	Number of layers	Weight of rammer (N)	Height of drop (m)	Mold volume (m^3)	Compaction energy (kJ/m^3)
DOTD TR 418/TR 432	25	3	24.475	0.3048	0.000944	592.7
CTB/CSB Specimen	34	1	24.475	0.3048	0.000424	592.7

At first, all the parts of the mold were assembled, and Petroleum jelly was applied inside the mold to facilitate the demolding of the specimen after compaction and curing (Figure 24a). Two clamps were attached to confine the mold in all the directions (Figure 24b). Then, the soil material treated with cement (i.e., CTB or CSB) was placed in small quantities using a small scoop inside the mold avoiding any loss of materials (Figure 24c). This process was continued until all the material was placed inside the mold. Then, compaction was done by placing the rammer directly onto the material surface and dropping it from a height of 12 in. (305 mm) as shown in Figure 24d. However, when the compaction was completed, it was observed that the compacted surface was not leveled or smooth (Figure 24e). Although efforts had been made during compaction to distribute 34 blows all over the surface of the specimen, the distribution was not equal in all directions. Moreover, the falling head of the rammer is circular in shape having a diameter of 4 in. (101.6 mm), while the mold is 3 in. in width by 6 in. in length. As a result, there was some overlapping between the blows which resulted in an uneven surface. Additionally, the corners of the mold were inaccessible to the rammer because of its circular shape.

An attempt was made to make the 0.6 in. (15.24 mm) notch in the middle of the specimen using the top part of the mold having a steel plate embedded. The length of the steel plate was 3 in. which was exactly equal to the width of the mold. So, it was quite difficult to make the notch using the steel plate embedded top part. Moreover, the breaking of a small portion of the top surface of the specimen was observed. However, the specimen was covered in plastic wraps (Figure 24f) and cured in the moist curing room for 7 days. After the 7 days, the specimen was demolded, and it was observed that the top surface (which was the bottom surface during compaction) over which the asphalt OT specimen is to be attached was quite level and smooth (Figure 24g). Additionally, only wrapping the specimen with plastic wraps seemed inadequate since moisture could still access the specimen as observed after a 7-day curing period. Because of all these issues, a second trial was conducted by the research team.

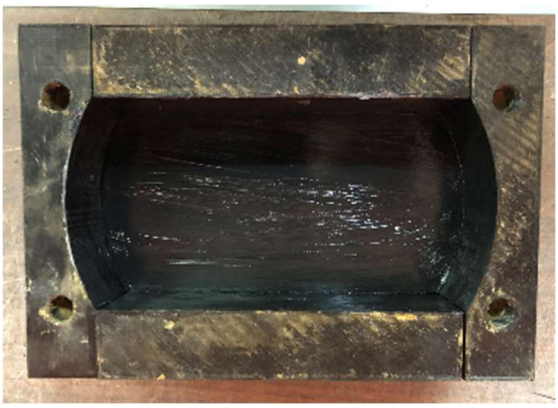

(a)

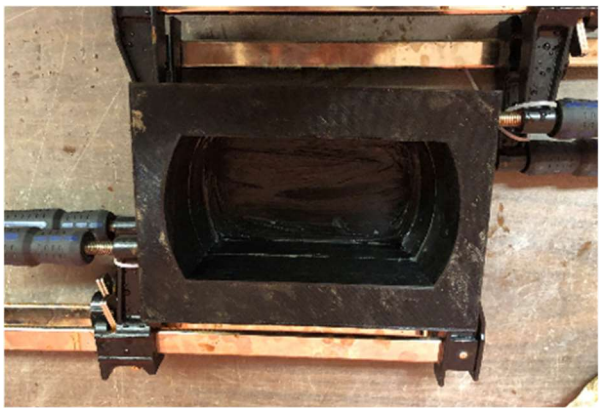

(b)

(c)

(d)

(e)

(f)

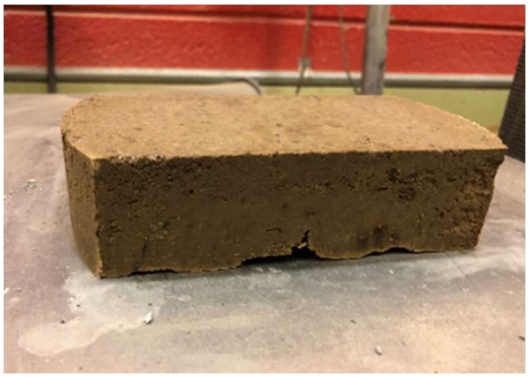

(g)

Figure 24. Compaction procedure during the first trial of CTB/CSB OT specimen preparation.

4.3.2. Second trial

Some modifications in the compaction procedure were adopted by the research team to obtain CTB/CSB OT specimens of desired surface smoothness. A wooden piece was sawed in the shape of the OT specimen (0.5 in. in thickness) and was used to evenly distribute rammer blows to the surface of the specimen. A sequence of blows was established and used during compaction to be consistent every time during compaction. The length of the steel plate in the top part of the printed mold was reduced slightly to facilitate easy notching. Moreover, in addition to using petroleum jelly, two long plastic wraps were placed inside the mold perpendicular to one another. The purpose of these two wraps was to cover the specimen surface inaccessible to water and to facilitate the easy demolding of the specimen. After compacting the specimen by dropping the rammer on the wooden piece, the surface of the compacted specimen was leveled and smooth. However, the effort to make the notch slightly shorter was unsuccessful. The entire assembly was then placed in a plastic bag which provided additional protection against water and kept inside the moist curing room for 7 days. After demolding, it was observed that both the top and bottom surface of the specimen were satisfactorily leveled and smooth. Figure 25 shows the compaction procedure followed in the second trial to prepare the CTB/CSB OT specimens. This trial was successful and was used for the rest of the study. Therefore, the research team prepared a step-by-step procedure for the preparation of CTB/CSB materials, mix design, and compaction provided in Appendix A.

(a)

(b)

(c)

(d)

(e)

(f)

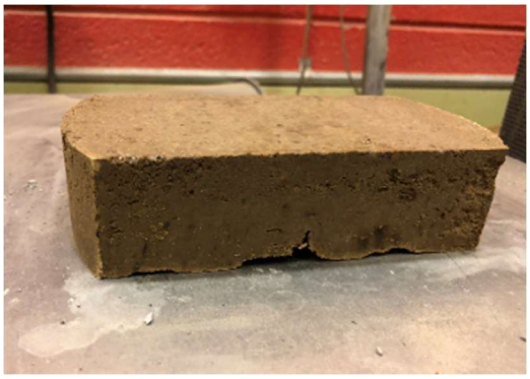

(g)

Figure 25. Compaction procedure during the second trial of CTB/CSB OT specimen preparation.

4.4. Preparation of HMA mixtures

4.4.1. Materials and properties

This study aims to evaluate the effect of the proposed modification on OT test setup on different common asphalt mixtures in Louisiana. Therefore, two asphalt binders commonly used in Louisiana were selected to prepare the asphalt mixtures. These binders included an unmodified

PG 67-22 and Styrene-Butadiene-Styrene (SBS) polymer-modified PG 76-22 binders. Asphalt binders were collected from Marathon Grayville Petroleum Refinery, Garyville, Louisiana. The experimental design of this project including variables is summarized in Table 6.

Table 6. Project experimental design.

Variable	Description
NMAS	0.5 in. (12.5 mm)
RAP Source	Single source (Fine and Coarse RAP)
Asphalt Binder	Unmodified binder: PG 67-22 Polymer-modified binder: PG 76-22
Asphalt Binder Content	Optimum asphalt binder content determined at N_{design}
RAP % (by weight of the aggregate blend)	0% and 20%
Testing Temperature	10°C ± 0.5°C and 25°C ± 0.5°C

The virgin aggregates that were used for the mixtures were supplied by Vulcan Materials Company from their Grand Rivers Quarry located in Lafayette, Louisiana. The supplied aggregates were Limestone (LS) that were 12-18 months old and were collected from stockpiles consisting of #89 LS, #78 LS, and #11 LS. The RAP aggregates were Diamond B and included fine RAP (F. RAP) and coarse RAP (C. RAP). Table 7, Table 8, and Table 9 summarize the properties of the asphalt binders, virgin aggregates, and RAP materials, respectively that have been used for the production of asphalt mixtures used in this project.

Table 7. Properties of the asphalt binders used in the HMA mixtures.

	Asphalt binders	
Binder grade	PG 67-22	PG 76-22
Modification	Unmodified	SBS-polymer modified
Sp. Gravity, Gb	1.031	1.036

Table 8. Gradations and properties of the virgin aggregates used in the HMA mixtures.

Virgin Aggregate Gradations			
Sieve sizes	**#89 LS**	**#11 LS**	**#78 LS**
25.0mm - 1"	100.0	100.0	100.0
19.0mm - 3/4"	100.0	100.0	100.0
12.5mm - 1/2"	100.0	100.0	93.0
9.5mm - 3/8"	95.1	100.0	50.1
4.75mm - #4	34.6	92.0	3.5
2.36mm - #8	8.6	63.0	1.2
1.18mm - #16	4.0	39.0	1.0
0.600mm - #30	3.0	25.0	1.0
0.300mm - #50	2.6	17.0	1.0
0.150mm - #100	2.3	13.0	0.9
0.075mm - #200	1.4	10.0	0.8
Virgin Aggregate Properties			
Bulk Sp. Gravity, Gsb	2.67	2.58	2.67
Apparent Sp. Gravity, Gsa	2.7	2.7	2.7
Absorption (%)	0.2	1.4	0.2
Fine Aggregate Angularity (FAA)	N. A	47	N.A.
Coarse Aggregate Angularity (CAA)	N. A	N. A	N.A.
Sand equivalency	N. A	69	N. A.

Table 9. Gradations and properties of the RAP materials used in the HMA mixtures.

RAP Gradations		
Sieve sizes	**F. RAP**	**C. RAP**
25.0mm - 1"	100.0	100.0
19.0mm - 3/4"	100.0	97.6
12.5mm - 1/2"	99.7	76.7
9.5mm - 3/8"	96.2	51.1
4.75mm - #4	70.5	31.4
2.36mm - #8	50.0	22.2
1.18mm - #16	38.3	17.6
0.600mm - #30	30.9	14.6
0.300mm - #50	20.4	10.2
0.150mm - #100	12.1	6.0
0.075mm - #200	8.7	3.7
RAP properties		
%Crushed	99.5	99.7
Fineness Modulus F.M.	4.7	6.7
Asphalt content, %AC	4.7	3.1
Bulk Sp. Gravity, Gsb	2.548	2.542
Effective Sp. Gravity, Gse	2.607	2.601
Apparent Sp. Gravity, Gsa	2.449	2.477

4.4.2. Hot-Mix-Asphalt (HMA) mixture design

In this study, two asphalt mixtures were prepared using virgin aggregates with 0% Reclaimed Asphalt Pavement (RAP) by the weight of the mixture. Moreover, another two mixtures were prepared using virgin aggregates with 20% RAP by the weight of the mixture to assess the effect of adding RAP aggregates on the performance of asphalt mixtures against reflective cracking. The RAP content was selected as 20% since it is the maximum allowable percentage of RAP that can be incorporated in asphalt mixtures under Section 502 of Louisiana Specifications. The aggregate stockpiles used for the mixtures without RAP included #89 LS, #78 LS, and #11 LS to produce mixtures with a 12.5-mm nominal maximum aggregate size (NMAS). Additionally, the aggregate stockpiles selected for the mixtures with RAP consisted of fine RAP and coarse RAP in addition to #89 LS, #78 LS, and #11 LS to produce mixtures with a 12.5-mm nominal maximum aggregate size (NMAS). The design aggregate structures for the mixtures produced in this study are illustrated in Figure 26.

The asphalt mixtures were prepared according to AASHTO R35, AASHTO M323, and Section 502 of the Louisiana Specifications that satisfied the volumetric and densification requirements. A Level 2 design ($N_{initial}$ = 7, N_{design} = 65, N_{final} =105 gyrations) was adopted in this study. Table 10 presents the Job-Mix Formula (JMF) for four different asphalt mixtures produced in this study and Table 11 summarizes details of the prepared asphalt mixtures, including the mixture code designations used in the report, the experimental plan, and testing temperatures.

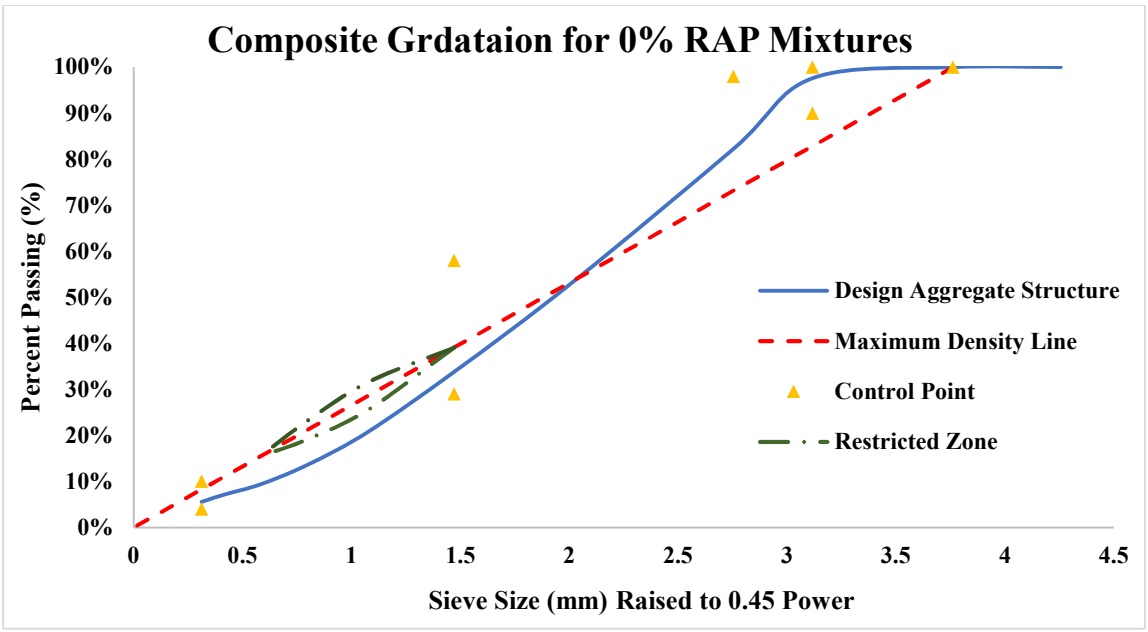

(a)

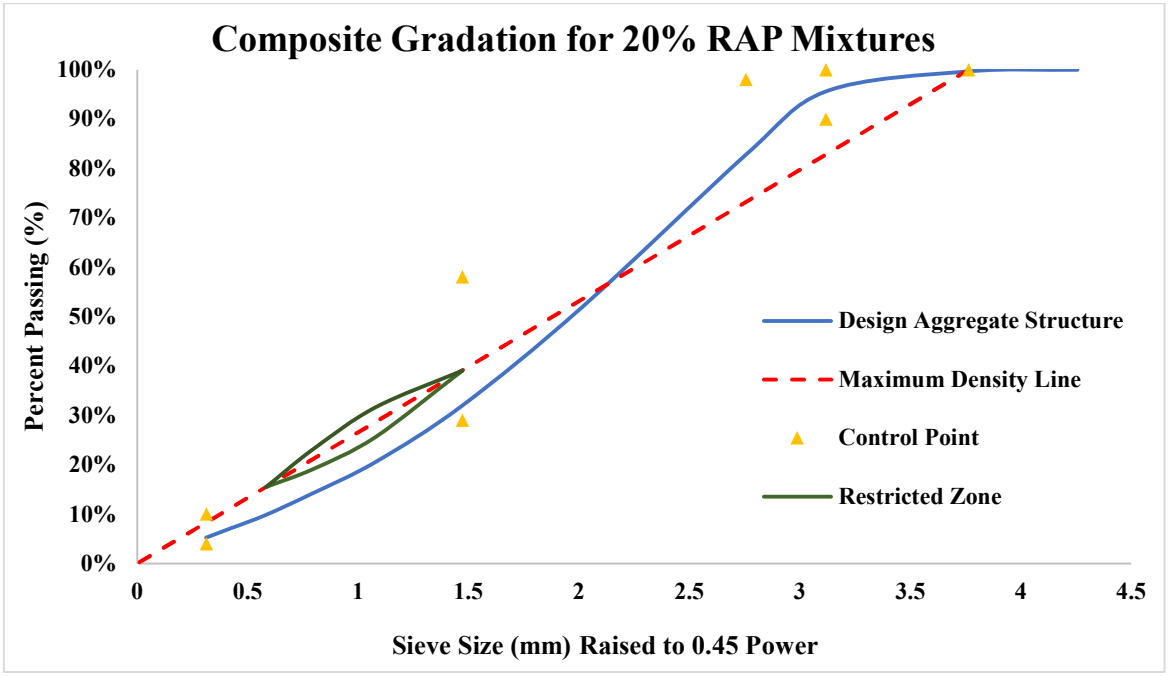

(b)

Figure 26. Design aggregate structure for the mixtures (a) without RAP and (b) with RAP.

Table 10. Job-Mix Formula (JMF) for the asphalt mixtures produced in this study.

Mix Code Designation		67-0RAP	76-0RAP	67-20RAP	76-20RAP
Mix Type		HMA			
NMAS		12.5 mm			
Aggregate Blend		15% #89LS 51% #11LS 34% #78LS 0% F. RAP 0% C. RAP		24% #89LS 37% #11LS 19% #78LS 7% F. RAP 13% C. RAP	
Binder type		PG 67-22	PG 76-22	PG 67-22	PG 76-22
Volumetric Properties	Criteria	Design Properties			
G_{mm}, N_d[2]	-	2.475	2.472	2.448	2.448
%AC	-	5.5	5.5	5.4	5.4
%Voids	3.5 – 4.5	4.4	3.2	2.8	3.5
%VMA	≥ 13.5 min	15.1	13.8	14.1	14.8
%VFA	69 - 80	75.1	77.0	79.7	76.6
%Dust/Effective Asphalt Ratio	0.6 – 1.6	1.2	1.2	1.1	1.1
Sieve Sizes		% Passing (Design Aggregate Blend)			
25.0mm - 1"		100		100	
19.0mm - 3/4"		100		100	
12.5mm - 1/2"		98		96	
9.5mm - 3/8"		82		83	
4.75mm - No. 4		53		52	
2.36mm - No. 8		34		32	
1.18mm - No. 16		21		21	
0.600mm - No. 30		14		14	
0.300mm - No. 50		9		10	
0.150mm - No. 100		7		7	
0.075mm - No. 200		6		5	

Table 11. Experimental matrix of the project.

Mixture Code Designation	Asphalt Binder	% RAP	Soil-cement base	Test Temperature (°C)
67-0RAP-10	PG 67-22	0	-	10
67-0RAP-25	PG67-22	0	-	25
67-0RAP-CTB-10	PG 67-22	0	CTB	10
67-0RAP-CTB-25	PG 67-22	0	CTB	25
67-0RAP-CSB-10	PG 67-22	0	CSB	10
67-0RAP-CSB-25	PG 67-22	0	CSB	25
67-20RAP-10	PG 67-22	20	-	10
67-20RAP-25	PG 67-22	20	-	25
67-20RAP-CTB-10	PG 67-22	20	CTB	10
67-20RAP-CTB-25	PG 67-22	20	CTB	25
67-20RAP-CSB-10	PG 67-22	20	CSB	10
67-20RAP-CSB-25	PG 67-22	20	CSB	25
76-0RAP-10	PG 76-22	0	-	10
76-0RAP-25	PG76-22	0	-	25
76-0RAP-CTB-10	PG 76-22	0	CTB	10
76-0RAP-CTB-25	PG 76-22	0	CTB	25
76-0RAP-CSB-10	PG 76-22	0	CSB	10
76-0RAP-CSB-25	PG 76-22	0	CSB	25
76-20RAP-10	PG 76-22	20	-	10

76-20RAP-25	PG76-22	20	-	25
76-20RAP-CTB-10	PG 76-22	20	CTB	10
76-20RAP-CTB-25	PG 76-22	20	CTB	25
76-20RAP-CSB-10	PG 76-22	20	CSB	10
76-20RAP-CSB-25	PG 76-22	20	CSB	25

4.5. Preparation of HMA OT specimens

In this study, the possibility/applicability of adding a CTB/CSB layer below the asphalt layer in evaluating the resistance to reflective cracking and simulating field conditions has been examined. Therefore, two types of OT specimens were prepared, mounted, and tested in OT testing setup, i.e., conventional OT specimens and composite OT specimens after adopting the proposed modifications.

4.5.1 Preparation of the conventional OT specimens

Conventional HMA OT specimens were prepared following Tex-248-F (version 2019). At first, five laboratory-molded cylindrical HMA specimens, having 6 in. (150 mm) diameter, and 4.5 ± 0.2 in. (115 ± 5 mm) height was prepared with air voids of 9 ± 1% in accordance with Tex-241-F. Then the specimens were cut perpendicularly to the top surface (Figure 27a) and the sides were trimmed so that the width of the specimens became 3 ± 0.02 in. (76 ± 0.5 mm) (Figure 27b). After discarding the cuttings, the top and bottom of each specimen were also trimmed so that the height of the specimens is 1.5 ± 0.02 in. (38 ± 0.5 mm), as shown in Figure 27c. The cuttings were discarded. The weight of the specimens was measured in water-submerged and saturated surface dry (SSD) condition following Tex-207-F. After that, the specimens were oven-dried at 104 ± 5°F (40 ± 3°C) for 5 hours to a constant weight. From the measured weights (oven-dried, submerged, and SSD) the mixture bulk specific gravity (G_{mb}) was calculated. Finally, the maximum specific gravity of the mixture (G_{mm}) obtained during mixture design, and G_{mb} was used to calculate the air-voids of trimmed specimens. The trimmed specimens having an air-void of 7 ± 1% were only selected for mounting and testing while the others were discarded. Prepared specimens were then glued to the base plates using JBWELD ClearWeld 2-part quick setting epoxy having a strength of 4,400 psi (30.3 MPa), setting time of 5 minutes, and curing time of 1 hour. The gluing procedure was consistent for all the specimens and complete adherence to Tex-248-F was maintained to minimize variability (Figure 28a). A 5-lb. weight is placed on the specimen to ensure intimate contact between the specimens (Figure 28b) and the base plates and the epoxy was allowed to cure overnight so that it can achieve sufficient bonding strength before testing.

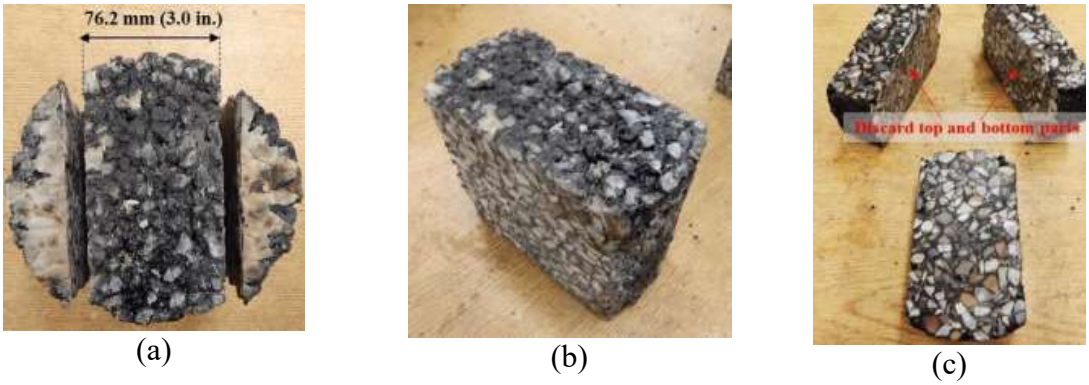

(a) (b) (c)

Figure 27. HMA OT specimen preparation: (a) cutting specimen perpendicular to the top surface, (b) after discarding the trimmed sides, and (c) trimmed final specimens.

Figure 28. Gluing and curing of OT specimen: (a) spreading epoxy, and (b) curing of epoxy overnight.

4.5.2 Preparation of the composite OT specimens

The composite specimens in accordance with the proposed modifications had two layers which included an HMA layer on top and a pre-notched CTB/CSB layer at the bottom. The top HMA layer was prepared following the same procedure as a conventional HMA OT specimen described earlier. The HMA layer was obtained after cutting and trimming the specimens to the final dimensions of the conventional HMA OT specimens (i.e., 6 in. (150 mm) diameter and 1.5 ± 0.02 in. (38 ± 0.5 mm) height). The CTB/CSB layer was prepared (with or without a notch) in accordance with the developed procedure mentioned in sub-section 4.3.2.

The CTB/CSB layer was attached with the OT base plates using JBWELD ClearWeld 2-part quick setting epoxy. The gluing procedure to attach the CTB/CSB layer to the base plates was the same as Tex-248-F. A dummy HMA OT specimen was placed on the CTB/CSB specimen to ensure intimate contact with the base plates, and the epoxy was allowed to cure overnight. A 5-lb. weight was not used in this case to avoid the chances of breaking the specimen.

In this study, two different approaches were attempted to accomplish bonding between the top and bottom layer. The first approach involved applying 16 g (0.035 lb.) of JBWELD ClearWeld 2-part quick setting epoxy on the CTB/CSB specimens following the same gluing procedure as described in Tex-248-F and then placing the HMA layer on top of the bottom layer. Finally, a dummy HMA specimen was placed on the composite specimen and allowed it to cure overnight. The final composite OT specimen prepared following is approach is shown in Figure 29.

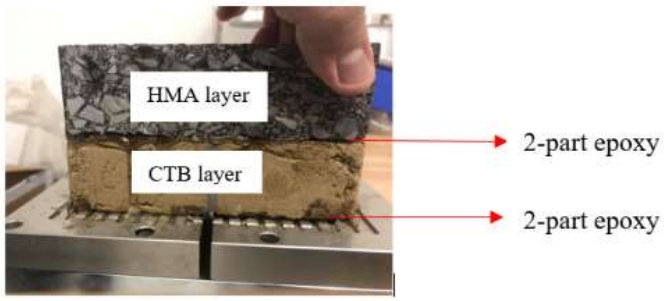

Figure 29. Final composite OT specimen where two layers are attached using 2-part epoxy.

However, prime coat is typically used in the field to attach asphalt layer over stabilized bases like CTB or CSB. Therefore, a second approach, which was the use of the MC-30 prime coat over the CTB/CSB layer at an application rate of 0.28 Gal/Sq Yd (as per the Louisiana Specification), to attach the top and bottom layer. In the field, the HMA layer is directly compacted when it is still hot and according to the Louisiana Specification, the temperature of the HMA to be compacted needs to be between 16-49°C (60-120°F). Therefore, first, the HMA layer was kept in the oven at 40°C (104°F) for 1 hour. The prime coat of 13 g (0.028 lb.) was applied uniformly on CTB/CSB layer and the warm HMA layer was placed on the top of the CTB/CSB layer. Then, a dummy HMA specimen was placed on the composite specimen and allowed to cure for 24 hours (see Figure 30).

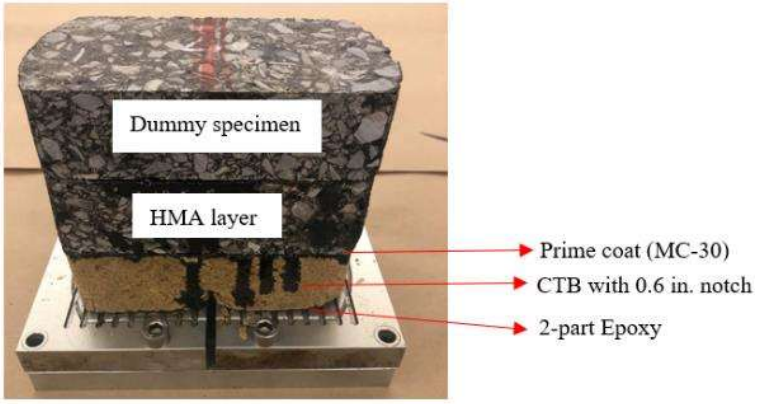

Figure 30. Final composite OT specimen where two layers are attached using prime coat.

4.6. OT testing procedure

All the specimens prepared for this study were tested using the OT vertical setup that came with an IPC Global Asphalt Standards Tester (AST), referred to as AsphaltQube (Figure 31a). The main components of the OT setup included a controlled temperature chamber for controlling the temperature, a crosshead, upper tension loading adaptor, overlay jig for specimen mounting, a load cell, and an external LVDT (Figure 31b). The specimens are glued to the steel base plates which were mounted on the Overlay jig vertically using bolts (Figure 31c). The upper half of the Overlay jig is stationary while the lower half attached to the load cell moves vertically downward and then upward applying tensile load on the specimen.

The testing is usually conducted at room temperature (25°C). In this study, testing of the OT specimens was performed at low-temperature (10°C) in addition to room temperature to investigate if the proposed modification of the OT setup can capture the effect of low temperature on the resistance to reflective cracking. This resulted in two different conditioning time for the OT specimens. The specimens to be tested in room temperature were conditioned for one hour before testing which was typical in accordance with the test standard (Tex-248-F). However, specimens prepared to be tested in low temperature were conditioned for three hours before testing. In all cases, a pre-test relaxation period of 10 minutes was used before testing.

Figure 31. Overlay tester: (a) IPC Global AsphaltQube, (b) major components of OT setup, and (c) mounted OT specimen.

Two types of loading can be used in OT while testing, i.e., one-phase loading and two-phase loading. One-phase loading is applied in a cyclic triangular waveform with a constant maximum displacement of 0.025 in. (0.63 mm) as shown in Figure 32a. On the other hand, two-phase loading has two phases where the first phase is a constant displacement waveform having a ram displacement of 0.007 in. (0.18 mm), and the second phase is similar to one-phase loading (Figure 32b). The two-phase loading is designed for advanced users and should be used for advanced mechanical analysis. Due to the simplicity in data analysis, one-phase loading was selected by the research team to be used during testing. The loading rate was 0.005 in./s (0.13 mm/s) and each loading cycle lasted for 10 seconds. Testing was conducted until a 93% reduction of the peak tensile load was achieved measured from the first loading cycle or when the testing reached 1,000

loading cycles. Throughout the testing period, the time, displacement, load, and the number of cycles to failure are measured.

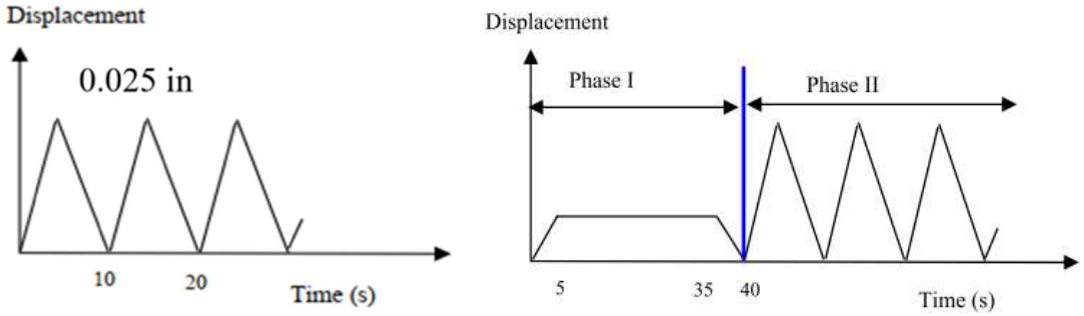

(a) (b)

Figure 32. Types of loading in OT testing: (a) One-phase, and (b) Two-phase (*72*).

4.7. Interpretation of OT testing data

The OT data included the time, displacement, and load corresponding to a certain number of loading cycles. Figure 33 shows the typical raw and processed data after the testing. The applied displacement, load, and corresponding time histories for the first ten cycles are illustrated in Figure 33. The hysteretic behavior of the test can be examined by plotting the displacement versus tensile load. The typical first hysteresis loop is shown in Figure 33b. Figure 33c shows the change in peak tensile load with respect to the number of cycles. The parameters that were calculated from the raw data included OT number of cycles to failure (N_{OT}), Critical Fracture Energy (G_c), and Crack Progression Rate (CPR).

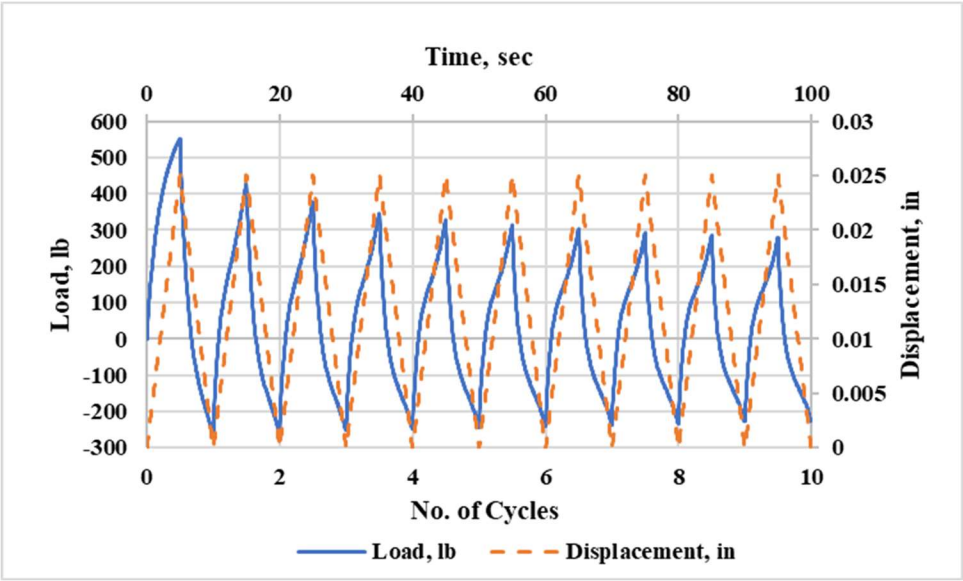

(a)

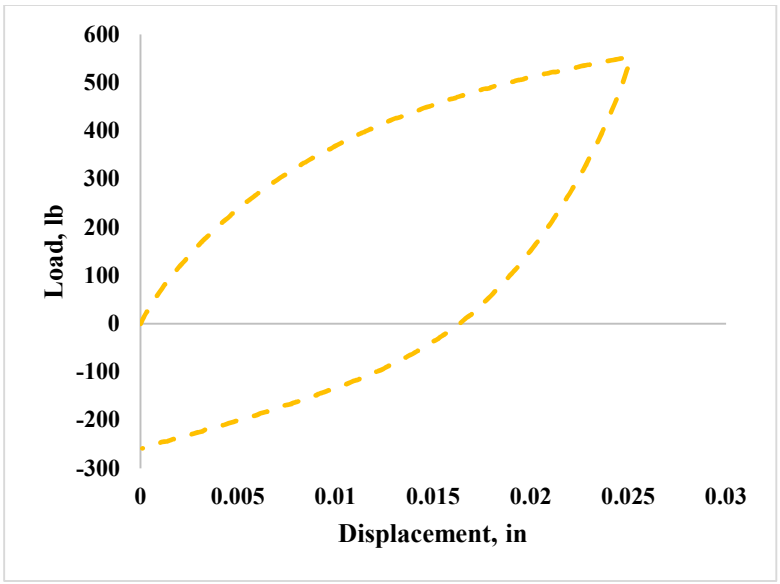

(b)

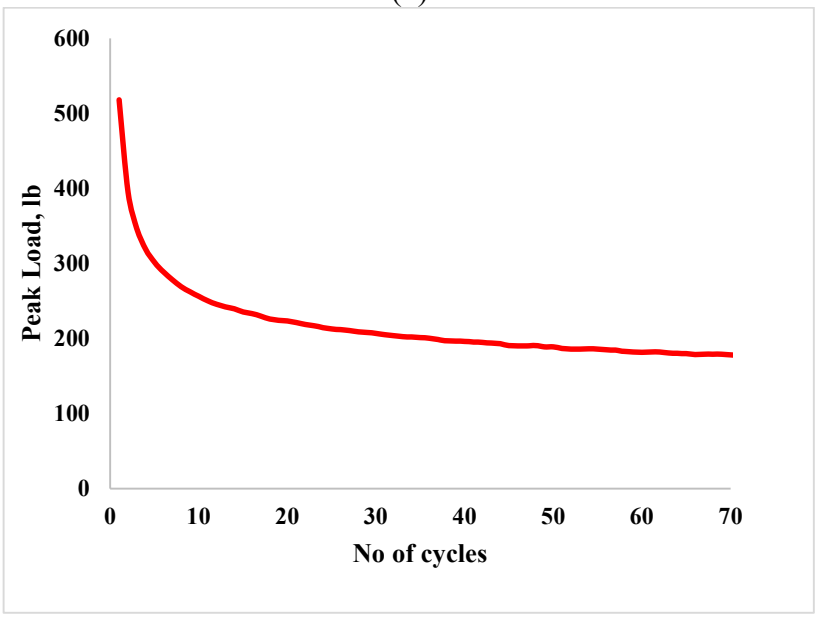

(c)

Figure 33. The typical raw and processed data after the testing.

4.7.1. The OT number of cycles to failure (N_{OT})

The loading cycle at which a 93% reduction of peak tensile load occurs, is referred to as the OT number of cycles to failure (N_{OT}). Alternatively, the test is stopped when a preset number of cycles (typically 1,000 as per Tex-248-F) is reached. The pass/fail criterion for the asphalt concrete mixtures with satisfactory cracking performance is a minimum of 300 loading cycles and asphalt mixtures that fail to meet the requirement might experience premature reflective cracking during its service life (*93*).

The main challenge to the widespread implementation of the OT test has been the high variability of the number of cycles to failure that is used as a performance index. Garcia et al. (*94*) noted that the high variability of the N_{OT} might be attributed to the limitations of the instrumentation used in

the OT devices. Load cells that are commonly installed in OT have capacities of 5,000 or 2,000 lb. with a precision of 0.1%. The reported loads are within 2-5 lb. of the actual values. When a 93% reduction of the peak load occurs the level of uncertainty in the measured loads can be up to 10% of the actual value. Therefore, the precision of the load cell has the potential to introduce a significant variability to calculate N_{OT} consistently using the current failure criterion. Because of this variability issue two new parameters, Critical Fracture Energy (Gc) and Crack Progression Rate (CPR) were developed to characterize the fracture, flexibility, and fatigue properties of the specimen during the crack initiation phase and propagation phase.

4.7.2. Critical Fracture Energy (Gc)

Critical Fracture Energy (Gc), a surrogate parameter to characterize the crack initiation stage of the OT test, is defined as the energy required to initiate a crack on the bottom of the specimen at the first loading cycle of the OT test. As shown in Figure 34, the area under the hysteresis loop of the first loading cycle is calculated first, and Gc is calculated using Equation 1:

$$G_c = \frac{w_c}{b * h} \quad [1]$$

where:
G_c = Critical Fracture Energy is the energy, lb.-in./in.^{2} (kN-mm^2);
w_c = fracture area, lb.-in. (kN-mm);
b = specimen width: 3 in. (76.2 mm); and
h = specimen height: 1.5 in. (38.1 mm).

An asphalt mixture should be tough enough to easily resist crack initiation. It indicates that the peak tensile load and the corresponding displacement need to be very high during the first loading cycle to yield modulus or energy-based parameters very high. Therefore, the higher the value of Gc is, the more energy the asphalt mixture will require to initiate the crack and exhibits greater resistance to reflective cracking.

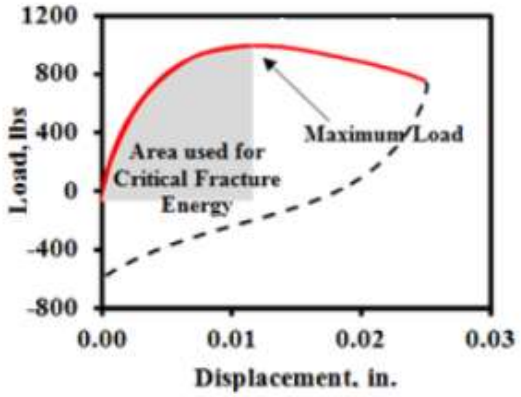

Figure 34. The area used to calculate the Critical Fracture Energy (Gc) from OT testing data (*63*).

4.7.3. Crack Progression Rate (CPR)

Crack Progression Rate (CPR) characterizes the flexibility and fatigue properties of specimens during the crack propagation phase. It is defined as the reduction in load required to propagate cracking under the cyclic loading conditions of the OT. From the OT data, the obtained number of loading cycles is plotted against maximum peak tensile load (also referred to as the crack driving

force) to obtain the load reduction curve. Then, a power equation is fitted to the load reduction curve. The power coefficient (β) of the power equation is termed as the Crack Resistance Index (CRI). To compare the results more consistently, the load reduction curve is normalized by the maximum load of the first cycle. A power equation is then fitted to the normalized load reduction curve in which the power term "b" is always negative. The absolute value of b is used for practical purposes and is referred to as Crack Propagation Rate (CPR). An asphalt mixture should be flexible enough to minimize the crack propagation rate after a crack is initiated. It indicates that the rate of loss of load and dissipation of the residual strength need to be slow through the application of the cyclic deformation. Therefore, a higher absolute value of the CPR indicates faster crack propagation through the asphalt mixture specimen and indicates shorter fatigue lives and vice versa.

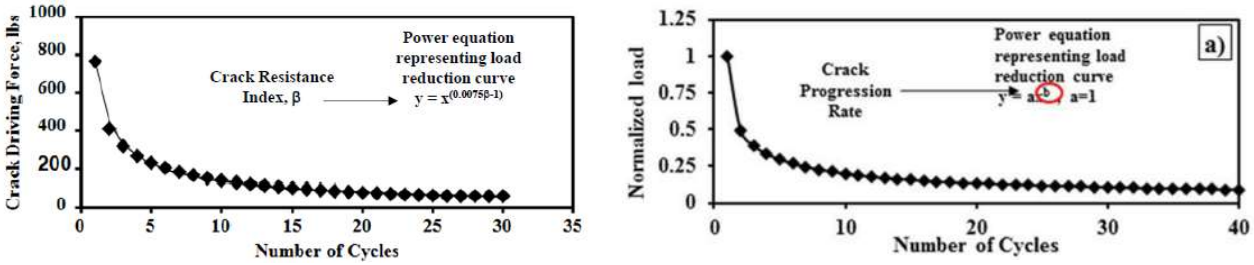

Figure 35. Graphical representation of the variation of crack driving force with the number of loading cycles and the calculation of (a) Crack Resistance Index (CRI), and (b) Crack Progression Rate (CPR) (*63*, *95*).

4.7.4. Cracking Interaction Plot

To better understand the cracking properties of mixtures using the proposed parameters, a cracking interaction plot is prepared by plotting Gc versus CPR (see Figure 36). For Gc, the proposed lower and upper limits are 7 and 21 kPa (1 and 3 in.-lb/in.^{2}), respectively (*88*). For CPR the threshold can be calculated based on the current pass/fail criteria of N_{OT}. The 93% load reduction in 300 cycles yields to CPR value of 0.47. So, as a preliminary failure limit, a CPR value of 0.5 is used to differentiate the good and poor cracking resistant asphalt mixtures (*94*). Therefore, based on the Cracking Interaction Plot shown in Figure 36, the asphalt mixtures should be ideally located inside the green shaded portion of the plot to be considered as crack resistance mixtures.

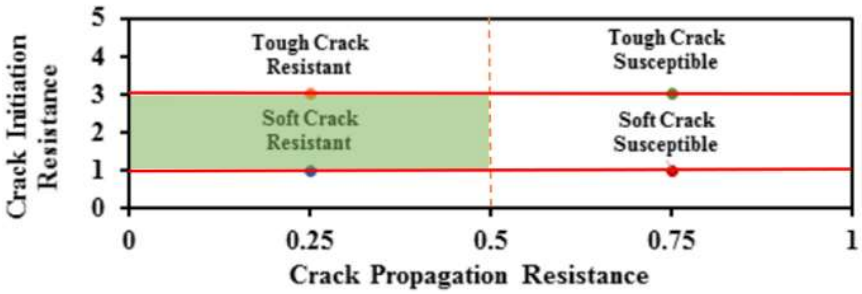

Figure 36. The OT cracking interaction plot (*88*).

From the design interaction plot, the cracking resistance of asphalt mixtures can be subjectively classified into four categories (*94*) which include:

a) Tough-Crack Resistant: Good resistance during crack initiation (Tough) and propagation (Flexible). Asphalt mixtures with acceptable cracking resistance should be in this quadrant.
b) Tough-Crack Susceptible: Asphalt mixtures with good resistance to crack initiation (Tough) and susceptible to crack propagation (Brittle).
c) Soft-Crack Resistant: Susceptible to crack initiation (Soft) but good resistance to attenuate the propagation of the crack (Flexible)
d) Soft-Crack Susceptible: AC mixtures with significantly poor resistance to crack initiation and propagation.

4.7.5 Statistical Analysis

In this study, a statistical analysis consisting of an Analysis of Variance (ANOVA) and a Tukey's HSD test was conducted. ANOVA at a 95% confidence level ($\alpha = 0.05$) was conducted to assess if the differences in performance indices (i.e., G_c, CPR, or N_{OT}) were statistically significant. The specimens were ranked using letters A, B, C, and so on. Two specimens sharing the same letter (i.e., A and A) indicates that the there was no significant difference between the performances of the specimens. In contrast, specimens sharing different letters (i.e., A and B) indicated significantly different performances.

5. ANALYSIS AND FINDINGS

5.1 Testing results of the composite OT specimens

The composite OT specimens where two layers (i.e., CTB/CSB without a notch and HMA) glued using 2-part epoxy were tested at two different temperatures and under one-phase loading at a maximum displacement of 0.025 in. (0.63 mm) until 93% peak tensile load reduction or 1,000 cycles of loading. It was observed that there was a crack initiation at the bottom of the CTB/CSB in early loading cycles as shown in Figure 37(a).

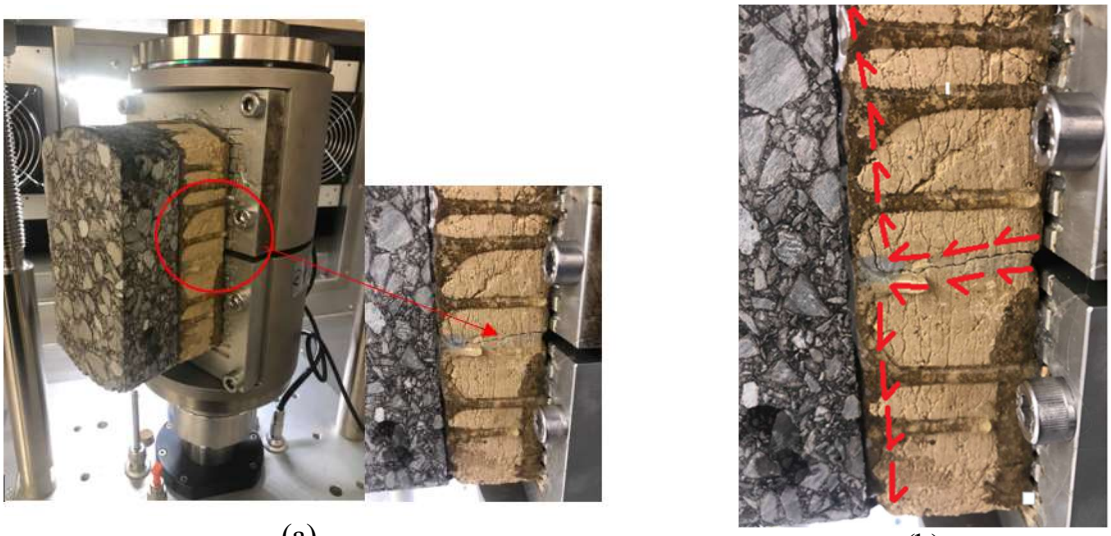

(a) (b)

Figure 37. Testing of composite OT specimens (a)crack initiation and propagation, (b) path of crack propagation.

However, as the number of loading cycles increased the crack propagated upward until the interface between the two layers and started to propagate parallel to the interface instead of advancing through the HMA layer. It occurred because the 2-part epoxy used between the interface was very strong (4,400 psi 24-hour tensile strength). Therefore, rather than simply gluing the two layers the epoxy itself became an additional layer between the two layers. As a result, the crack started to propagate parallel to the interface (see Figure 37b) rather than advancing through the HMA layer which made the mechanism of reflective cracking (i.e., the formation of a crack in the base and propagating to the upper layer) to become invalid.

The research team in this study attempted to test the composite OT specimens where MC-30 prime coat was used as the bonding material between the two layers. However, when the specimens with a notch at the bottom layer were mounted vertically on the Overlay Jig the lower half of the CTB layer broke from the location of the crack and the HMA layer above it also slipped and separated from the bottom layer. The same problem also occurred when composite specimens without a notch in the CTB/CSB layer were attempted to be mounted vertically in the Overlay Jig where the HMA layer was separated from the bottom layer.

These problems mentioned earlier might occur due to the inability of the prime coat to work as a gluing material between the interface. In the field, the prime coat is applied on the stabilized base, and HMA loose mixture is directly compacted over the base while the asphalt mixture is still hot. In the proposed OT setup, the HMA layer was prepared and compacted separately. The composite OT specimens were prepared by pouring prime coat over the CTB/CSB at room temperature,

placing the HMA layer on the bottom layer after being heated in the oven at 40°C for 1 hour and curing for 24 hours. Due to the difference in compaction methods between field and laboratory, the prime coat failed to create bonding between the two layers. Additionally, testing was conducted in a vertical setup rather than in a horizontal setup. The prime coat was not strong enough to resist that downward movement of the HMA layer due to gravity. Testing composite specimens in a horizontal OT setup might solve the problem.

Overall, the modified OT proposed in this study was unsuccessful. More research is needed to find a better way of testing HMA overlays constructed over a pre-cracked stabilized base against reflective cracking.

5.2 Testing results of the conventional OT specimens

In this study, three replicate specimens were prepared for OT testing from each asphalt mixture designation mentioned earlier in Table 11. These replicates were tested in two different temperatures and under one-phase loading at a maximum displacement of 0.025 in. (0.63 mm) until 93% peak tensile load reduction or 1,000 cycles of loading. The load, displacement, and time histories as well as the hysteresis behavior during the first loading cycle for each tested replicate are shown in Appendix B. Table 12 summarizes the N_{OT}, G_c, and CPR results calculated for all tested specimens using the data collected from the OT tests.

From Table 12, it can be observed that only the specimens prepared with unmodified PG 67-22 binder and 20% RAP and tested at low temperature (10°C) reached the failure criterion. It means the use of softer asphalt binder, incorporation of 20% RAP, and low temperature testing made this mixture fail before reaching 1,000 loading cycles. The average number of cycles to failure (N_{OT}) for this mixture was 324 which means this mixture might not experience premature reflective cracking during its service life. However, the COV is higher (i.e., 31%) than the acceptable limit (COV $\leqslant$ 30%). For the other mixtures, it was not possible to calculate NOT because no specimen exhibited a 93% maximum tensile load reduction before reaching 1,000 loading cycles. The mixtures prepared in this study were unaged which might result in the majority of the specimens (i.e., 87.5%) not to fail within 1,000 loading cycles.

In general, it can be observed from Table 12, that the specimens tested at low temperature exhibited higher critical fracture energy (G_c) values, which exceeds the soft crack-resistant limit (>3 lb-in./in^2), as compared with the specimens tested at room temperature. On the other hand, the specimens tested at low temperature exhibited lower Crack Progression Rate (CPR) values as compared with the specimens tested at room temperature. The CPR values of all the specimens were lower than the acceptance limit (i.e., 0.5) to become crack susceptible. The COV values for both G_c and CPR were lower than 30% which indicated good repeatability of the collected data. The average hysteresis behavior of all the specimens is presented in Figure 38. To comparatively evaluate the performance of the specimens, the normalized load reduction curves are superimposed. The average variation of the normalized peak load with respect to loading cycles obtained for all the specimens is summarized in Figure 39. The abscissa is converted into a logarithmic scale. The acceptable limit (i.e., Normalized Peak Load vs No of cycles plot using CPR = 0.5) is also shown in Figure 39.

From Table 12, it can be observed that only the specimens prepared with unmodified PG 67-22 binder and 20% RAP and tested at low temperature (10°C) reached the failure criterion. It means

the use of softer asphalt binder, incorporation of 20% RAP, and low temperature testing made this mixture fail before reaching 1,000 loading cycles. The average number of cycles to failure (N_{OT}) for this mixture was 324 which means this mixture might not experience premature reflective cracking during its service life. However, the COV is higher (i.e., 31%) than the acceptable limit (COV ≤ 30%). For the other mixtures, it was not possible to calculate N_{OT} because no specimen exhibited a 93% maximum tensile load reduction before reaching 1,000 loading cycles.

Table 12. The OT results for all specimens tested in this study.

Mixture	Sp.	Avg. Air Voids (%)	Avg. Max Tensile load (lb)	N_{OT}	Gc (lb.-in/in^2)				CPR			
					Gc	Avg.	STD	COV (%)	CPR	Avg.	STD	COV (%)
PG76-0RAP-25C	1	7.6	553.3	N/A	2.064	2.134	0.120	5.6	0.238	0.235	0.010	4.4
	2				2.273				0.243			
	3				2.066				0.223			
PG76-0RAP-10C	1	7.5	1189.1	N/A	6.900	6.627	0.292	4.4	0.180	0.170	0.09	5.1
	2				6.661				0.164			
	3				6.319				0.166			
PG67-0RAP-25C	1	7.1	527.1	N/A	2.957	2.392	0.489	20.5	0.211	0.243	0.029	11.8
	2				2.126				0.266			
	3				2.094				0.253			
PG67-0RAP-10C	1	7.3	1277.1	N/A	3.669	4.309	0.555	12.9	0.171	0.172	0.007	4.1
	2				4.655				0.179			
	3				4.603				0.165			
PG76-20RAP-25C	1	7.2	595.1	N/A	1.744	1.778	0.116	6.5	0.325	0.276	0.045	16.2
	2				1.907				0.237			
	3				1.907				0.224			
PG76-20RAP-10C	1	7.1	1037.2	N/A	3.209	3.497	0.273	7.8	0.129	0.145	0.018	12.5
	2				3.528				0.142			
	3				3.753				0.165			
PG67-20RAP-25C	1	7.4	509.0	N/A	1.979	1.949	0.151	7.7	0.219	0.215	0.003	1.5
	2				1.786				0.213			
	3				2.083				0.214			
PG67-20RAP-10C	1	7.3	1303.2	437	3.705	4.653	0.821	17.7	0.178	0.195	0.015	7.6
	2			288	5.094				0.202			
	3			246	5.159				0.206			

In general, it can be observed from Table 12 that the specimens tested at low temperature exhibited higher critical fracture energy (G_c) values, which exceeds the soft crack-resistant limit (>3 lb-in./in^2), as compared with the specimens tested at room temperature. On the other hand, the specimens tested at low temperature exhibited lower Crack Progression Rate (CPR) values as compared with the specimens tested at room temperature. The CPR values of all the specimens were lower than the acceptance limit (i.e., 0.5) to become crack susceptible. The COV values for both G_c and CPR were lower than 30% which indicated good repeatability of the collected data. The average hysteresis behavior of all the specimens is presented in Figure 38. To comparatively evaluate the performance of the specimens, the normalized load reduction curves are superimposed. The average variation of the normalized peak load with respect to loading cycles

obtained for all the specimens is summarized in Figure 39. The abscissa is converted into a logarithmic scale. The acceptable limit (i.e., Normalized Peak Load vs No of cycles plot using CPR = 0.5) is also shown in Figure 39.

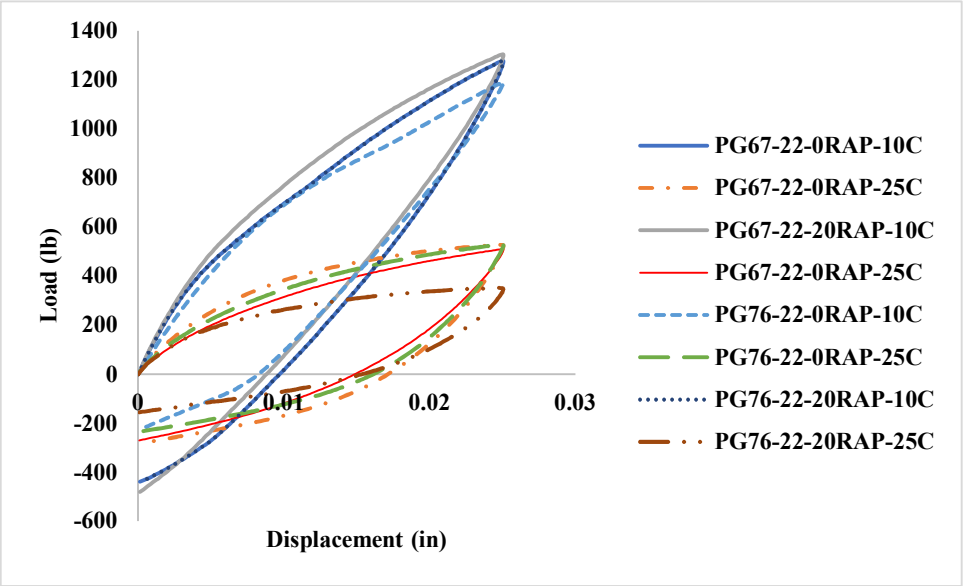

Figure 38. Average first loop hysteresis behavior for all the specimens tested in this study.

It can be observed from Figure 38 that, all the specimens tested in this study exhibited similar hysteresis behaviors. For most cases, specimens prepared with 20% RAP exhibited steeper hysteresis loops as compared with the specimens prepared with 0% RAP.

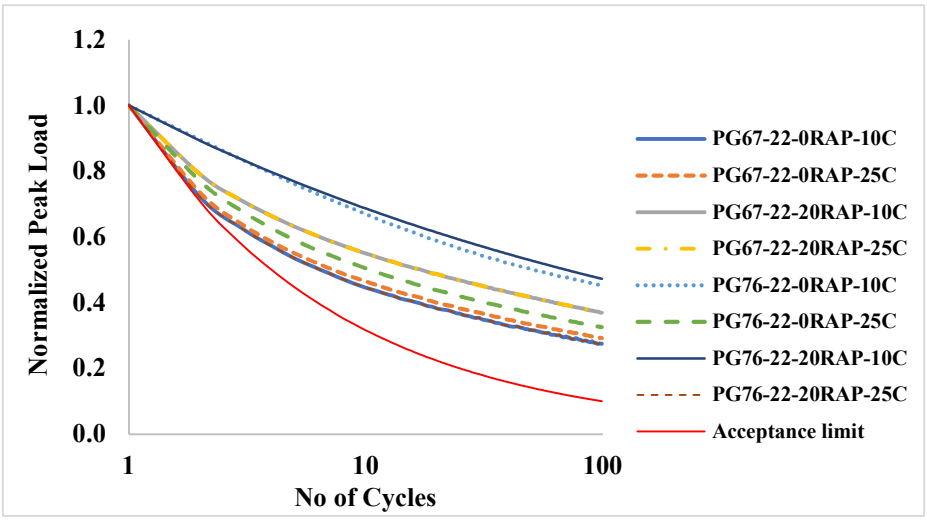

Figure 39. The average normalized peak load reduction curves for all the specimens tested in this study.

From Figure 39, it can be observed that all the replicates showed similar normalized load reduction curves. The average load reduction curve is satisfactorily above the acceptance limit curve and therefore, shows good reflective cracking performance during the crack propagation phase.

5.2.1. Effect of test temperature

In general, for all the mixtures of this study, the average maximum tensile load carried by the mixtures was approximately two times higher when tested at low temperature (10°C) as compared with room temperature (25°C). Therefore, the G_c values increased when test temperature was changed from room temperature to low temperature where the differences in performances were statistically significant (i.e., p-value < 0.001). However, when tested at low temperature (10°C), the critical fracture energy exceeds the upper limit of the soft crack-resistant zone for all the cases. It means the resistance of the specimens during crack initiation was enhanced at low temperature. Gc values for all the specimens were within the acceptable limit (COV < 30%). The PG 76-22-0RAP-10C showed the maximum G_c value (i.e., 6.63 lb-in/in^2) and thereby, exhibited best performance in crack initiation stage as expected. On the other hand, PG76-20RAP-25C, with minimum G_c value (i.e., 1.78 lb-in/in^2) performed worst in crack propagation.

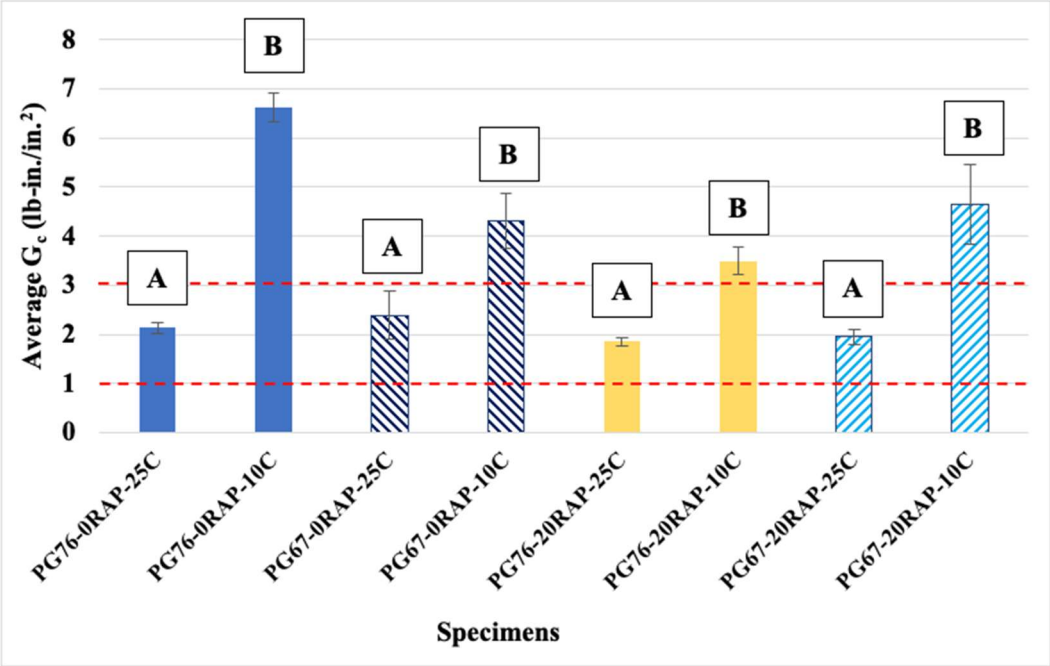

Figure 40. Comparison of the average critical fracture energy (G_c) values of the specimens based on change in test temperature.

The CPR values obtained for all the replicates were below the preliminary failure limit (CPR = 0.5) as presented in Figure 41. It means all the specimens became more flexible to attenuate the crack propagation after crack initiation. For all the specimens, the average CPR values were lower when the mixtures were tested at low temperature (10°C) as compared to room temperature (25°C) where the difference in performances were statistically significant (i.e., p-value < 0.001). It means a decrease in test temperature increased the flexibility of the specimens and therefore, increased the ability of the specimens to attenuate crack propagation. The PG76-20RAP-10C samples showed the minimum average CPR value (i.e., 0.145) which indicates best performance in crack propagation while PG76-20RAP-25C samples, with the maximum average CPR value (i.e., 0.243), exhibited worst performance in attenuating crack propagation. Overall, based on G_c and CPR, specimens prepared with PG 76-22 binder and 20% RAP and tested at room temperature provided the worst performance against reflective cracking. The specimens with PG 76-22, 0% RAP and tested at low temperature exhibited best performance in resisting reflective cracking.

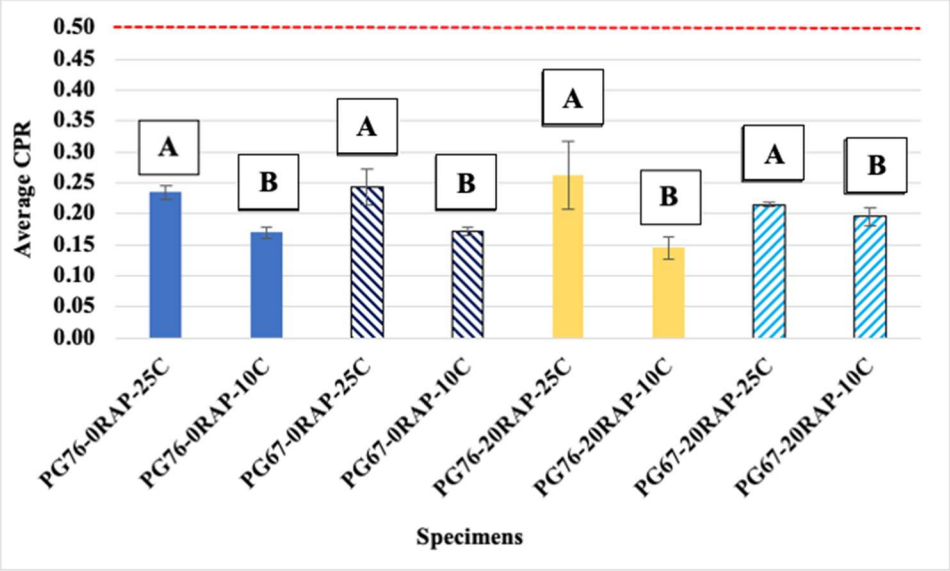

Figure 41. Comparison of the average Crack Progression Rate (CPR) values of the specimens based on change in test temperature.

The average G_c value from each tested specimen is plotted against the average CPR value to obtain the cracking interaction plot as shown in Figure 42. The error bars represent ±1 standard deviation. It can be observed that when the specimens are tested at low temperature all the specimens become stiffer and behave as tough crack resistant. On the other hand, the specimens exhibited soft crack resistant behavior when tested at room temperature. Overall, a reduction in temperature from room to low temperature resulted in the asphalt mixtures to change their behavior from soft crack-resistant mixtures to tough crack-resistant mixtures.

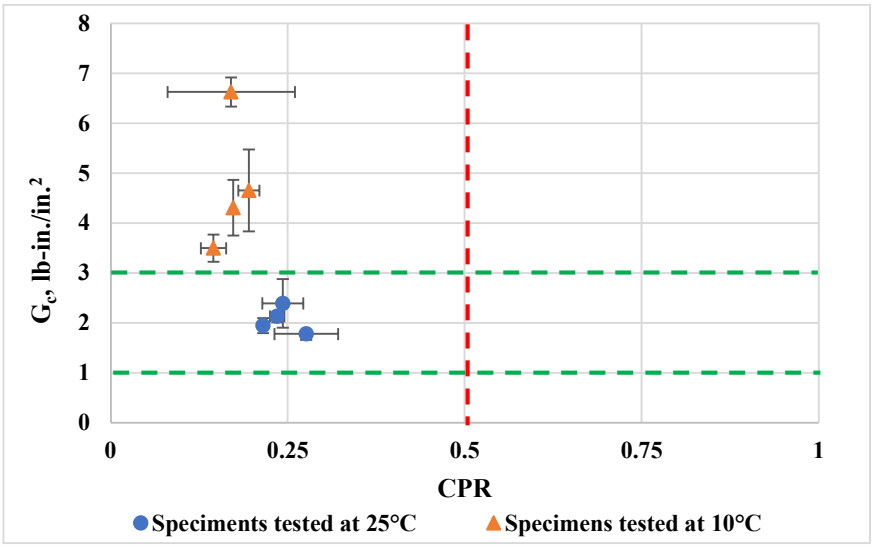

Figure 42. Cracking interaction plot for all the specimens tested – effect of testing temperature.

5.2.2 Effect of binder type

To evaluate the effect of binder type on the reflective cracking performance of the tested asphalt mixture specimens, the G_c and CPR values were plotted, as shown in Figure 43 and Figure 44,

respectively. The average G_c values from each tested mixture were plotted against the average CPR values to obtain the cracking interaction plot as shown in Figure 45. The error bars shown in all these figures represented ±1 standard deviation.

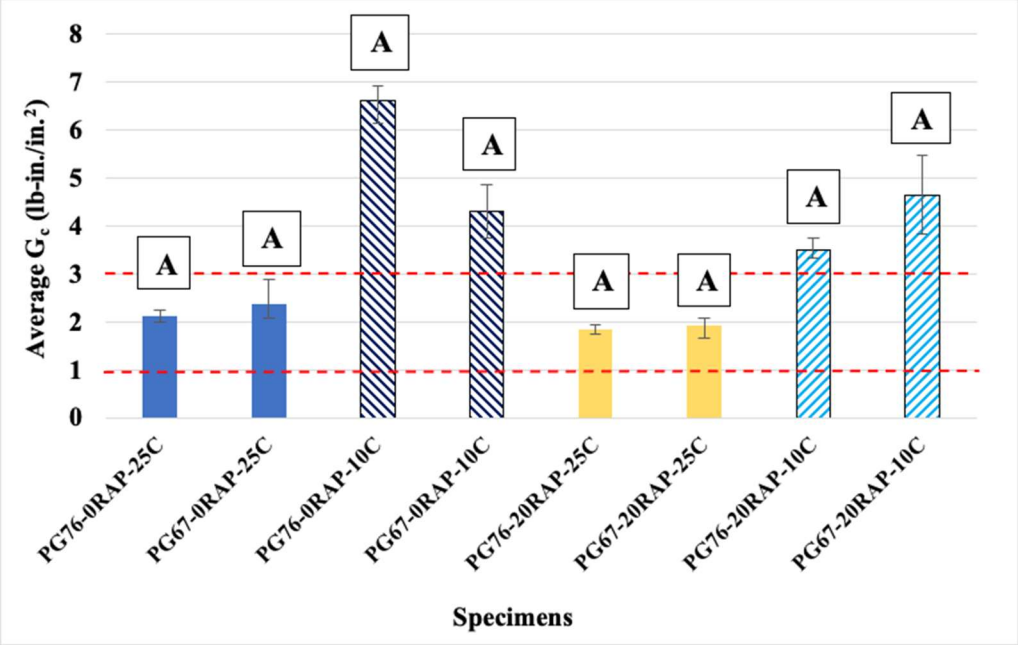

Figure 43. Comparison of the average critical fracture energy (G_c) values of specimens based on change in binder type.

From Figure 43, it can be observed that specimens prepared with PG 67-22 exhibited higher G_c values as compared with the specimens prepared with PG 76-22. It means that, except for PG 67-0RAP-10C, the use of softer binder (unmodified PG 67-22) enhanced the resistance of the specimens to crack initiation which aligned with the findings from the literature (*42*). This opposite trend for PG 67-0RAP-10C might be attribute to the use of stiffer, SBS polymer-modified binder combined with low-temperature testing. These factors might result in an unexpected increase in G_c value for PG76-0-RAP-25C as compared with PG 67-0RAP-10C. However, the differences in G_c values were statistically insignificant (i.e., p-value = 0.77).

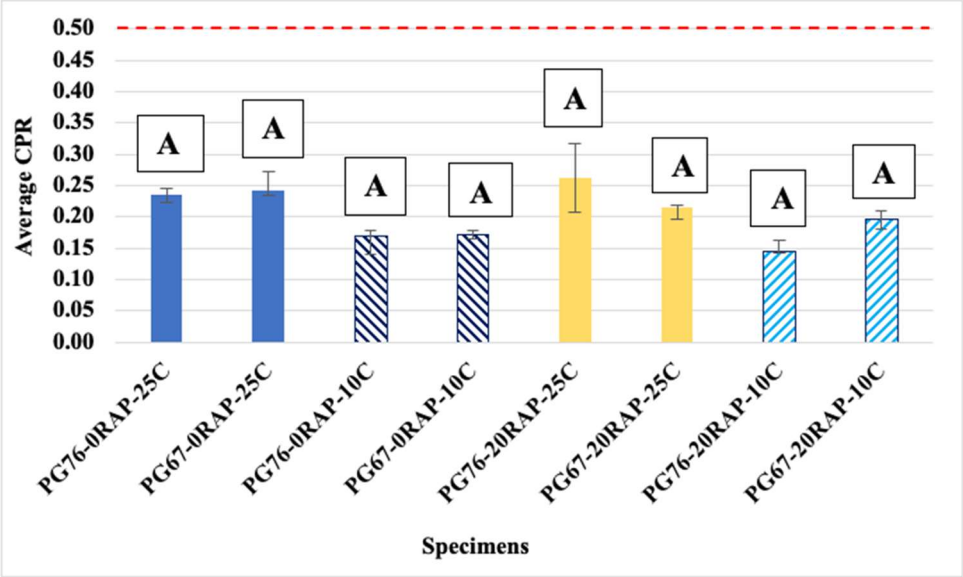

Figure 44. Comparison of the average Crack Progression Rate (CPR) values of specimens based on change in binder type.

From Figure 44, it can be seen that no observable trend in CPR was found when the binder type was changed from PG 76-22 to PG 67-22 and the differences in CPR values were statistically insignificant (i.e., p-value = 0.85). Similarly, the cracking interaction plot (Figure 45) showed that the specimens sometimes behaved as tough crack-resistant while sometimes showed soft crack-resistant behavior. However, CPR values should decrease when a softer binder is used as compared with the use of a stiffer binder (*42*). Further research is needed by incorporating more binder types in the test matrix to understand the true effect of changing binder type on the reflective cracking performance.

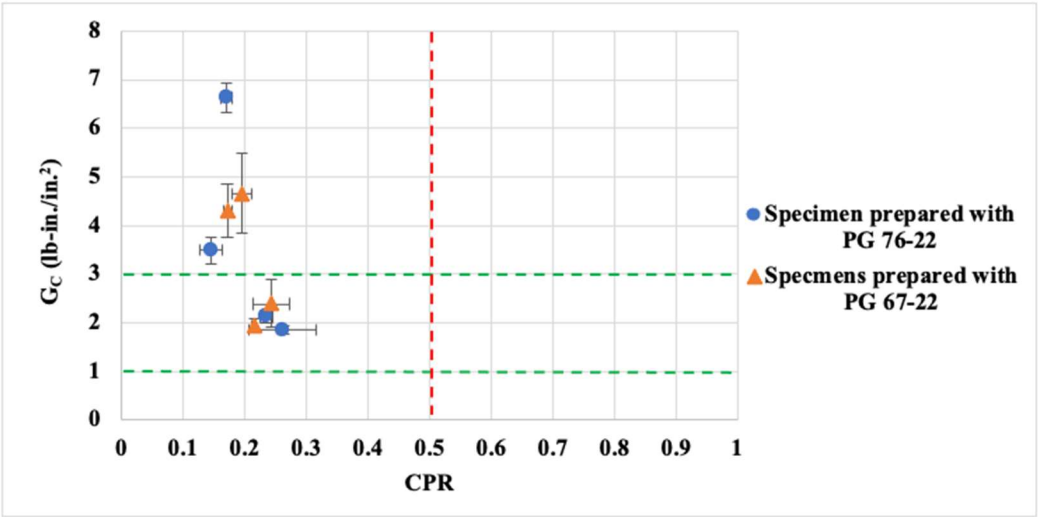

Figure 45. Cracking interaction plot for the specimens tested – effect of binder type.

5.2.3. Effect of RAP content

To evaluate the effect of binder type on the reflective cracking performance of asphalt mixture specimens, the G_c and CPR values were plotted as shown in Figure 46 and Figure 47, respectively.

The average G_c values were plotted against the average CPR values to obtain the cracking interaction plot as shown in Figure 45. The error bars shown in all these figures represented ±1 standard deviation.

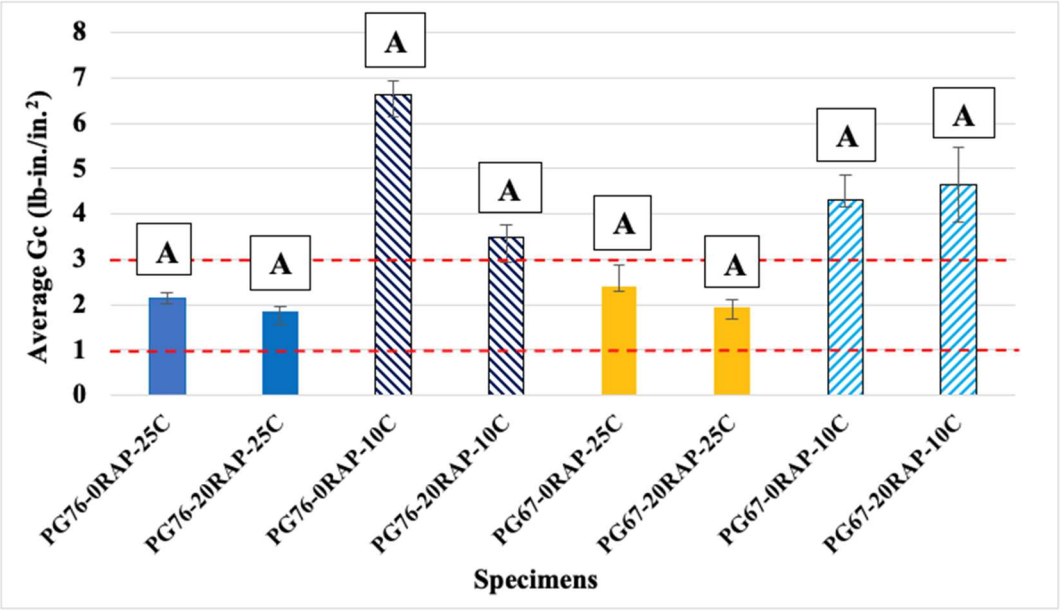

Figure 46. Comparison of the average critical fracture energy (G_c) values of specimens based on change in RAP content.

From Figure 46, it can be observed that, except for PG 67-20RAP-10C the average G_c values decreased when 20% RAP was incorporated into the asphalt mixtures as compared with the asphalt mixture specimens prepared with no RAP. It means that the addition of RAP resulted in the mixtures to become susceptible to crack initiation which aligned with the findings from the literature (*42*). This opposite trend for PG 67-20RAP-10C might be attribute to the combined use of softer binder and low temperature testing which resulted in an unexpected increase in Gc value as compared with PG67-0RAP-10C. However, the differences in G_c values were statistically insignificant (i.e., p-value = 0.19).

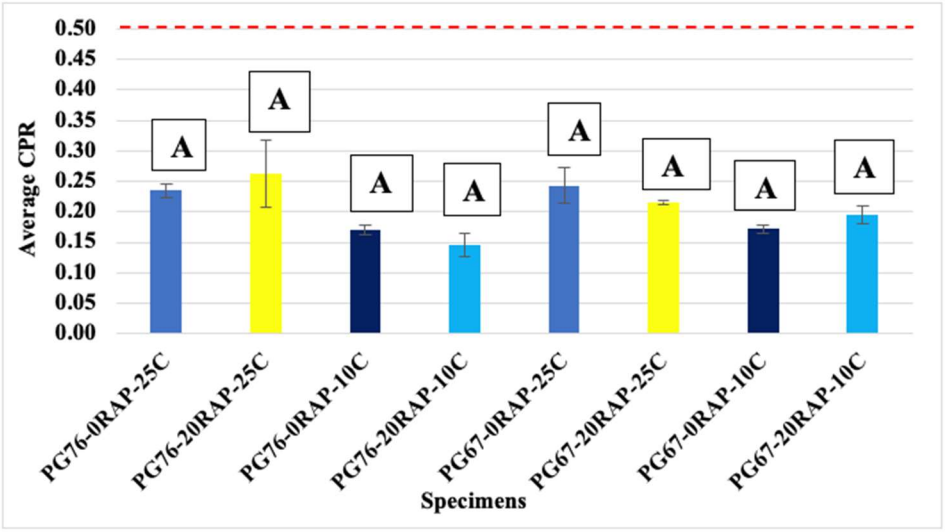

Figure 47. Comparison of the average Crack Progression Rate (CPR) values of the specimens based on change in RAP content.

From Figure 47, it can be seen that there was no observable trend in CPR when the RAP content was changed from 0% to 20%. The differences in CPR values were statistically insignificant (i.e., p-value = 0.85). The cracking interaction plot presented in Figure 48 the specimens sometimes behaved as tough crack-resistant while sometimes showed soft crack-resistant behavior.

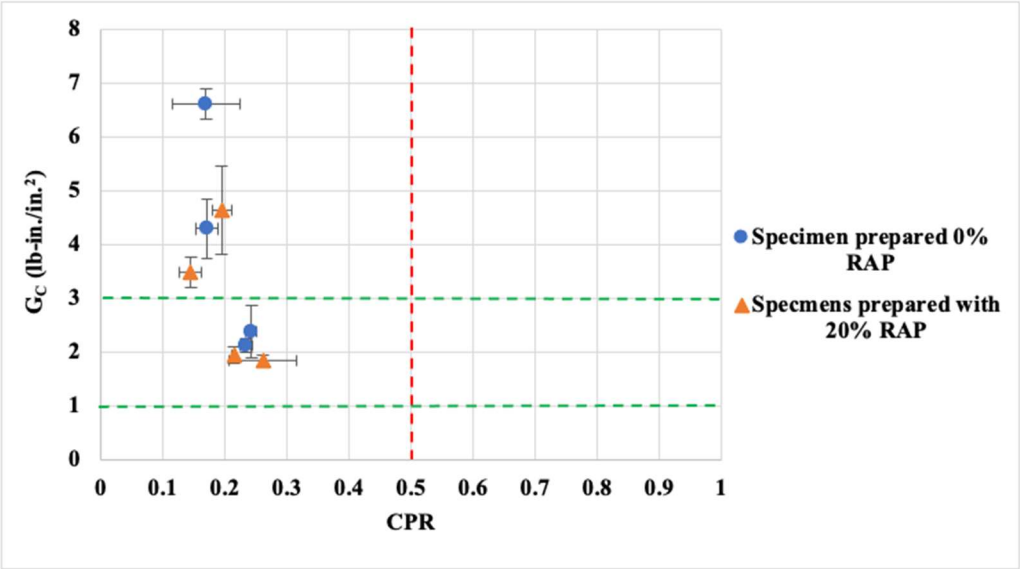

Figure 48. Cracking interaction plot for all the specimens tested – effect of RAP content.

6. CONCLUSION

In this project, an in-depth literature review of the available laboratory tests that simulate reflective cracking phenomenon has been conducted and the best device to simulate thermally-induced reflective cracking in the laboratory was chosen. An attempt has been made in this study is to propose a modification of the test setup selected earlier to test and evaluate an asphalt mixture layer on top of a simulated Cement-Treated Base (CTB) or Cement-Stabilized Base (CSB) layer against reflective cracking. Additionally, the reflective cracking performance of various asphalt mixtures was evaluated using the conventional OT setup. The major findings obtained from this research project are listed below:

- Most of the available test setups that attempt to simulate reflective cracking evaluate the effectiveness of different HMA overlays or anti-reflective cracking products and their resistance to reflective cracking.
- No experimental study has been carried out only to evaluate the resistance of asphalt mixtures to reflective cracking where HMA overlay is constructed above a layer with cracks in its surface.
- The Texas Transportation Institute (TTI) Overlay Tester (OT) is the most suitable equipment to study the performance of asphalt mixtures against thermally-induced reflective cracking in the laboratory due to performance-based results, rapid testing time, reasonable repeatability of the test data, lower equipment cost, strong lab-to-field correlation and the availability of the standard test procedure.
- The attempt of this study to modify the conventional OT setup for better mimicking the field reflective cracking was unsuccessful. The epoxy glue used to attach the HMA layer with the underlying CTB/CSB layer was very strong which prevented the crack to propagate to the HMA layer. When the prime coat was used as a substitute for glue, the prime coat was unable to generate any bond between the top and bottom layers. As a result, the HMA layer slipped when the composite OT specimen was mounted in the vertical OT setup. Testing composite specimens in a horizontal OT setup might solve the problem. Further research is necessary to find a better way of testing HMA overlays constructed over a pre-cracked stabilized base against reflective cracking.
- Only the specimens prepared with unmodified PG 67-22 binder and 20% RAP mixture and tested at low temperature in the conventional OT setup reached the failure criterion. For the other mixtures, it was not possible to calculate N_{OT} because no specimen exhibited a 93% maximum tensile load reduction before reaching 1,000 loading cycles.
- The COV% values for both Critical Fracture Energy (G_c) and Crack Progression Rate (CPR) were well below 30% which indicated good repeatability of the collected data.
- In the conventional OT setup, the G_c values of the specimens increased when testing temperature was decreased from room to low temperature and the difference in performances were statistically significant. The opposite trend was true for Crack Progression Rate (CPR) which decreased with a decrease in test temperature and the performances were significantly different. Overall, the cracking interaction plot showed that a reduction of test temperature from room to low resulted in the asphalt mixtures to change their behavior from soft crack-resistant to tough crack-resistant specimens. The

specimens prepared with PG 76-22, 0% RAP and tested at low temperature exhibited best performance reflective cracking.

- When tested in conventional OT setup, specimens prepared with unmodified softer binder (PG 67-22) exhibited higher G_c values in most cases as compared with the specimens prepared with SBS polymer-modified, stiffer binder (PG 76-22) where the performances were statistically equivalent. On the contrary, no observable trend was found in CPR values when binder type was changed since the specimens sometimes behaved as tough crack-resistant while sometimes showed soft crack-resistant behavior. Further research is necessary to understand the true effect of changing binder type on the reflective cracking performance.
- In most cases, the average G_c values decreased when 20% RAP was incorporated into the asphalt mixtures as compared with the asphalt mixture specimens prepared with no RAP However, like the effect of changing binder type, no observable trend was found in CPR values due to the incorporation of RAP to the asphalt mixtures.
- All the specimens tested in this study using conventional OT setup exhibited CPR values well below the limit to become crack susceptible which indicated good performance in crack propagation stage or fatigue cracking.

REFERENCES

1. Baek, J, and Al-Qadi, I. L. Finite Element Method Modeling of Reflective Cracking Initiation and Propagation: Investigation of the Effect of Steel Reinforcement Interlayer on Retarding Reflective Cracking in Hot-Mix Asphalt Overlay. *Transportation Research Record: Journal of the Transportation Research Board,* 2006 :32–42. https://doi.org/10.3141/1949-04.

2. Mushota, C., Mwale, M. C., Mutembo, G., Muya, M., and Walubita, L. F. Reflective Cracking on Cement Treated Base (CTB) Pavements in Zambia: An Analytical Study. *Application of Nanotechnology in Pavements, Geological Disasters, and Foundation Settlement Control Technology GSP,* 2014. 244:62–69.

3. Adaska, W. S., and Luhr, D. R. Control of Reflective Cracking in Cement-Stabilized Pavements. In *Proceedings of the 5th International RILEM Conference*, 2004: 309–316.

4. Petit, C., Al-Qadi, I. L, and Millien, A. Cracking in Pavements- Mitigation, Risk Assessment and Prevention. In *Proceedings of the 5th International RILEM Conference,* 2004.

5. Elseifi, M., and Bandaru, R. *Cost Effective Prevention of Reflective Cracking of Composite Pavement*. FHWA/LA.11/478 4, U.S. Department of Transportation, 2011.

6. Owusu-Antwi, E. B., Khazanovich, L., and Titus-Glover, L. Mechanistic-Based Model for Predicting Reflective Cracking in Asphalt Concrete–Overlaid Pavements. *Transportation Research Record*, 1998.

7. Loria-Salazar, L. G. *Reflective Cracking of Flexible Pavements : Literature Review, Analysis Models, and Testing Methods*. University of Nevada, Reno, 2008.

8. Elseifi, M., and Dhakal, N. Mitigation Strategies of Reflection Cracking in Pavement. Final Report 541, 2015.

9. Germann, F. P., and Lytton, R. L. *Methodology for Predicting the Reflection Cracking Life of Asphalt Concrete Overlays*. Technical Report, FHWA/TX-79/09+207-5, 1979. College Station, Texas 77843-3135.

10. Halsted, G. E, Luhr, D. R., and Adaska, W. S. Guide to Cement-Treated Base (CTB), 2006.

11. Alneami, A. H., and Almudadi, T. H. A Laboratory Tool Used to Evaluate the Reflective Cracking in Overlay Asphalt Pavement. *Al-Rafidain Engineering,* 2006. 19 (3): 11–25.

12. Kader, P., Baran, R. G., and Gordon, R. G. The Performance of CTB Pavements under Accelerated Loading - The Beerburrum ALF Trail 1986/87, 1989. Victoria, Australia.

13. Caltabiano, M.A., and Rawlings, R. E. Treatment of Reflection Cracks in Queensland. In *Proceedings of the 7th International Conference on Asphalt Pavements, The University of Nottingham, U.K,* 1992.

14. Kota, P. B. V. S., Scullion, T., and Little, D. N. "Investigation of Performance of Heavily Stabilized Bases in Houston, Texas District." *Transportation Research Record: Journal of the Transportation Research Board*, 1995.

15. Little, D. N., Scullion, T., Kota, P. B. V. S., and Bhuiyan, J. *Guidelines for Mixture Design of Stabilized Bases and Subgrades*. Technical Report, FHWA/TX-95/1287-3-F, College Station, Texas 77843-3135, 1992.

16. Metcalf, J.B., Rassoulian, M., Romanoschi, S., and Yougqi, L. "The Louisiana Accelerated Loading Facility Report 2: Experiment 1, Phase III." Louisiana Transportation Research Center, Baton Rouge, 1988.

17. Cho, Yoon-Ho, Lee, K. and Ryu, S. "Development of Cement-Treated Base Material for Reducing Shrinkage Cracks." *Transportation Research Record: Journal of the Transportation Research Board,* 2006. 1952 (1): 134–43. https://doi.org/10.3141/1952-15.

18. Halsted, G. E. Minimizing Reflective Cracking in Cement-Stabilized Pavement Bases. *Nova Scotia Pavement Maintenance and Preservation Session*, 2010. 1–10.

19. Chen, Dar-hao, Won, M., Scullion, T., and Bilyeu, J. Minimizing Reflective Cracking With Applications of the Rolling Dynamic Deflectometer and Overlay Tester. In *National Conference on Preservation, Repair, and Rehabilitation of Concrete Pavements, St. Louis Missouri*, 2009. 3–14.

20. Von Quintus, H. L., Lytton, R. L., Mallela, J., Weiss, W., and Shen, S. *Techniques for Mitigation of Reflective Cracks*, Final Report AAPTP 05-04, Airfield Asphalt Pavement Technology Program. Auburn, AL, 2009.

21. Hughes, J. J., and Al-Qadi, I. L. *Evaluation of Steel Paving Mesh*, FHWA Construction Report, FHWA-PA-2002-001, 2001.

22. Zhou, F, and Scullion, T. *Overlay Tester: A Rapid Performance Related Crack Resistance Test*. Technical Report, FHWA/TX-05/0-4467-2, College Station, Texas 77843-3135, 2005.

23. Gaarkeuken, G., Scarpas, A., and de Boundt, A. H.. The Causes and Consequences of Secondary Cracking. Report 7-96-203-23. Division of Road and Railway Construction, Faculty of Civil Engineering, TU-Delft, The Netherlands, 1996.

24. Baek, J. Modeling reflective cracking development in hot-mix asphalt overlays and quantification of control techniques (Doctoral dissertation, University of Illinois at Urbana-Champaign), 2010 .

25. Zhou, F., and Sun, L. Reflection Cracking in Asphalt Overlay on Existing PCC. In *Proceedings of the 9th International Conference on Asphalt Pavements,* 2002.

26. Marchand, J. P., and Goacolou, H. Cracking in Wearing Courses. In *Proceedings of the 5th International Conference on the Structural Design of Asphalt Pavements, Delft*, 1882. 741–777.

27. Portland Cement Association. *Soil-Cement Construction Handbook-Engineering Bulletin,* 1995.

28. Halsted, G. E, Luhr, D. R., and Adaska, W. S. Guide to Cement-Treated Base (CTB), 2006.

29. LaDOTD. Method of Test for Determining the Minimum Cement Content for Incorporation into Soils, Soil-Aggregate, or Aggregate Mixtures for Stabilization and Treatment, DOTD TR 432, 2002.

30. LaDOTD. Method of Test for Moisture-Density Relationships, DOTD TR 418M, 1998.

31. Ismail, A., Baghini, M. S., Karim, M. R., Shokri, F., Al-Mansob, R. A., Firoozi, A. A., and Firoozi, A. A. Laboratory investigation on the strength characteristics of cement-treated base. *Applied mechanics and materials*, 2014. 507:353-360.

32. Adaska, W. S., & Luhr, D. R. Control of reflective cracking in cement stabilized pavements. *In Proceedings of 5th international RILEM conference on cracking in pavements*, 2004. 309-316.

33. Gallego, J., and Prieto, J. N. 2006. New Laboratory Equipment for Study of Reflective Cracking in Asphalt Overlays. *Transportation Research Record,* 2006. 1970 (1): 215–222. https://doi.org/10.3141/1970-25.

34. Prieto, J. N., Gallego, J., and Pérez, I. Application of the Wheel Reflective Cracking Test for Assessing Geosynthetics in Anti-Reflection Pavement Cracking Systems. *Geosynthetics International*, 2007. 14 (5): 287–97. https://doi.org/10.1680/gein.2007.14.5.287..

35. Bennert, T. *Flexible Overlays for Rigid Pavements.* Final Report, FHWA-NJ-2009-014, 2010.

36. Lytton, R. L. Use of Geotextiles for Reinforcement and Strain Relief in Asphalt Concrete. *Geotextiles and Geomembranes,* 1989. 8 (3): 217–37. https://doi.org/10.1016/0266-1144(89)90004-6.

37. Zhou, F., Hu, S., Hu, X., & Scullion, T. *Mechanistic-empirical asphalt overlay thickness design and analysis system*. Report No. FHWA/TX-09/0-5123-3. Texas Transportation Institute, 2009.

38. Williams, R. C., Buss, A., & Chen, C. Reflective crack mitigation guide for flexible pavements, 2015.

39. Sebesta, S. Use of microcracking to reduce shrinkage cracking in cement-treated bases. *Transportation Research Record*, 2005. 1936(1), 2-11.

40. Sebesta, S., & Scullion, T. *Effectiveness of minimizing reflective cracking in cement-treated bases by microcracking*. Report No. FHWA/TX-05/0-4502-1, 2009.

41. F. Zhou, D. Newcomb, C. Gurganus, S. Banihashemrad, M. Sakhaeifar, E. S. Park, and R. L. Lytton. Field Validation of Laboratory Tests to Assess Cracking Resistance of Asphalt Mixtures: An Experimental Design. *Field Validation of Laboratory Tests to Assess Cracking Resistance of Asphalt Mixtures: An Experimental Design*, 2016. https://doi.org/10.17226/23608.

42. Zhou, F., S. Im, S. Hu, D. Newcomb, and T. Scullion. Selection and Preliminary Evaluation of Laboratory Cracking Tests for Routine Asphalt Mix Designs. *Road Materials and Pavement Design*, Vol. 18, 2017, pp. 62–86. https://doi.org/10.1080/14680629.2016.1266741.

43. Millien, A., Dragomir, M. L., Wendling, L., Petit, C., and Iliescu, M. Geogrid Interlayer Performance in Pavements: Tensile-Bending Test for Crack Propagation. In *Proceedings of the 7th RILEM International Conference on Cracking in Pavements*, 2012. 1209–1218.

44. Molenaar, A. Evaluation of Pavement Structure with Emphasis on Reflective Cracking. In *Proceedings of the 2nd International RILEM Conference on Reflective Cracking in Pavements*, 1993. 21–48.

45. De Bondt, A. H. *Anti-Reflective Cracking Design of Reinforced Asphalt Overlays*, Ph.D. Dissertation, Department of Civil Engineering, Delft University of Technology, Delft, the Netherlands, 1998.

46. Di Benedetto, H., Neji, J., Antoine, J. P., and Pasquier, M. Apparatus for Laboratory Study of Cracking Resistance. In *Proceedings of the 2nd International RILEM Conference on Reflective Cracking in Pavements*, 1993. 179–186.

47. Dempsey, B. J. Development and Performance of Interlayer Stress-Absorbing Composite in Asphalt Concrete Overlays. *Transportation Research Record: Journal of the Transportation Research Board,* 2002. 1809 (1): 175–183.

48. Tschegg, E. K, Stanzl-Tschegg, S. E., and Litzka, J. New Testing Method to Characterize Mode I Fracturing of Asphalt Aggregate Mixtures. In *Proceedings of 2nd International RILEM Conference on Reflective Cracking in Pavements*, 1993. 236–245.

49. Montestruque, G., Rodrigues, R., Nods, M., and Elsing, A. Stop of Reflective Crack Propagation with the Use of Pet Geogrid as Asphalt Overlay Reinforcement. *5th International RILEM Conference on Cracking in Pavements*, 2004, 231–238.

50. Yu, B., Lu, Q., and Yang, J. Evaluation of Anti-Reflective Cracking Measures by Laboratory Test. *International Journal of Pavement Engineering,* 2013. 14(6): 553–60. https://doi.org/10.1080/10298436.2012.721547.

51. Sobhan, K., Crooks, T., Tandon,V., and Mattingly, S. Laboratory Simulation of the Growth and Propagation of Reflection Cracks in Geogrid Reinforced Asphalt Overlays. *Proceedings of the 5th International RILEM Conference on Cracking in Pavements-Mitigation, Risk Assesment and Prevention,* 2004. 4 (1): 589–596.

52. Denolf, K., Visscher, J. D., and Vanelstraete, A. Performance of Anti-Cracking Interface Systems on Overlaid Cement Concrete Slabs – Development of Laboratory Test to Simulate Slab Rocking. In *Proceedings of the 7th RILEM International Conference on Cracking in Pavements*, 2012. 1169–80. https://doi.org/10.1007/978-94-007-4566-7_111.

53. Grzybowska, W. Wojtowicz, J., and Fonferko, L. C. Application of GeoSynthetics to Overlays in Cracow Region of Poland." In *Proceedings of the 2nd International RILEM Conference on Reflective Cracking in Pavements*, 1993, 290-298.

54. Gallego, J., and Prieto, J. N. "Development of New Laboratory Equipment for the Study of Reflective Cracking in Asphalt Overlays." *Asphalt Overlays and Infrastructure Distress, 2006*.

55. Gibney, A, Lohan, G., and Moore, V. Laboratory Study of Resistance of Bituminous Overlays to Reflective Cracking. *Transportation Research Record: Journal of the Transportation Research Board,* 2007. 1809 (1): 184–90. https://doi.org/10.3141/1809-20.

56. Gonzalez-Torre, I., Calzada-Perez, M. A., Vega-Zamanillo, A., and Castro-Fresno, D. Evaluation of Reflective Cracking in Pavements Using a New Procedure That Combines Loads

with Different Frequencies. *Construction and Building Materials*, 2015. 75: 368–374. https://doi.org/10.1016/j.conbuildmat.2014.11.030.

57. Pais, J. The Reflective Cracking in Flexible Pavements. *Romanian Journal of Transport Infrastructure,* 2013. 2 (1): 63–87. https://doi.org/10.1515/rjti-2015-0012.

58. Dumas, Ph., and Vecoven, J. 1993. "Processes Reducing Reflective Cracking: Synthesis of Laboratory Tests." In *Proceedings of the 2nd International RILEM Conference on Reflective Cracking in Pavements*, 220–226.

59. Tamagny, P., Wendling, L., and Piau, J. M. A New Explanation of Pavement Cracking from Top to Bottom: The Visco-Elasticity of Asphalt Materials. In *Proceedings of the 5th International RILEM Conference on Cracking in Pavements-Mitigation, Risk Assesment and Prevention.*, 2004. 425–32.

60. Moreno-Navarro, F., and Rubio-Gámez, M. C. UGR-FACT Test for the Study of Fatigue Cracking in Bituminous Mixes. *Construction and Building Materials,* 2013. 43: 184–90. https://doi.org/10.1016/j.conbuildmat.2013.02.024.

61. Pais, J. The Reflective Cracking in Flexible Pavements. *Romanian Journal of Transport Infrastructure,* 2013. 2 (1): 63–87. https://doi.org/10.1515/rjti-2015-0012.

62. Yu, B., Cao, B., and Yang, J. Laboratory Simulation of Reflective Cracking by Load. In *Proceedings of the AR2009 Conference, Nanjing, China*, 2009.

63. Tex-248-F. Test Procedure for Overlay Test, 2017.

64. Cleveland, G. S., Lytton, R. L. and Button, J. W. Reinforcing Benefits of Geosynthetic Materials in Asphalt Concrete Overlays Using Pseudo Strain Damage Theory. *Transportation Research Board*, 2003.

65. Button, J. W., and Hunter, T. G. *Synthetic Fibers in Asphalt Paving Mixtures.* Final Report, College Station, Texas 77843-3135, 1984.

66. Button, J. W., J. A. Epps, and R. L. Lytton. *Laboratory Evaluation of Miraf Fabrics for Pavement Overlays*. College Station, Texas 77843-3135, 1983.

67. Button, J. W., and J. A. Epps. *Evaluation of Fabric Interlayers*. College Station, Texas 77843-3135, 1982.

68. Pickett, D. L, and Lytton, R. L. *Laboratory Evaluation of Selected Fabrics for Reinforcement of Asphaltic Concrete Overlays*. Technical Report, College Station, Texas 77843-3135, 1983.

69. Button, J. W., and Lytton, R. L. Evaluation of Fabrics, Fibers, and Grids in Overlays. In *Proceedings of the International Conference on Structural Design*. The University of Michigan, 1987.

70. Cleveland, G. S., Lytton, R. L. and Button, J. W. Using Pseudostrain Damage Theory to Characterize Reinforcing Benefits of Geosynthetic Materials in Asphalt Concrete Overlays. *Transportation Research Record: Journal of the Transportation Research Board*, 2007. 1849 (1): 202–211. https://doi.org/10.3141/1849-22.

71. Zhou, F., Hu, S., Chen, D., and Scullion, T. Overlay Tester: Simple Performance Test for Fatigue Cracking. *Transportation Research Record: Journal of the Transportation Research Board*, 2007. 2001 (1): 1–8. https://doi.org/10.3141/2001-01.

72. Zhou, F., and Scullion, T. *Upgraded Overlay Tester and Its Application To Characterize Reflection Cracking Resistance of Asphalt Mixtures*. Technial Report, FHWA/TX-04/0-4467-1, College Station, Texas 77843-3135, 2003.

73. Walubita, L.F., Faruk, A.N., Zhang, J. and Hu, X. Characterizing the cracking and fracture properties of geosynthetic interlayer reinforced HMA samples using the Overlay Tester (OT). *Construction and Building Materials*, 2015. *93*: 695-702.

74. Li, J., Oh, J., Naik, B., Simate, G.S. and Walubita, L.F. Laboratory characterization of cracking-resistance potential of asphalt mixes using overlay tester. *Construction and Building Materials*, 2014. 70: 130-140.

75. Ozer, H., Al-Qadi, I.L., Kanaan, A.I. and Lippert, D.L. Performance characterization of asphalt mixtures at high asphalt binder replacement with recycled asphalt shingles. *Transportation Research Record*, 2013. 2371(1): 105-112.

76. Walubita, L. F., Faruk, A. N., Koohi, Y, Luo, R., Scullion, T., and Lytton, R. L. *The Overlay Tester (OT): Comparison with Other Crack Test Methods and Recommendations for Surrogate Crack Tests.* Technical Report, FHWA/TX-13/0-6607-2, College Station, Texas 77843-3135, 2012.

77. Walubita, L. F., Faruk, A. N., Das, G., Tanvir, H. A., Zhang, J., and Scullion, T. *The Overlay Tester: A Sensitivity Study to Improve Repeatability and Minimize Variability in the Test Results.* Technical Report, FHWA/TX-12/0-6607-1, College Station, Texas 77843-3135, 2012.

78. Chowdhury, A, Button, J. W., and Lytton, R. L. *Tests of HMA Overlays Using Geosynthetics to Reduce Reflection Cracking*. Technical Report, FHWA/TX-10/0-1777-3, College Station, Texas 77843-3135, 2009.

79. Cleveland, G. S., Button, J. W., and Lytton, R. L. *Geosynthetics in Flexible and Rigid Pavement Overlay Systems to Reduce Reflection Cracking.* Technical Report, FHWA/TX-02/1777-1, College Station, Texas 77843-3135, 2003.

80. Zhou, F., Im, S., Hu, S., Newcomb, D., & Scullion, T. Selection and preliminary evaluation of laboratory cracking tests for routine asphalt mix designs. *Road Materials and Pavement Design*, 2017. 18(1): 62-86.

81. Mogawer, W. S., Austerman, A. J., Bonaquist, R., & Roussel, M. Performance characteristics of thin-lift overlay mixtures: High reclaimed asphalt pavement content, recycled asphalt shingles, and warm-mix asphalt technology. *Transportation Research Record*, 2011. 2208(1), 17-25.

82. Porras, J. D., Hajj, E. Y., Sebaaly, P. E., Kass, S., and Liske, T. Performance evaluation of field-produced warm-mix asphalt mixtures in Manitoba, Canada. *Transportation Research Record*, 2012. 2294(1), 64-73.

83. Al-Qadi, I. L., Lippert, D. L., Wu, S., Ozer, H., Renshaw, G., Murphy, T. R., and Said, I. M. *Utilizing Lab Tests to Predict Asphalt Concrete Overlay Performance.* Illinois Center for Transportation/Illinois Department of Transportation, 2017.

84. Pan, P., Kuang, Y., Hu, X., and Zhang, X. A comprehensive evaluation of rejuvenator on mechanical properties, durability, and dynamic characteristics of artificially aged asphalt mixture. *Materials*, 2018. 11(9), 1554.

85. Garcia, V. M., & Miramontes, A. Understanding Sources of Variability of Overlay Test Procedure. *Transportation Research Record,* 2015. 2507(1), 10-18.

86. Garcia, V. M., Miramontes, A., Garibay, J., Abdallah, I., and Nazarian, S. *Evaluation of Operational Variables That Can Improve Overlay Tester Results.* Report No. 16-2317, 2016.

87. Garcia, V. M., Miramontes, A., Garibay, J., Abdallah, I., Carrasco, G., Lee, R., and Nazarian, S. Alternative methodology for assessing cracking resistance of hot mix asphalt mixtures with overlay tester. *Road Materials and Pavement Design*, 2017. 18(4): 388-404.

88. Garcia, V. M., Miramontes, A., Garibay, J., Abdallah, I., and Nazarian, S. Assessing Crack Susceptibility of Asphalt Concrete Mixtures with Overlay Tester. *Journal of Testing and Evaluation*, 2018. 46(3): 924-933.

89. Garcia, V.M., Garibay, J., Abdallah, I., and Nazarian, S. Evaluation of Interchangeability of Commercially Available Overlay Tester Devices. *Airfield and Highway Pavements 2019: Testing and Characterization of Pavement Materials*, 2019. 20-28.

90. Zhou, F., Karki, P., and Im, S. Development of a Simple Fatigue Cracking Test for Asphalt Binders. Transportation Research Record, 2017. 2632(1), 79-87.

91. Cao, W., Wang, Y., & Wang, C. (2019). Fatigue characterization of bio-modified asphalt binders under various laboratory aging conditions. *Construction and Building Materials*, 2019. 208:686-696.

92. LaDOTD. Louisiana Standard Specifications for Roads and Bridges, 2018.

93. Zhou, F., Hu, S., and Scullion, T. *Integrated Asphalt (Overlay) Mixture Design, Balancing Rutting and Cracking Requirements*. Technical Report, FHWA/TX-06/0-5123-1, 2006.

94. Garcia, V., A Cracking Methodology to Assess Fracture and Fatigue Properties of Asphalt Concrete Mixtures using Overlay Tester. Open Access Theses & Dissertations, 2016.

95. Garcia, V., Miramontes, A., Garibay, J., Abdallah, I., and Nazarian, S. *Improved overlay tester for fatigue cracking resistance of asphalt mixtures*. Research Report 0-6815-1. Center for Transportation Infrastructure Systems, The University of Texas at El Paso, El Paso, TX, 2017.

APPENDIX A: PROPOSED PROCEDURRE OF PREPARING CTB/CSB SPECIMENS

Sample

Obtain a representative sample of the soil to be stabilized/treated weighing 1,400 g (3.09 lb.).

Procedure

A. Sample Preparation
   1. Prepare the sample in accordance with DOTD TR 411M. Discard any material retained on the 4.75 mm (No. 4) sieve.
   2. Record the optimum moisture content (DB) from the moisture-density relationship (i.e., 14.4%).
   3. Determine the design moisture content (DM) to the nearest 0.1% using Equation A1:

$$DM = DB + V \quad [A1]$$

where:
DB = optimum moisture content (%) for raw or lime treated material; and
V = constant (1.0% for A-4, A-6 or lime treated soils and 0.5% for other soils)

   4. Dry the representative portion to a constant mass in accordance with DOTD TR 403 and TR 411M to eliminate the effects of hygroscopic moisture.
   5. Remove the dried material from the oven within 24 hours of beginning specimen preparation. Place the material in a container and seal it to protect it from moisture contamination coming from the air during its cooling period.

B. Specimen preparation
   1. Pour the required quantity of dry soil (i.e., 690 g for CTB or 653 g for CSB) in each of two separate mixing pans.
   2. Determine the quantity of water needed to bring each portion to the slaked moisture content (M) using Equation A2:

$$M = \frac{K\,(DM - 5)}{100} \quad [A2]$$

where:
K = mass of test specimen (dry soil + cement); and
DM = design moisture content, %

   3. Add the proper quantity of slake water to each portion and mixed thoroughly.
   4. Cover and protect each portion to which slake water has been added to keep constant moisture content. Allow the portions to slake for a minimum of 30 minutes.
   5. Add a proper quantity of cement (6% and 12% by weight of dry soil) to each portion (i.e., 41.4 g for CTB or 78.4 g for CSB) and mix thoroughly.
   6. Determine the quantity of net water (N) using the following Equation A3:

$$N = L + 0.05K \quad [A3]$$

where:
L = Evaporation = 0.01 x K

   7. Add the proper quantity of net water to each specimen immediately to each portion and mix thoroughly. Record the time of net water addition.

8. Cover the test specimens and protect those to keep a constant moisture content. Allow the specimens to stand for 60 minutes. Time the beginning of molding specimens was to ensure that the molding of specimens is completed within 90 minutes of cement addition.

C. Molding the specimens

1. Assemble the mold by combining all the parts (Figure A1a). Attach the collar and use clamps parallel to the longitudinal direction to provide adequate confinement (Figure A1b)

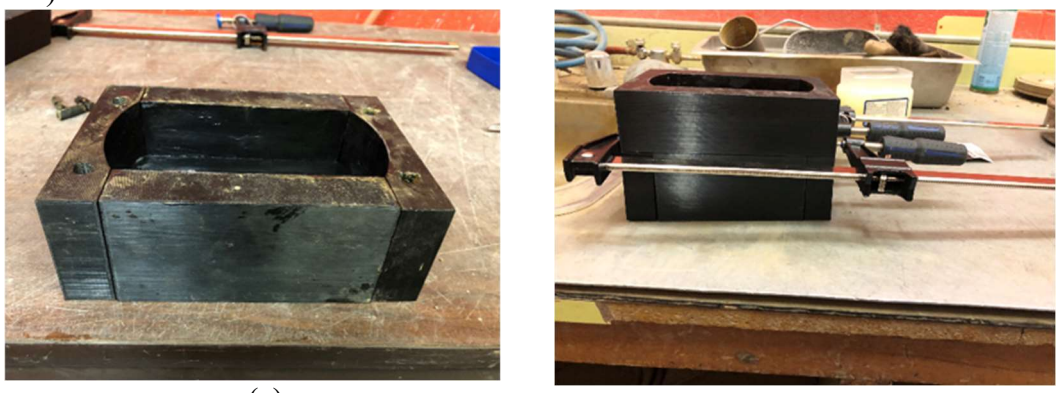

(a) (b)

Figure A1. Assembling the mold and attaching the clamps.

2. Place two long plastic wraps perpendicular to each other inside the mold (Figure A2)

Figure A2. Placing plastic wraps inside the mold.

3. Using a small scoop take the treated/stabilized soil in small quantity from the mixing pan and pour it slowly inside the mold carefully avoiding any loss of materials (Figure A3a). Distribute the soil evenly inside the mold using a spatula (Figure A3b). Repeat this process repeated until the entire portion (i.e., 690 g for CTB or 653 g for CSB) is inside the mold.

(a)

(b)

Figure A3. Pouring soil inside the mold using a scoop and spreading it evenly using a spatula.

D. Compaction of the specimens, curing, and demolding

1. The soil in the mold is compacted using a manual rammer (Figure A4). The manual rammer is a metal 5.5 ± 0.05 lb rammer with a circular striking face and a diameter of 2.0 ± 0.01 in. It is arranged to control the height of drop to 12 ± 0.06 in. The compaction is done in one layer and with 34 blows. The number of blows required was calculated to yield the same compaction energy used during the determination of moisture density relationship or minimum cement content (Table 4).

Figure A4. The 5.5 lb. manual rammer used during compaction.

2. Place a wooden piece (having the same shape as the OT specimen) on the poured soil to facilitate uniform load distribution during compaction (Figure A5).

Figure A5. Placement of a wooden piece to facilitate compaction.

3. Conduct compaction by putting the blows over the wooden piece. Provide a total of 34 blows in a way so that the blows are evenly distributed over the specimen. To do this, a sequence was followed as shown in Table A1.

Table A1. The sequence of blows used for compaction.

Phase	Number of blows and location	Location of blows
1	5	Center
2	5	Left, right, left, right, and left
3	5	Center
4	5	Left, right, left, right, and left
5	5	Center
6	5	Left, right, left, right, and left
7	4	Center
Total	34	-

4. Remove the collar and the wooden piece after the end of compaction (Figure A6).

Figure A6. Specimen surface after removing the collar and wooden piece.

5. Notch the specimen using the top part where a steel plate embedded in the middle of the bottom surface.

6. Cover the top surface of the compacted specimen using the remaining portion of the plastic wrap placed before (Figure A7). Put the assembly in a plastic bag so that the specimen becomes inaccessible to moisture.

Figure A7. Wrapping the top surface of the specimen using plastic wraps.

7. Put the specimen inside the assembly in the moist curing room for a curing period of 7 days.
8. After 7 days demold, cover, and protect the specimen for testing.

APPENDIX B: THE LOAD, DISPLACEMENT, TIME HISTORIES, AND THE HYSTERESIS BEHAVIOR DURING THE FIRST LOADING CYCLE FOR EACH TESTED REPLICATE

B.1. Asphalt mixtures (PG 76-22 + 0% RAP) tested at room temperature (25°C)

Three replicates of OT specimens with PG 76-22 asphalt binder and 0% RAP aggregates were tested in OT at room temperature (25°C) under one-phase loading at a maximum displacement of 0.025 in. (0.63 mm) until 93% peak tensile load reduction or 1,000 cycles of loading. For this mixture type (PG 76-22 and 0% RAP), it was impossible to calculate N_{OT} since all the specimens withstood 1,000 cycles before reaching 93% peak tensile load reduction. All specimens were able to withstand more than 300 loading cycles which means this mixture type shows satisfactory cracking performance & might not experience premature reflective cracking during its service life.

All the specimens prepared with PG 76-22 and 0% RAP, and tested at room temperature exhibited similar load, displacement, and time histories as well the hysteresis behavior during the first loading cycle as shown in Figure B1 and Figure B2. It ensures consistency of the raw data obtained from OT testing at room temperature. The maximum tensile load carried by each specimen, average maximum tensile load and standard deviation are presented in Figure B3. Additionally, the reduction of peak load (crack driving force) with number of cycles is shown in Figure B4.

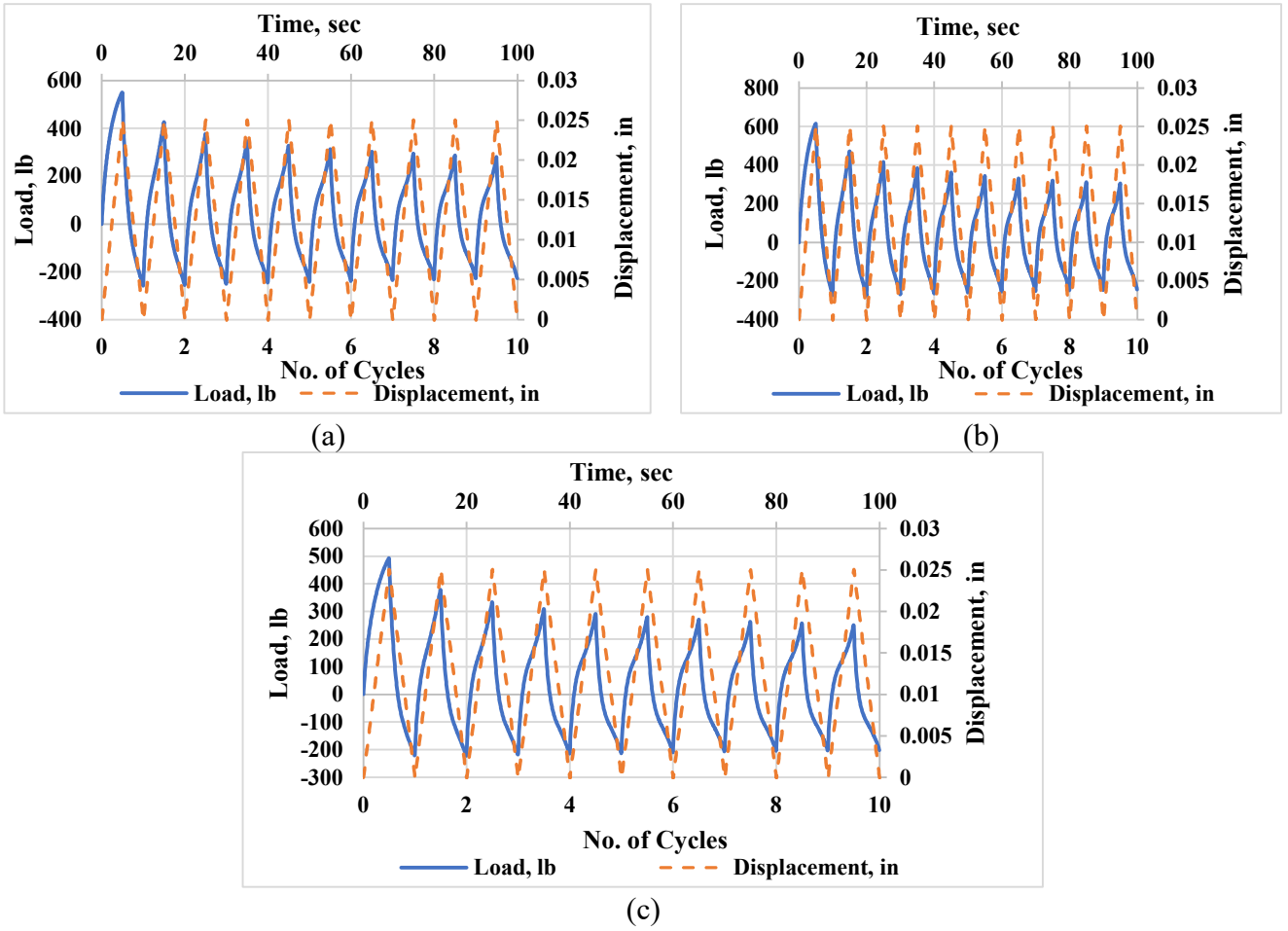

Figure B1. OT load, displacement, and time histories for (a) PG76-22-0RAP-25C-1, (b) PG76-22-0RAP-25C-2, and (c) PG76-22-0RAP-25C-3.

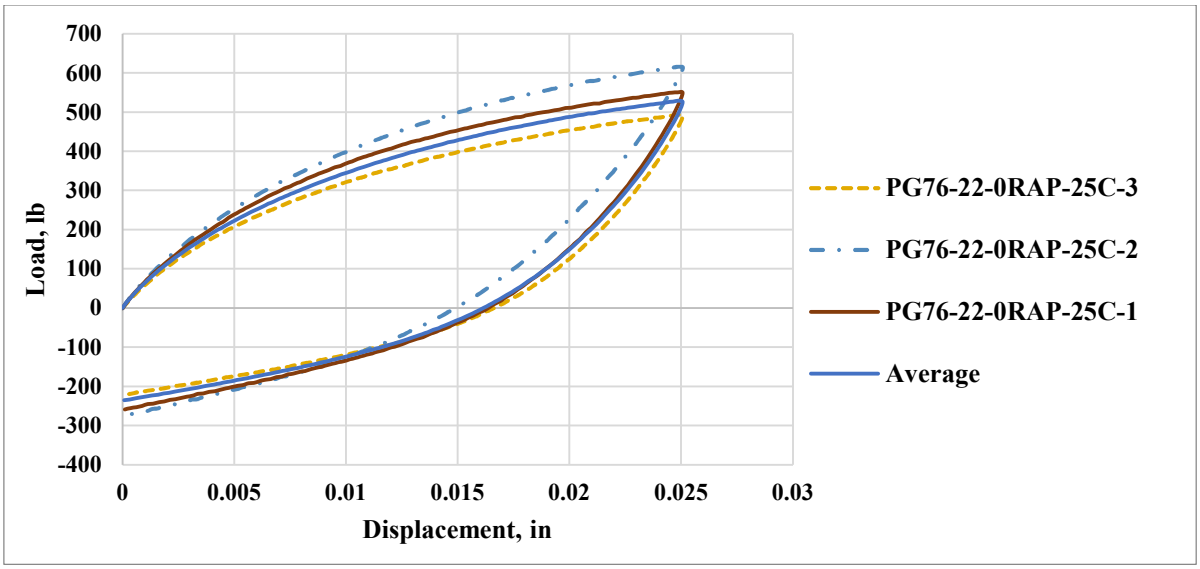

Figure B2. The first hysteresis loops of the OT specimens prepared with PG 76-22 + 0% RAP tested at room temperature.

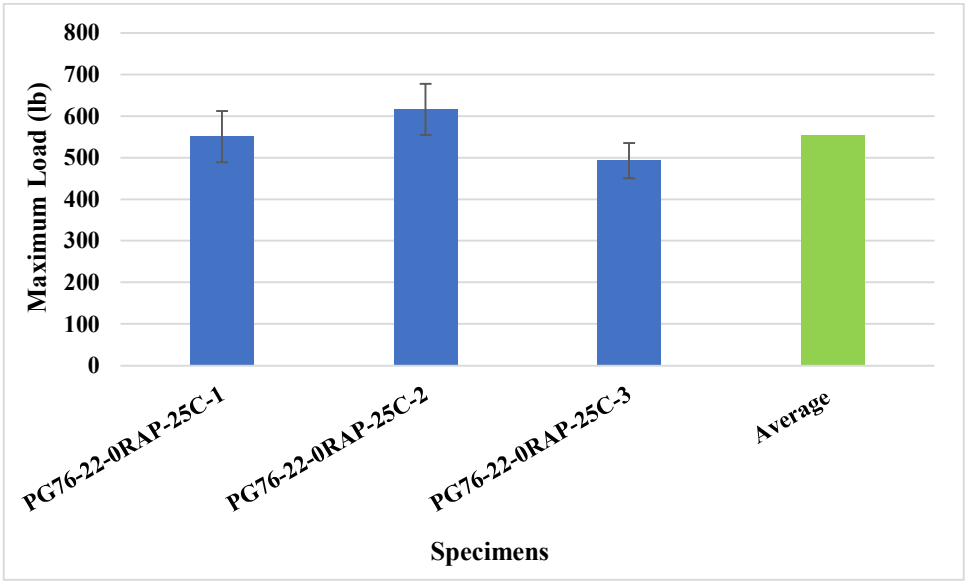

Figure B3. Maximum tensile load carried by OT specimens during the first loading cycle, prepared with PG 76-22 + 0% RAP and tested at room temperature.

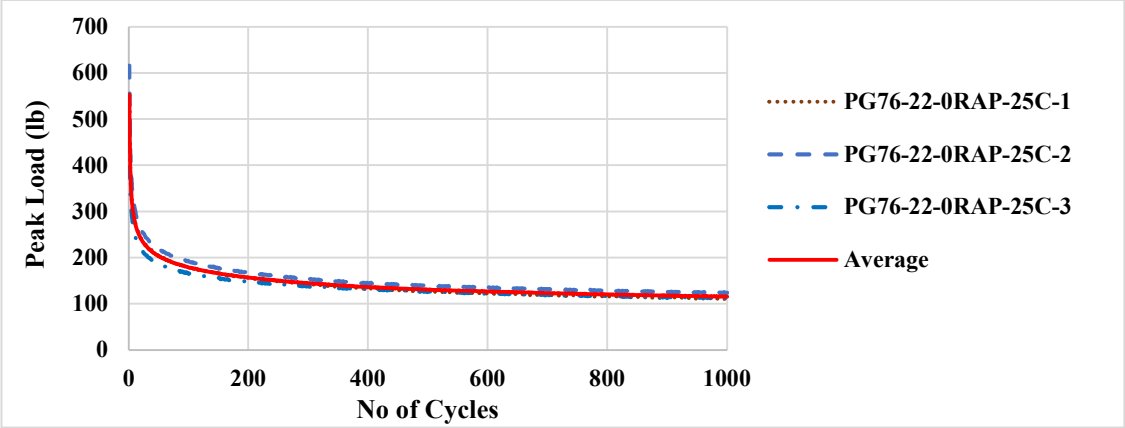

Figure B4. Reduction of crack driving force with respect to loading cycles for the OT specimens, prepared with PG 76-22 + 0% RAP and tested at room temperature.

To comparatively evaluate the performance of the replicates, the normalized load reduction curves for all replicates are superimposed. The variation of the normalized peak force with respect to loading cycles obtained for all the replicates and the average behavior is summarized in Figure B5. The abscissa is converted into a logarithmic scale. The acceptance limit (i.e., Normalized Peak Load vs No of cycles plot using CPR = 0.5) is also shown in Figure B5.

From Figure B5 it can be observed that all the replicates showed similar normalized load reduction curves. The average load reduction curve is satisfactorily above the acceptance limit curve and therefore, shows good reflective cracking performance during the crack propagation phase.

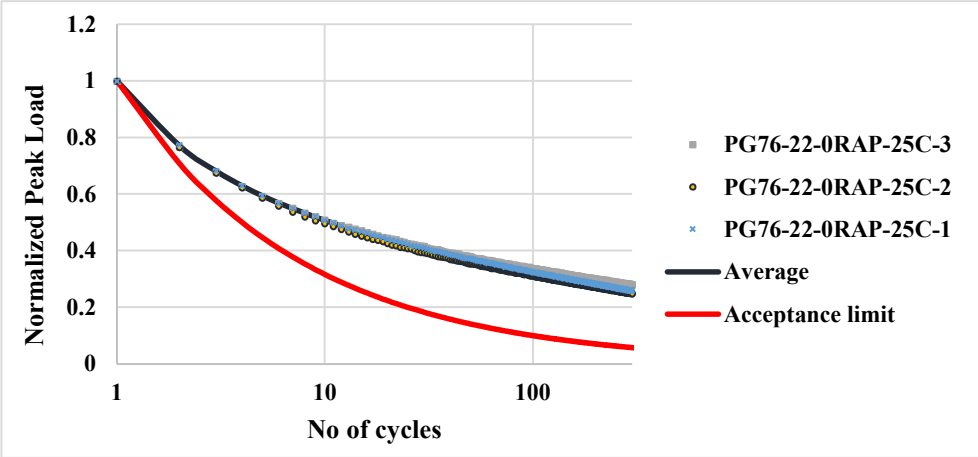

Figure B5. Normalized load reduction curves for all the replicates tested at room temperature.

B.2. Asphalt mixtures (PG 76-22 + 0% RAP) tested at low temperature (10°C)

Three replicates of OT specimens prepared with PG 76-22 asphalt binder and 0% RAP aggregates were tested in OT at low temperature (10°C) under one-phase loading at a maximum displacement of 0.025 in. (0.63 mm) until 93% peak tensile load reduction or 1000 cycles of loading. For this mixture type (PG 76-22 and 0% RAP) it was not possible to calculate N_{OT} since all the specimens withstood 1000 cycles before reaching 93% peak tensile load reduction. All the specimens were able to withstand more than 300 loading cycles which means this mixture type shows satisfactory

cracking performance and might not experience premature reflective cracking during its service life.

All the specimens prepared with PG 76-22 and 0% RAP and tested at low temperature exhibited similar load, displacement, and time histories as well the hysteresis behavior during the first loading cycle as shown in Figure B6 and Figure B7, respectively. It ensures the consistency of the raw data obtained from OT testing at room temperature. The maximum tensile load carried by each specimen, average maximum tensile load and standard deviation is presented in Figure B8. Additionally, the reduction of peak load (crack driving force) through the number of cycles is shown in Figure B9.

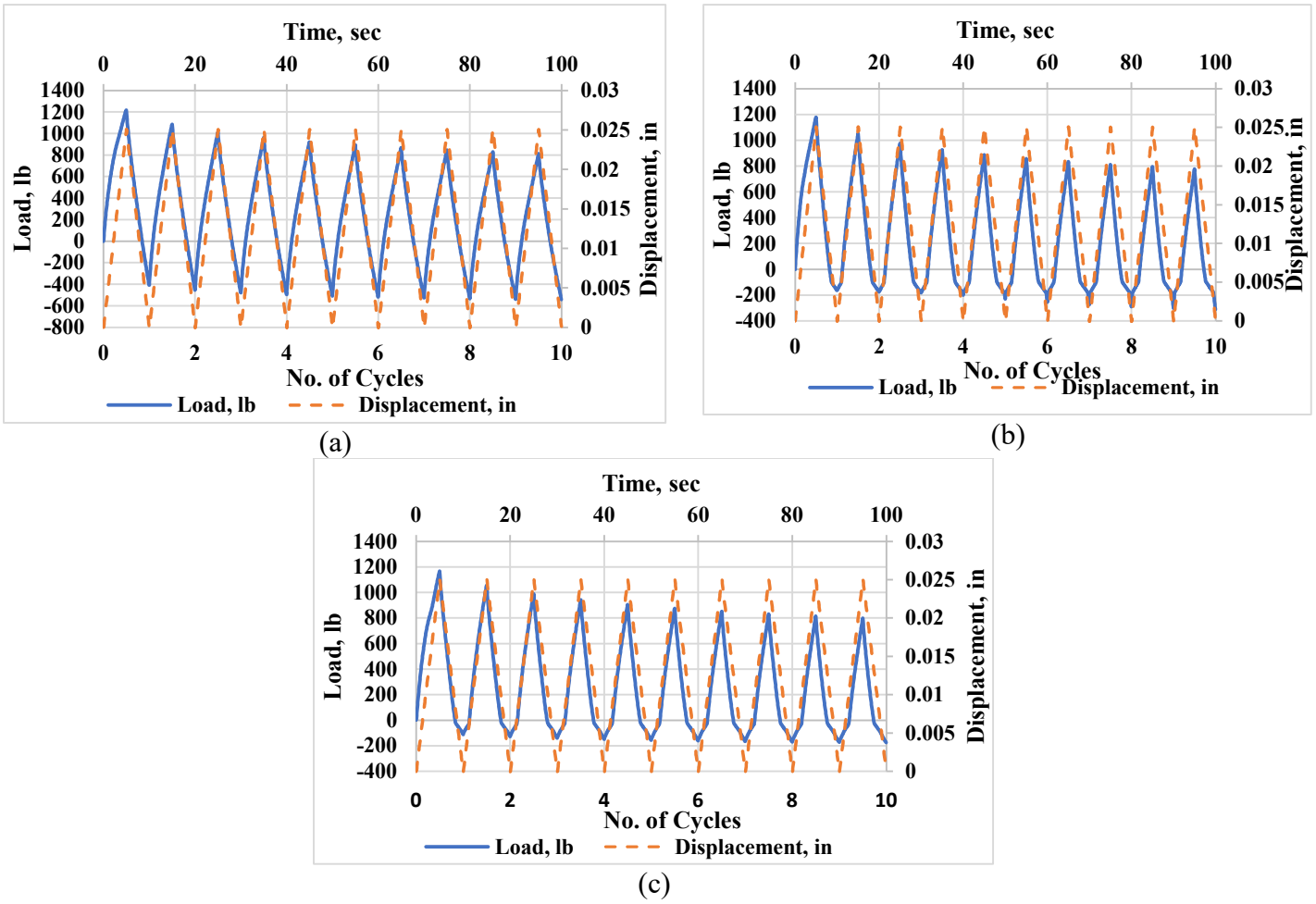

Figure B6. OT load, displacement, and time histories for (a) PG76-22-0RAP-10C-1, (b) PG76-22-0RAP-10C-2, and (c) PG76-22-0RAP-10C-3.

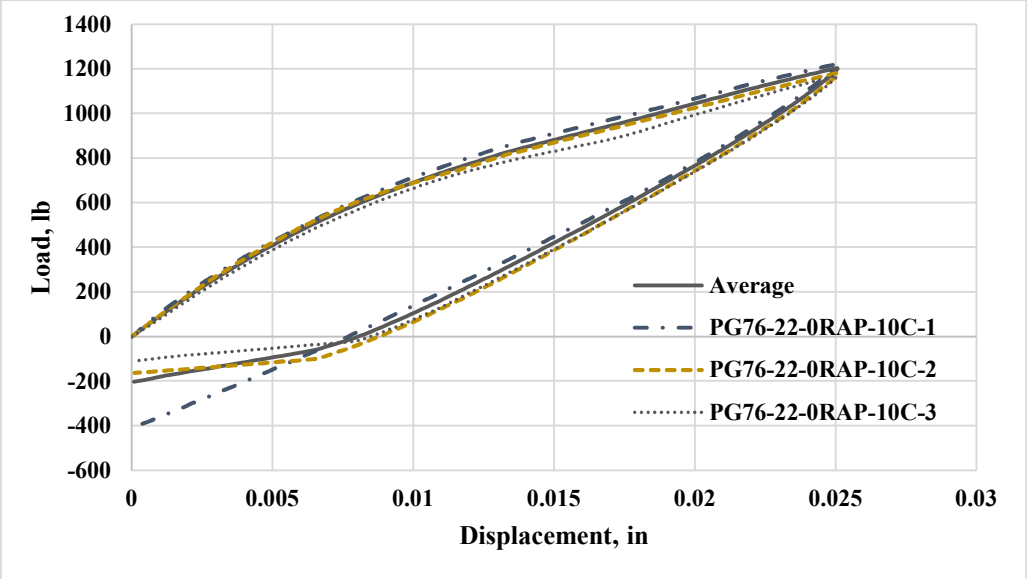

Figure B7. The first hysteresis loops of the OT specimens prepared with PG 76-22 + 0% RAP and tested at low temperature.

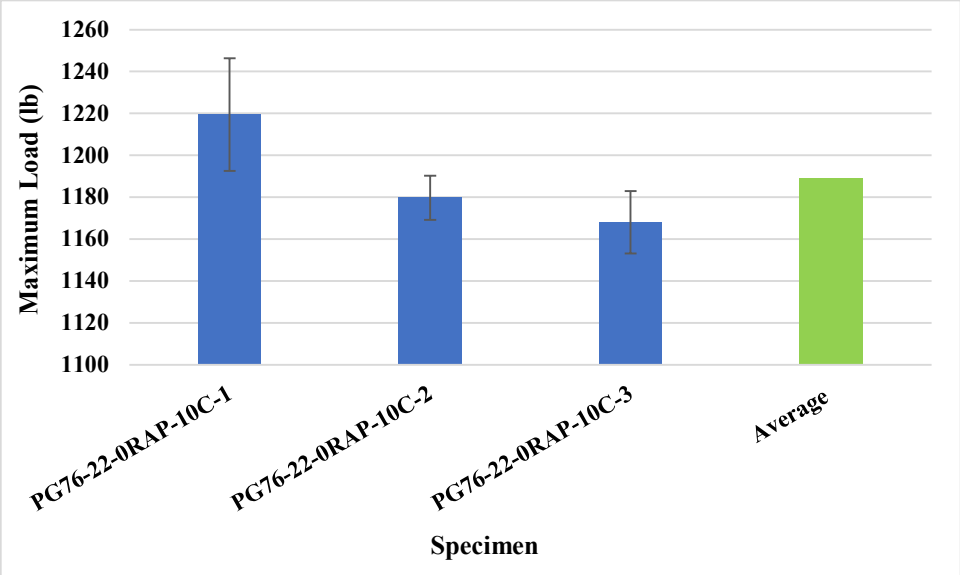

Figure B8. Maximum tensile load carried by OT specimens during the first loading cycle, prepared with PG 76-22 + 0% RAP and tested at low temperature.

To comparatively evaluate the performance of the replicates, the normalized load reduction curves for all replicates are superimposed. The variation of the normalized peak force with respect to loading cycles obtained for all the replicates and the average behavior is summarized in Figure B10. The abscissa is converted into a logarithmic scale. The acceptable limit (i.e., Normalized Peak Load vs No of cycles plot using CPR = 0.5) is also shown in Figure B10.

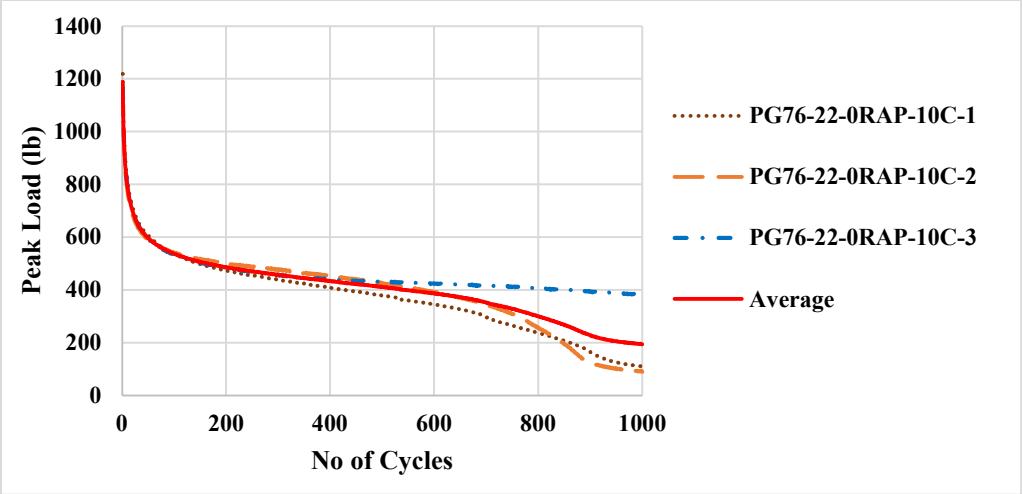

Figure B9. Reduction of crack driving force with respect to loading cycles for the OT specimens, prepared with PG 76-22 + 0% RAP and tested at low temperature

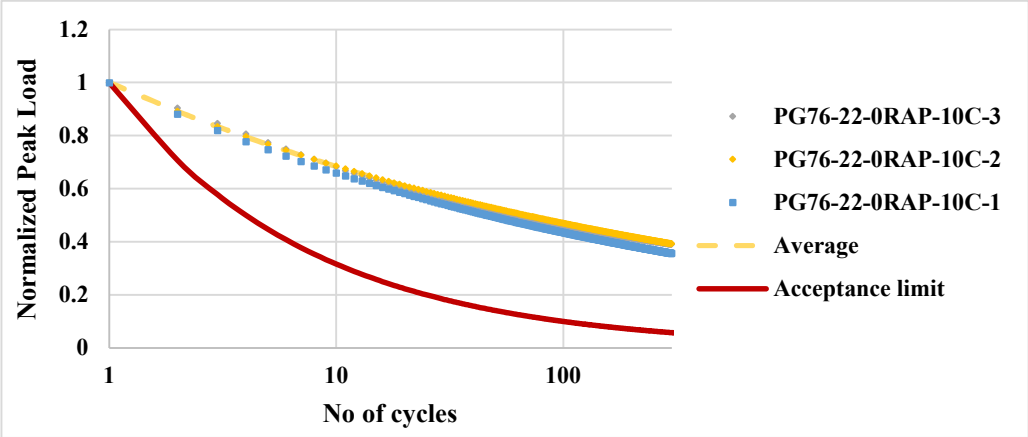

Figure B10. Normalized load reduction curves for all the replicates tested at low temperature.

From Figure B10, it can be observed that all the replicates showed similar normalized load reduction curves. The average load reduction curve is satisfactorily above the acceptance limit curve and therefore, shows good reflective cracking performance during the crack propagation phase.

B.3. Asphalt mixtures (PG 67-22 + 0% RAP) tested at room temperature (25°C)

Three replicates of OT specimens prepared with PG 67-22 asphalt binder and 0% RAP aggregates were tested in OT at room temperature (25°C) under one-phase loading at a maximum displacement of 0.025 in. (0.63 mm) until 93% peak tensile load reduction or 1000 cycles of loading. For this mixture type (PG 67-22 and 0% RAP) it was not possible to calculate N_{OT} since all the specimens withstood 1000 cycles before reaching 93% peak tensile load reduction. All the specimens were able to withstand more than 300 loading cycles which means this mixture type shows satisfactory cracking performance and might not experience premature reflective cracking during its service life.

All the specimens prepared with PG 67-22 and 0% RAP and tested at room temperature exhibited similar load, displacement, and time histories as well the hysteresis behavior during the first loading cycle as shown in Figure B11 and Figure B12. It ensures the consistency of the raw data obtained from OT testing at room temperature. The maximum tensile load carried by each specimen, average maximum tensile load and standard deviation is presented in Figure B13. Additionally, the reduction of peak load (crack driving force) through the number of cycles is shown in Figure B14.

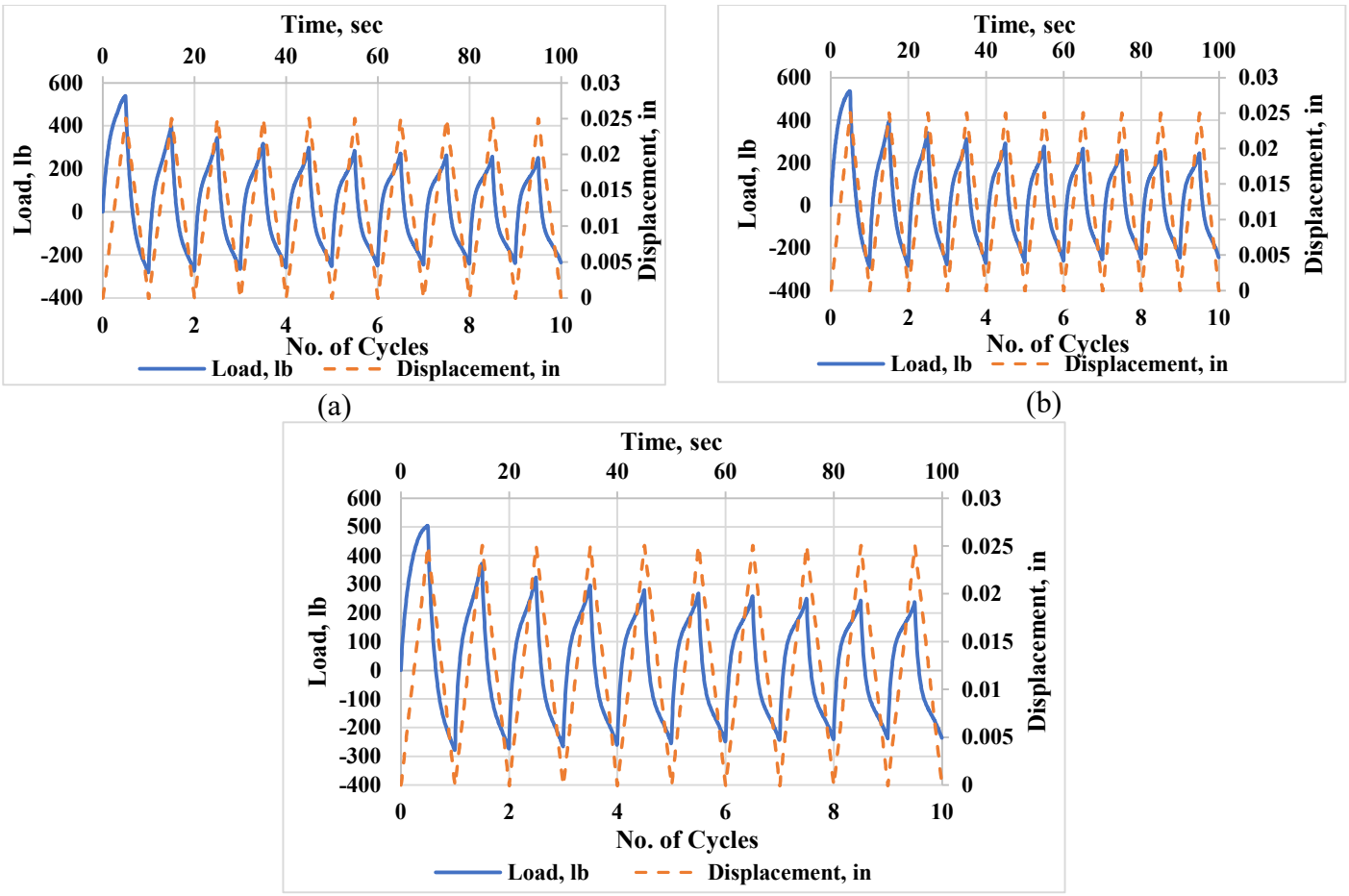

Figure B11. OT load, displacement, and time histories for (a) PG67-22-0RAP-25C-1, (b) PG67-22-0RAP-25C-2, and (c) PG67-22-0RAP-25C-3.

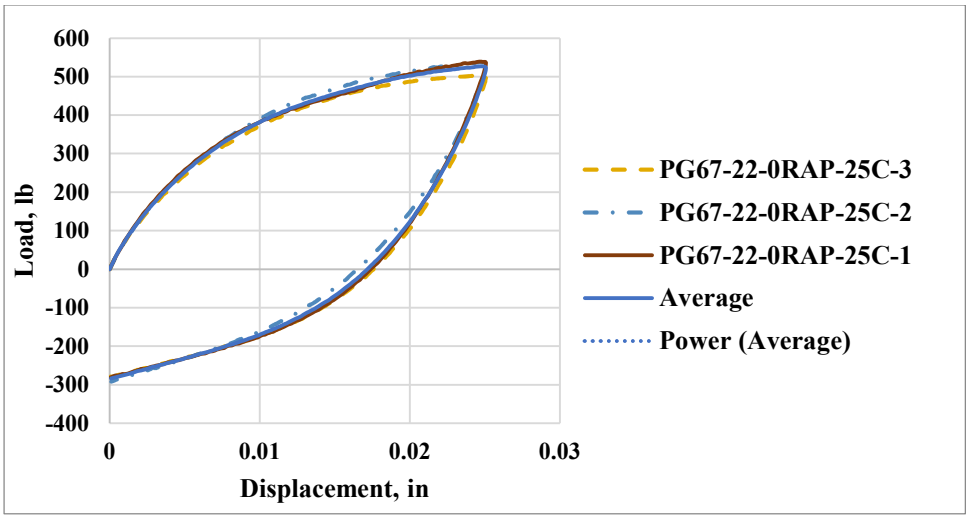

Figure B12. The first hysteresis loops of the OT specimens prepared with PG 67-22 + 0% RAP and tested at room temperature.

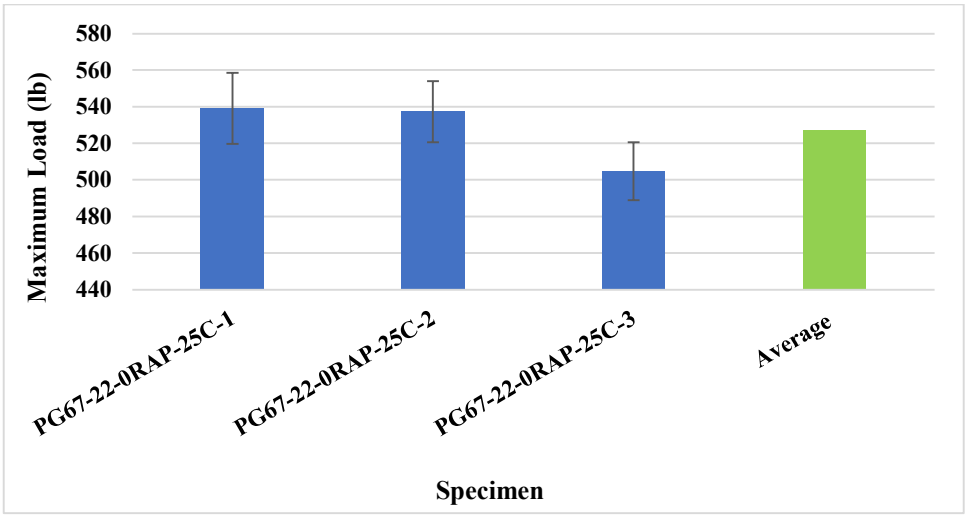

Figure B13. Maximum tensile load carried by OT specimens during the first loading cycle, prepared with PG 67-22 + 0% RAP and tested at room temperature.

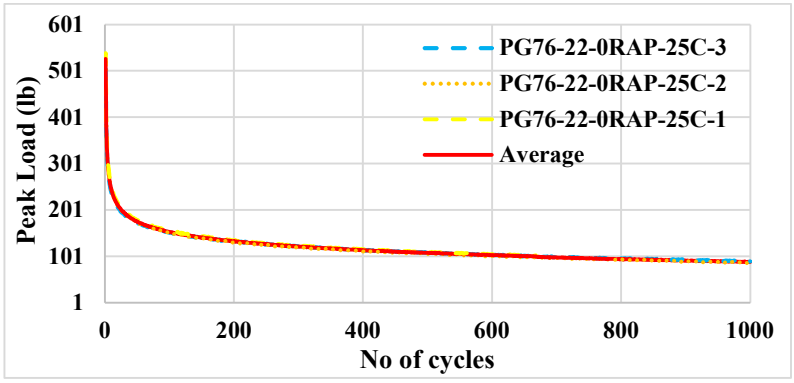

Figure B14. Reduction of crack driving force with respect to loading cycles for the OT specimens, prepared with PG 76-22 + 0% RAP and tested at room temperature.

To comparatively evaluate the performance of the replicates, the normalized load reduction curves for all replicates are superimposed. The variation of the normalized peak force with respect to loading cycles obtained for all the replicates and the average behavior is summarized in Figure B15. The abscissa is converted into a logarithmic scale. The acceptable limit (i.e., Normalized Peak Load vs No of cycles plot using CPR = 0.5) is also shown in Figure B15.

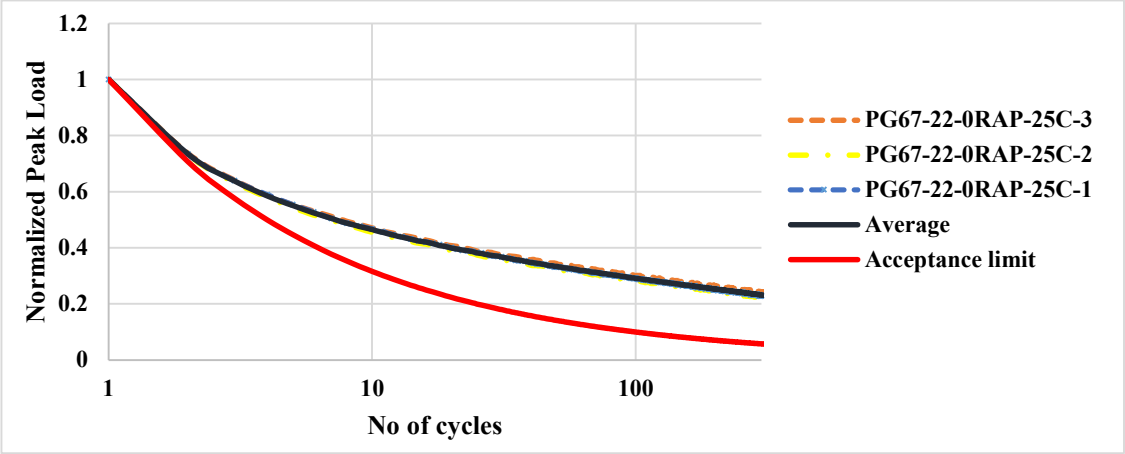

Figure B15. Normalized load reduction curves for all the replicates of PG 67-22 + 0% RAP mixture tested at room temperature.

From Figure B15 it can be observed that all the replicates showed similar normalized load reduction curves. The average load reduction curve is satisfactorily above the acceptance limit curve and therefore, shows good reflective cracking performance during the crack propagation phase.

B.4. Asphalt mixtures (PG 67-22 + 0% RAP) tested at low temperature (10°C)

Four replicates of OT specimens prepared with PG 67-22 asphalt binder and 0% RAP aggregates were tested in OT at low temperature (10°C) under one-phase loading at a maximum displacement of 0.025 in. (0.63 mm) until 93% peak tensile load reduction or 1000 cycles of loading. For this mixture type (PG 76-22 and 0% RAP) it was not possible to calculate N_{OT} since all the specimens withstood 1000 cycles before reaching 93% peak tensile load reduction. All the specimens were able to withstand more than 300 loading cycles which means this mixture type shows satisfactory cracking performance and might not experience premature reflective cracking during its service life.

All the specimens prepared with PG 67-22 and 0% RAP and tested in low temperature exhibited similar load, displacement, and time histories as well the hysteresis behavior during the first loading cycle as shown in Figure B16 and Figure B17. It ensures the consistency of the raw data obtained from OT testing at room temperature. The maximum tensile load carried by each specimen, average maximum tensile load and standard deviation is presented in Figure B18. Additionally, the reduction of peak load (crack driving force) through the number of cycles is shown in Figure B19.

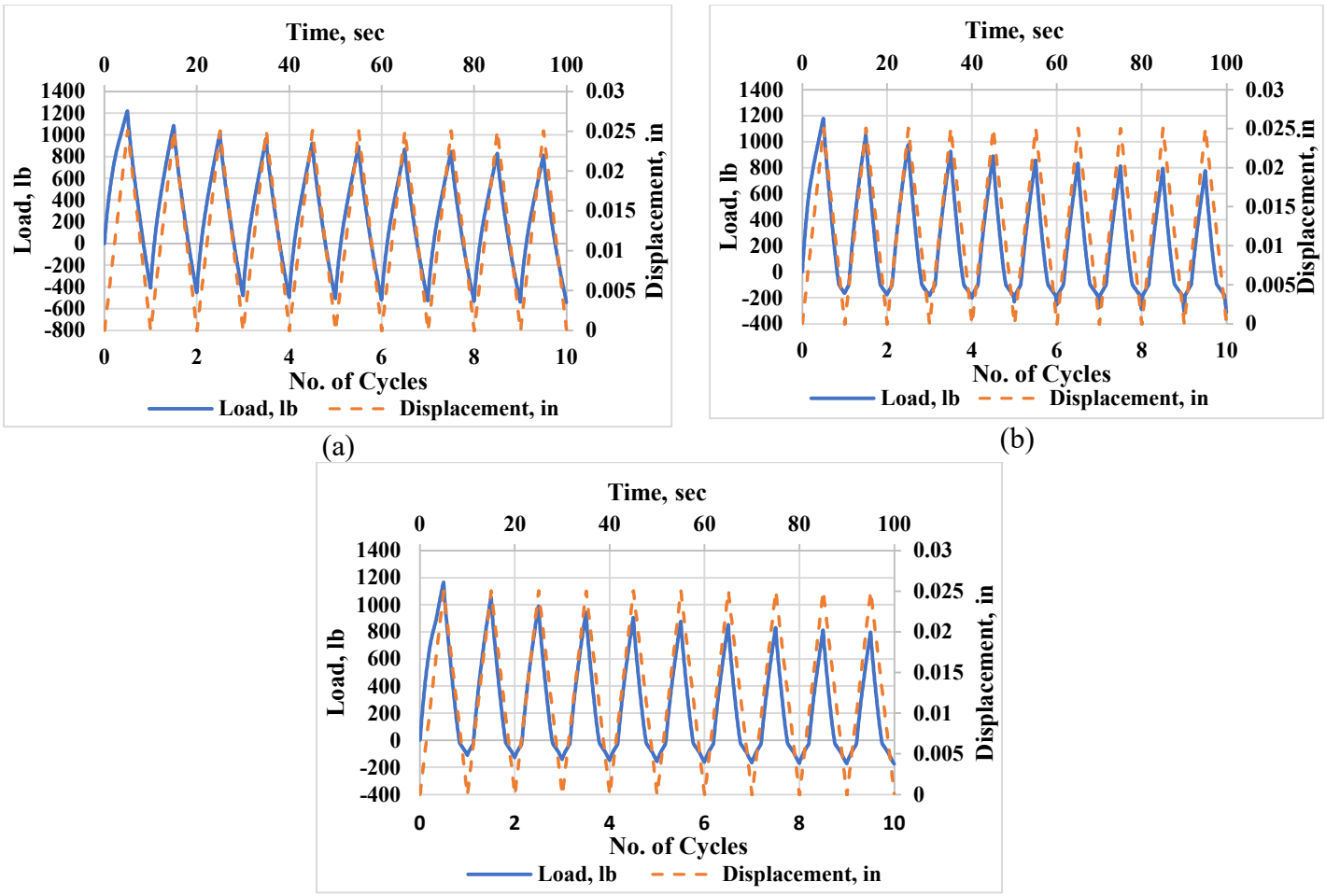

Figure B16. OT load, displacement, and time histories for (a) PG67-22-0RAP-10C-1, (b) PG67-22-0RAP-10C-2, and (c) PG67-22-0RAP-10C-3.

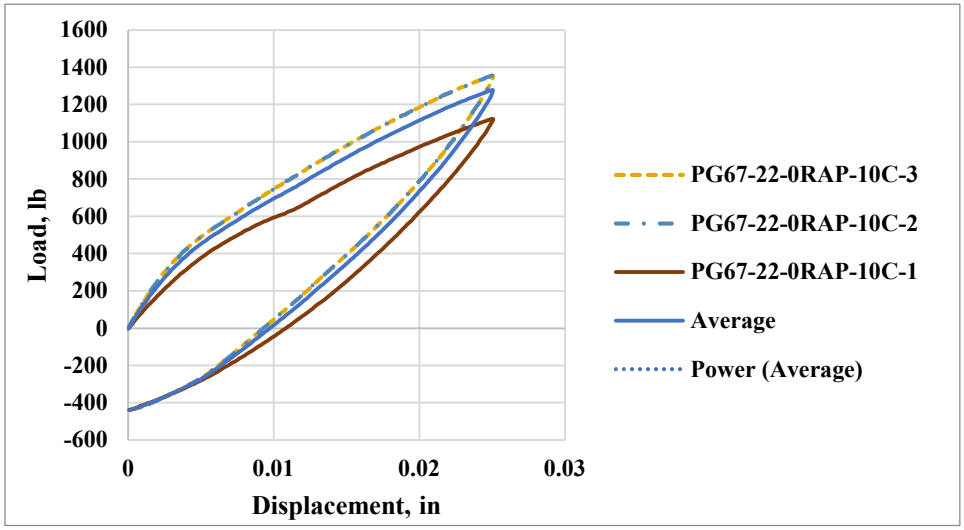

Figure B17. The first hysteresis loops of the OT specimens prepared with PG 67-22 + 0% RAP tested at low temperature.

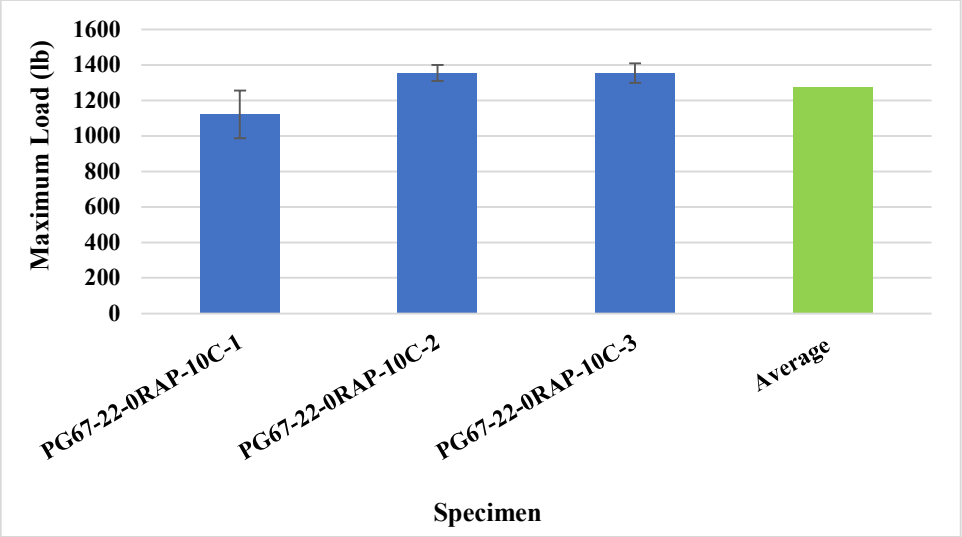

Figure B18. Maximum tensile load carried by OT specimens during the first loading cycle, prepared with PG 67-22 + 0% RAP and tested at low temperature.

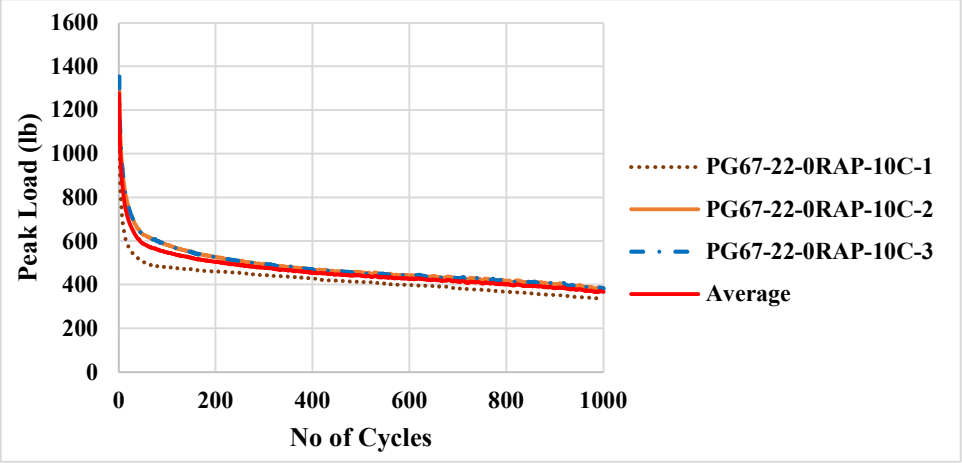

Figure B19. Reduction of crack driving force with respect to loading cycles for the OT specimens, prepared with PG 67-22 + 0% RAP and tested at low temperature.

To comparatively evaluate the performance of the replicates, the normalized load reduction curves for all replicates are superimposed. The variation of the normalized peak force with respect to loading cycles obtained for all the replicates and the average behavior is summarized in Figure B20. The abscissa is converted into a logarithmic scale. The acceptable limit (i.e., Normalized Peak Load vs No of cycles plot using CPR = 0.5) is also shown in Figure B20.

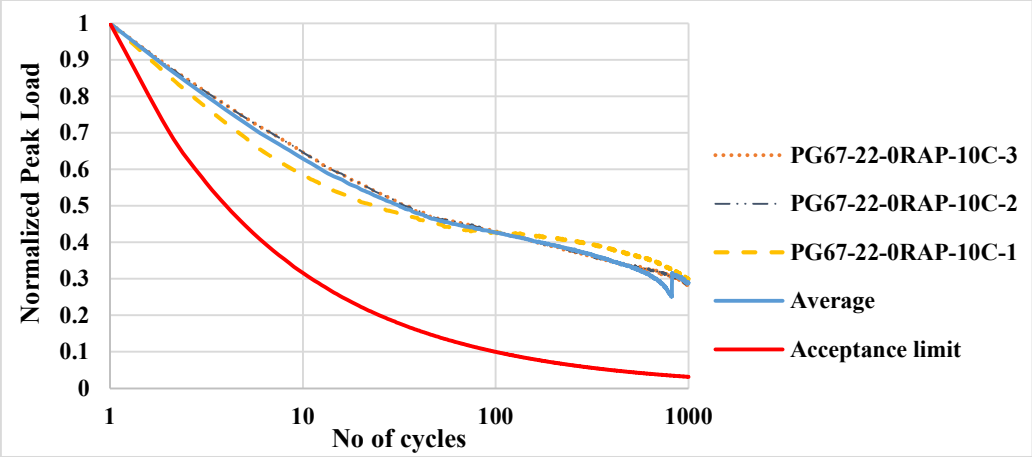

Figure B20. Normalized load reduction curves for all the replicates tested at low temperature.

From Figure B20 it can be observed that all the replicates showed similar normalized load reduction curves. The average load reduction curve is satisfactorily above the acceptance limit curve and therefore, shows good reflective cracking performance during the crack propagation phase.

B.5. Asphalt mixtures (PG 76-22 + 20% RAP) tested at room temperature (25°C)

Three replicates of OT specimens prepared with PG 76-22 asphalt binder and 20% RAP aggregates were tested in OT at room temperature (25°C) under one-phase loading at a maximum displacement of 0.025 in. (0.63 mm) until 93% peak tensile load reduction or 1000 cycles of loading. For this mixture type (PG 76-22 and 20% RAP) it was not possible to calculate N_{OT} since all the specimens withstood 1000 cycles before reaching 93% peak tensile load reduction. All the specimens were able to withstand more than 300 loading cycles which means this mixture type shows satisfactory cracking performance and might not experience premature reflective cracking during its service life.

All the specimens prepared with PG 76-22 and 20% RAP and tested in room temperature exhibited similar load, displacement, and time histories as well the hysteresis behavior during the first loading cycle as shown in Figure B21 and Figure B22. It ensures the consistency of the raw data obtained from OT testing at room temperature. The maximum tensile load carried by each specimen, average maximum tensile load and standard deviation is presented in Figure B23. Additionally, the reduction of peak load (crack driving force) through the number of cycles is shown in Figure B24.

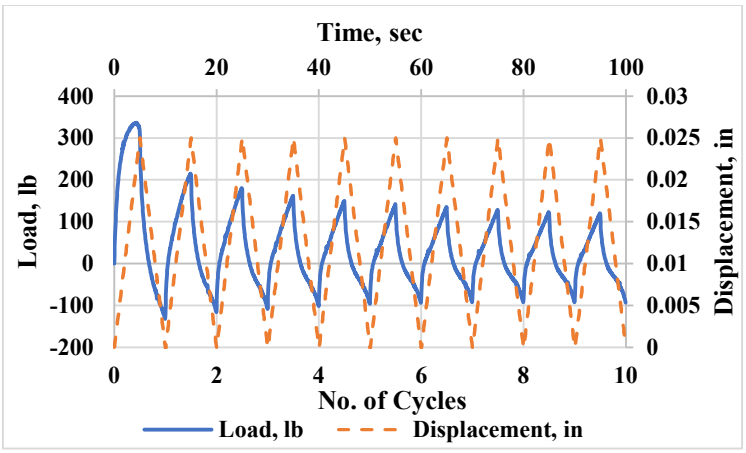

(a)

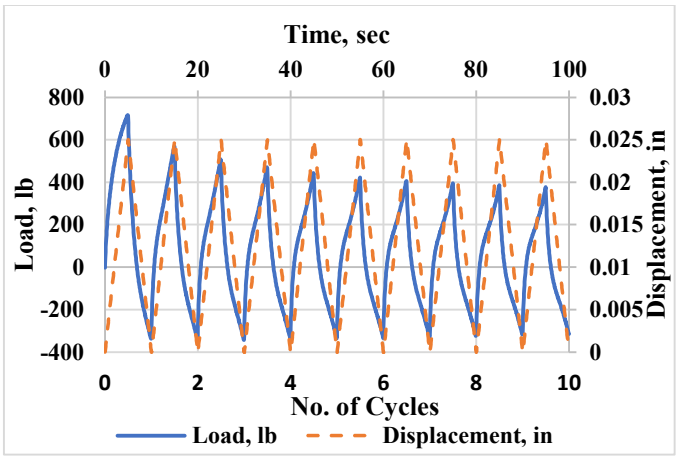

(b)

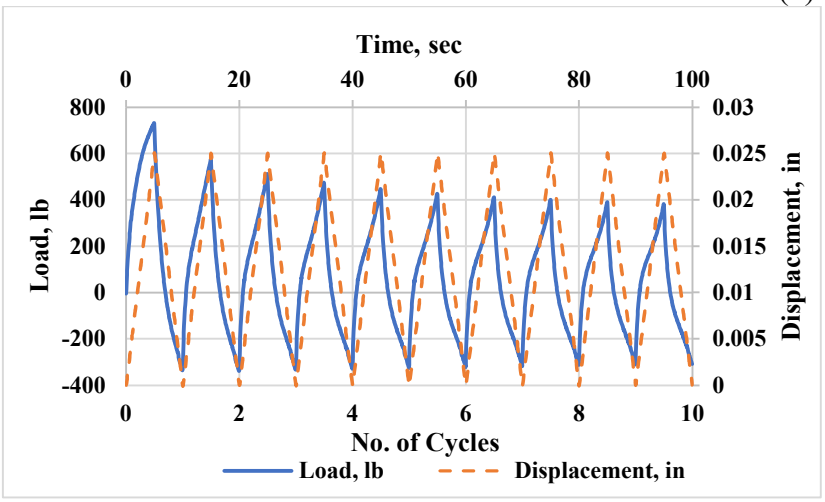

Figure B21. OT load, displacement, and time histories for (a) PG76-22-20RAP-25C-1, (b) PG76-22-20RAP-25C-2, and (c) PG76-22-20RAP-25C-3.

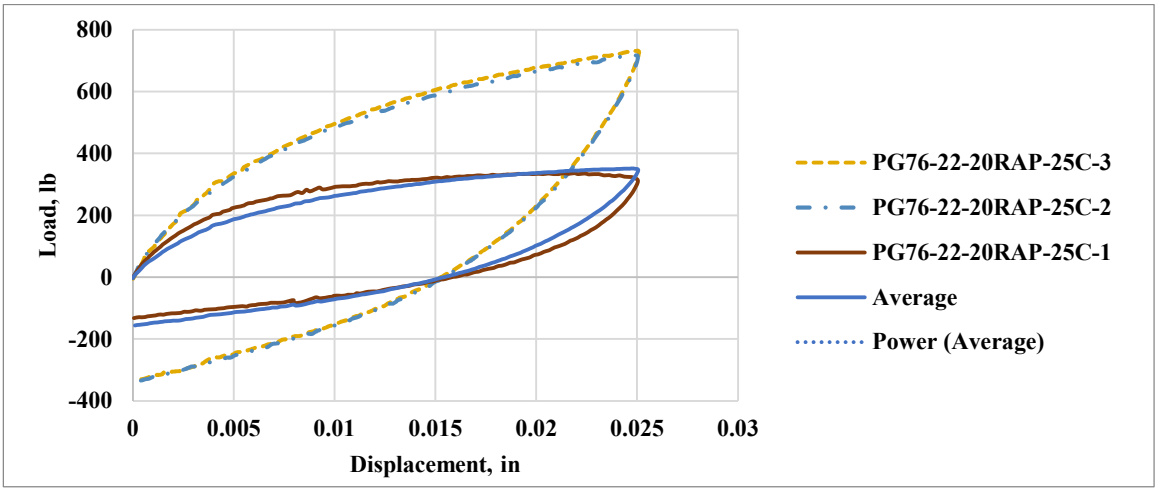

Figure B22. The first hysteresis loops of the OT specimens prepared with PG 76-22 + 20% RAP tested at room temperature.

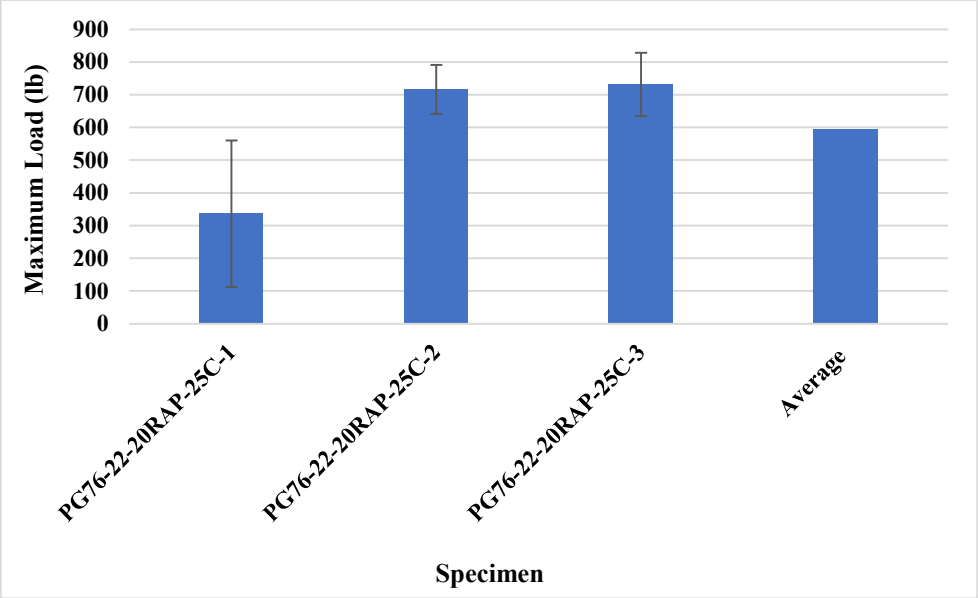

Figure B23. Maximum tensile load carried by OT specimens during the first loading cycle, prepared with PG 76-22 + 20% RAP and tested at room temperature.

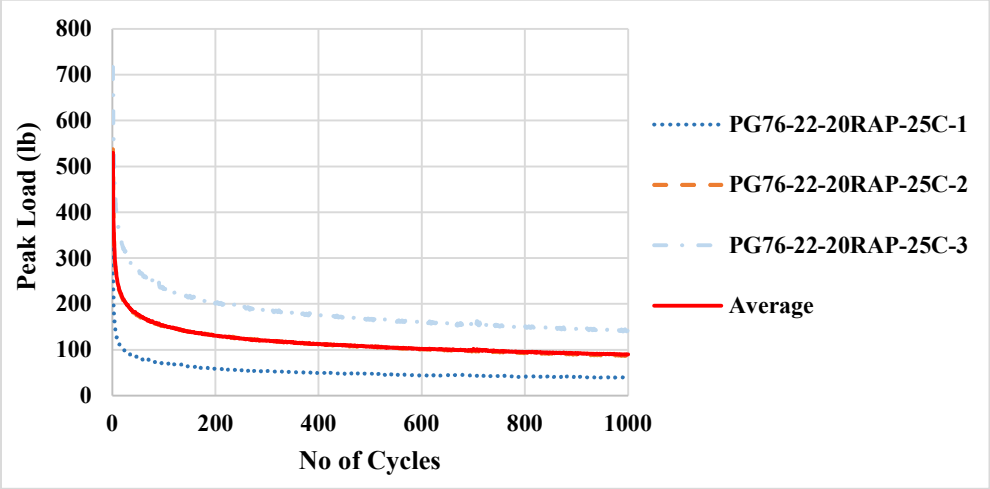

Figure B24. Reduction of crack driving force with respect to loading cycles for the OT specimens, prepared with PG 76-22 + 20% RAP and tested at low temperature.

To comparatively evaluate the performance of the replicates, the normalized load reduction curves for all replicates are superimposed. The variation of the normalized peak force with respect to loading cycles obtained for all the replicates and the average behavior is summarized in Figure B25. The abscissa is converted into a logarithmic scale. The acceptable limit (i.e., Normalized Peak Load vs No of cycles plot using CPR = 0.5) is also shown in Figure B25.

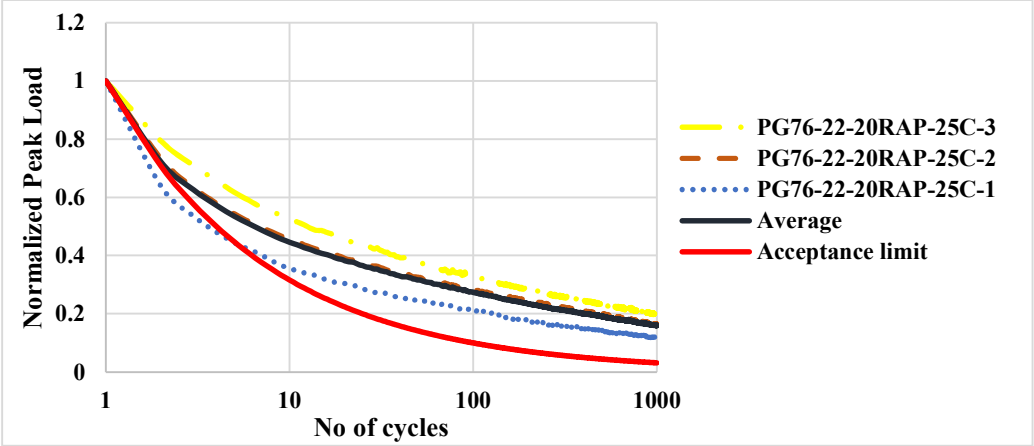

Figure B25. Normalized load reduction curves for all the replicates tested at low temperature.

From Figure B25 it can be observed that all the replicates showed similar normalized load reduction curves. The average load reduction curve is satisfactorily above the acceptance limit curve and therefore, shows good reflective cracking performance during the crack propagation phase.

B.6. Asphalt mixtures (PG 76-22 + 20% RAP) tested at low temperature (10°C)

Three replicates of OT specimens prepared with PG 76-22 asphalt binder and 20% RAP aggregates were tested in OT at low temperature (10°C) under one-phase loading at a maximum displacement of 0.025 in. (0.63 mm) until 93% peak tensile load reduction or 1000 cycles of loading. For this mixture type (PG 76-22 and 0% RAP) it was not possible to calculate N_{OT} since all the specimens withstood 1000 cycles before reaching 93% peak tensile load reduction. All the specimens were able to withstand more than 300 loading cycles which means this mixture type shows satisfactory cracking performance and might not experience premature reflective cracking during its service life.

All the specimens prepared with PG 76-22 and 20% RAP and tested in low temperature exhibited similar load, displacement, and time histories as well the hysteresis behavior during the first loading cycle as shown in Figure B26 and Figure B27. It ensures the consistency of the raw data obtained from OT testing at room temperature. The maximum tensile load carried by each specimen, average maximum tensile load and standard deviation is presented in Figure B28. Additionally, the reduction of peak load (crack driving force) through the number of cycles is shown in Figure B29.

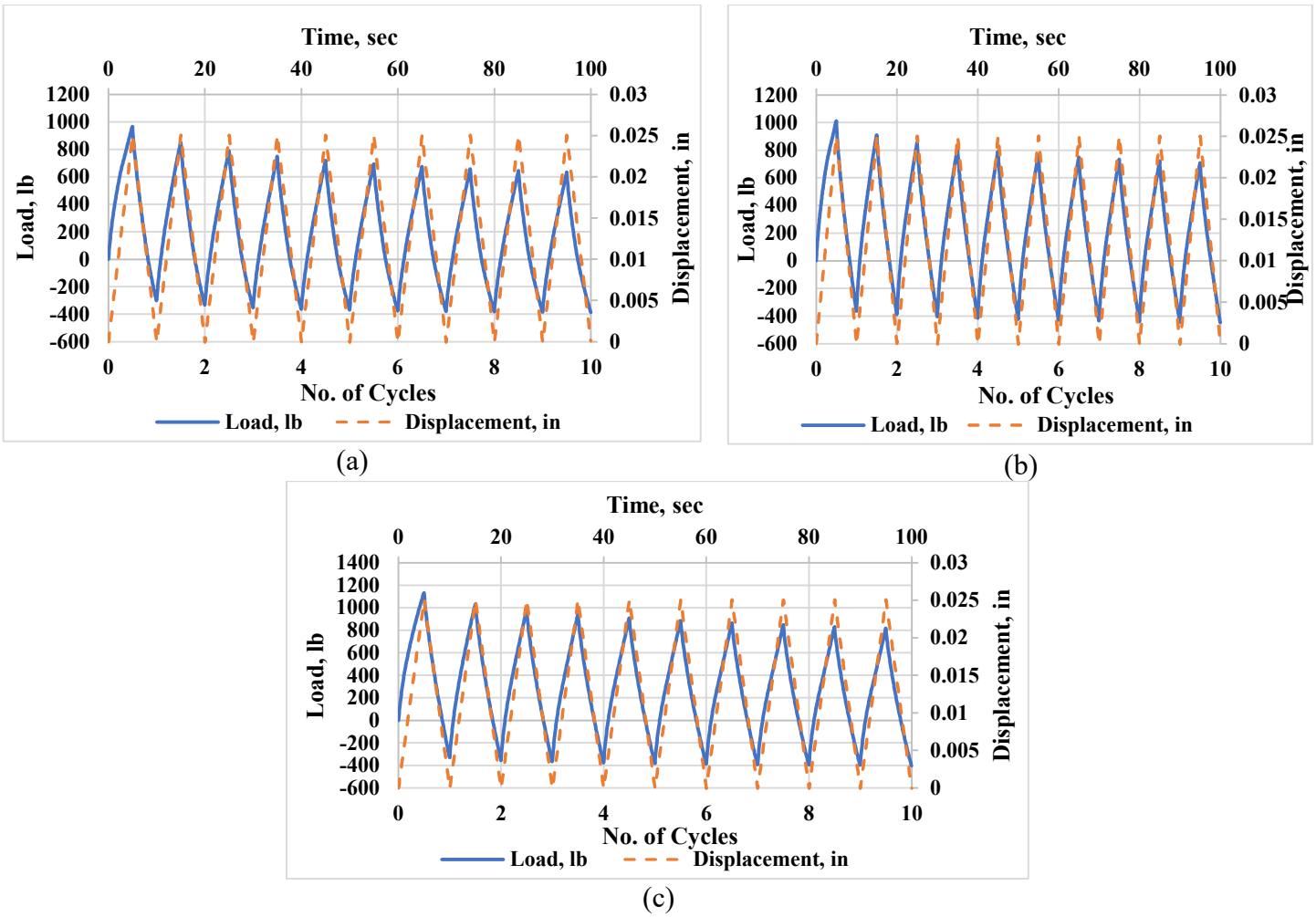

Figure B26. OT load, displacement, and time histories for (a) PG76-22-20RAP-10C-1, (b) PG76-22-20RAP-10C-2, and (c) PG76-22-20RAP-10C-3.

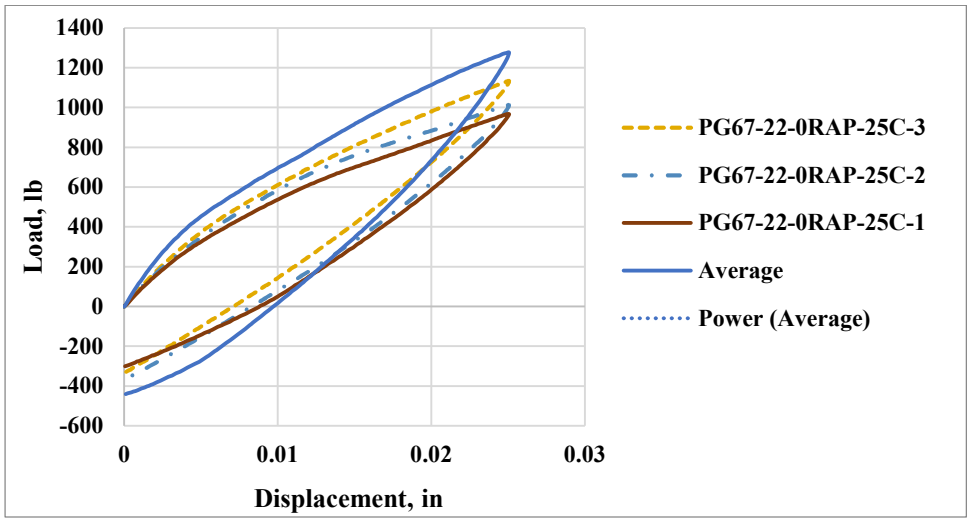

Figure B27. The first hysteresis loops of the OT specimens prepared with PG 76-22 + 20% RAP tested at low temperature.

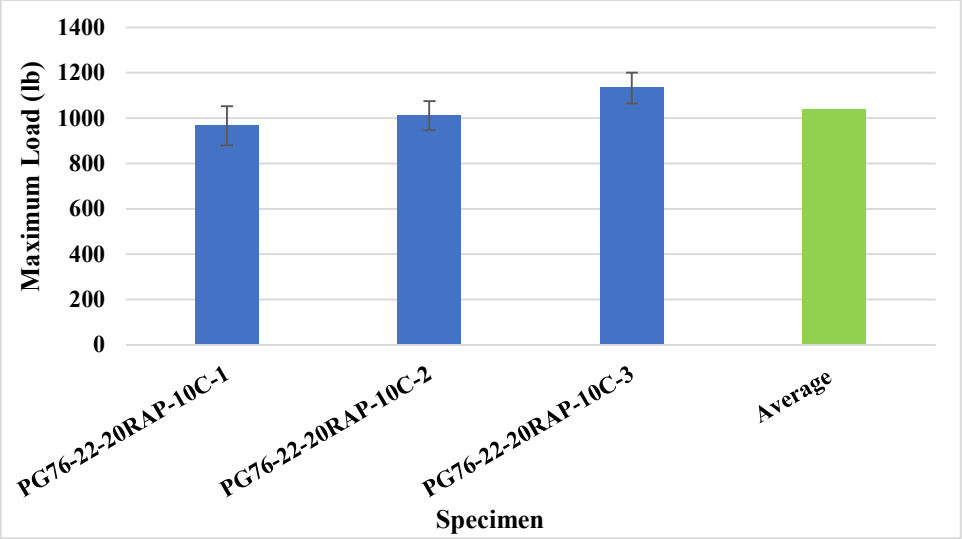

Figure B28. Maximum tensile load carried by OT specimens during the first loading cycle, prepared with PG 67-22 + 0% RAP and tested at low temperature.

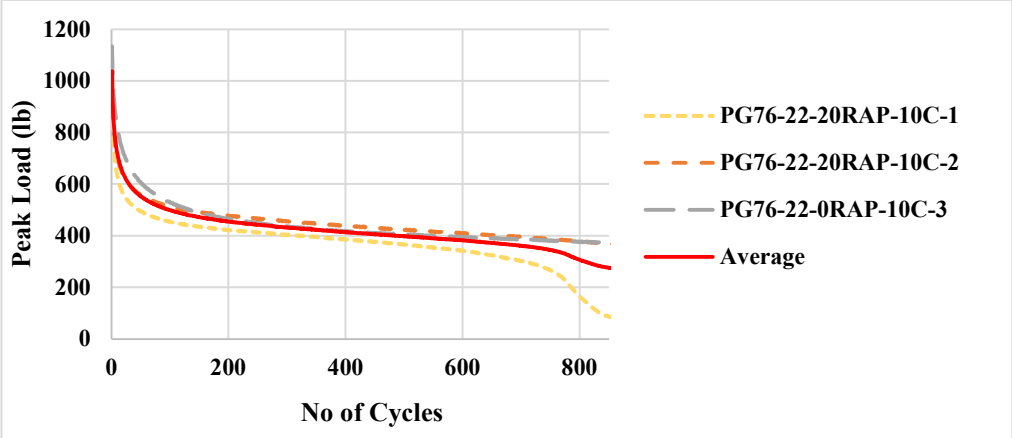

Figure B29. Reduction of crack driving force with respect to loading cycles for the OT specimens, prepared with PG 76-22 + 0% RAP and tested at low temperature.

To comparatively evaluate the performance of the replicates, the normalized load reduction curves for all replicates are superimposed. The variation of the normalized peak force with respect to loading cycles obtained for all the replicates and the average behavior is summarized in Figure B30. The abscissa is converted into a logarithmic scale. The acceptable limit (i.e., Normalized Peak Load vs No of cycles plot using CPR = 0.5) is also shown in Figure B30.

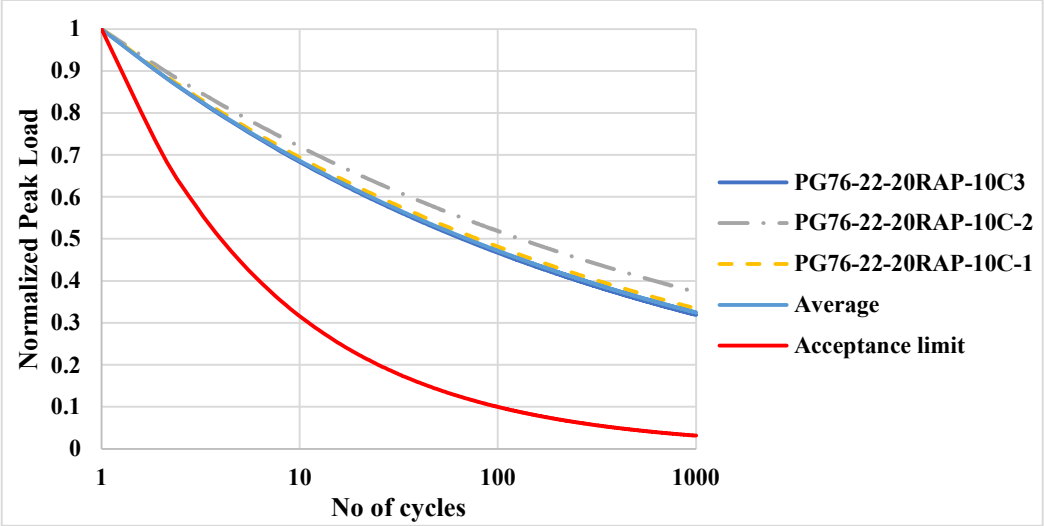

Figure B30. Normalized load reduction curves for all the replicates tested at low temperature.

From Figure B30 it can be observed that all the replicates showed similar normalized load reduction curves. The average load reduction curve is satisfactorily above the acceptance limit curve and therefore, shows good reflective cracking performance during the crack propagation phase.

B.7. Asphalt mixtures (PG 67-22 + 20% RAP) tested at room temperature (25°C)

Three replicates of OT specimens prepared with PG 67-22 asphalt binder and 20% RAP aggregates were tested in OT at room temperature (25°C) under one-phase loading at a maximum displacement of 0.025 in. (0.63 mm) until 93% peak tensile load reduction or 1,000 cycles of loading. For this mixture type (PG 76-22 and 20% RAP) it was not possible to calculate N_{OT} since all the specimens withstood 1,000 cycles before reaching 93% peak tensile load reduction. All the specimens were able to withstand more than 300 loading cycles which means this mixture type shows satisfactory cracking performance and might not experience premature reflective cracking during its service life.

All the specimens prepared with PG 67-22 and 20% RAP and tested in room temperature exhibited similar load, displacement, and time histories as well the hysteresis behavior during the first loading cycle as shown in Figure B31 and Figure B32. It ensures the consistency of the raw data obtained from OT testing at room temperature. The maximum tensile load carried by each specimen, average maximum tensile load and standard deviation is presented in Figure B33. Additionally, the reduction of peak load (crack driving force) through the number of cycles is shown in Figure B34.

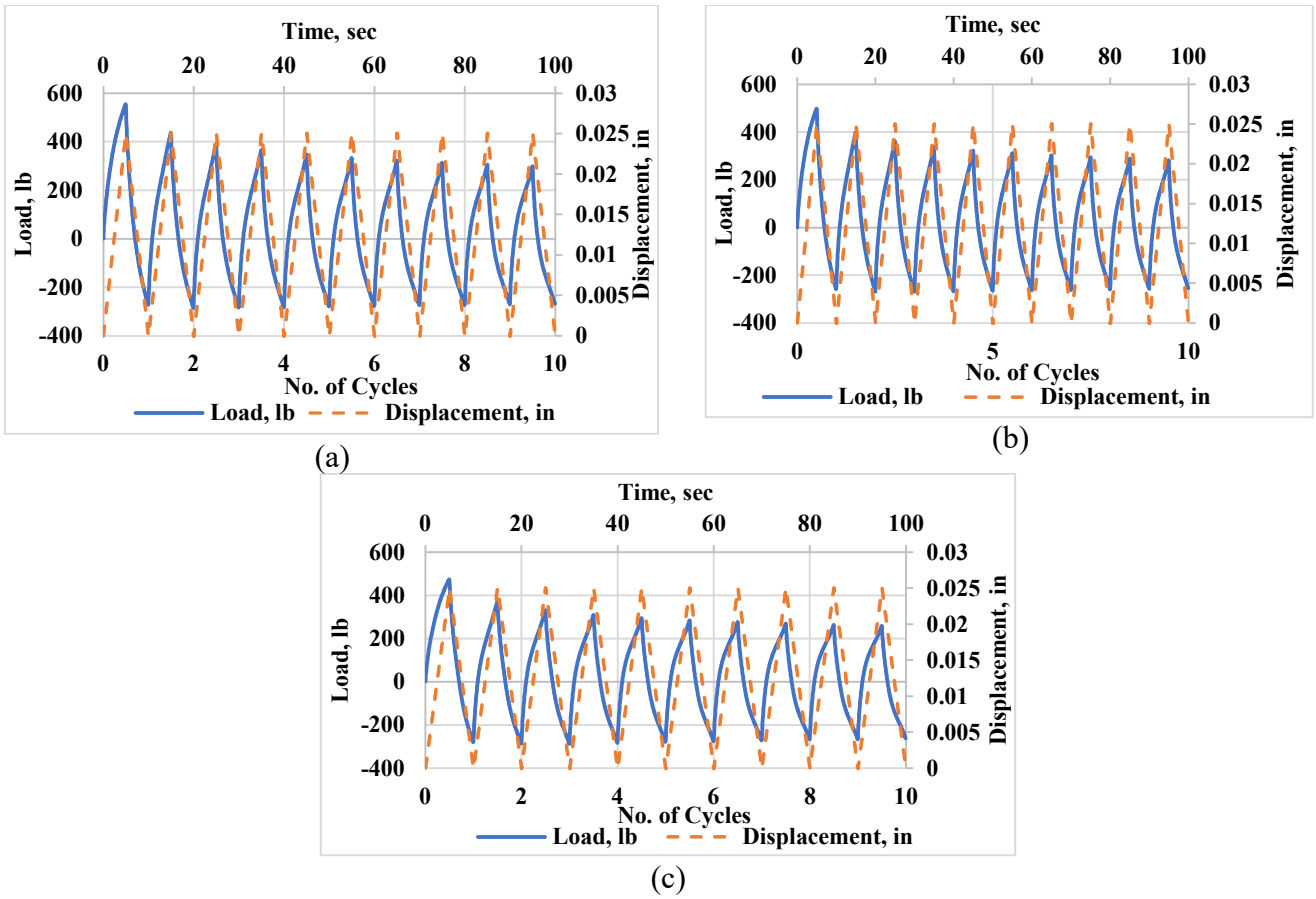

Figure B31. OT load, displacement, and time histories for (a) PG67-22-20RAP-25C-1, (b) PG67-22-20RAP-25C-2, and (c) PG67-22-20RAP-25C-3.

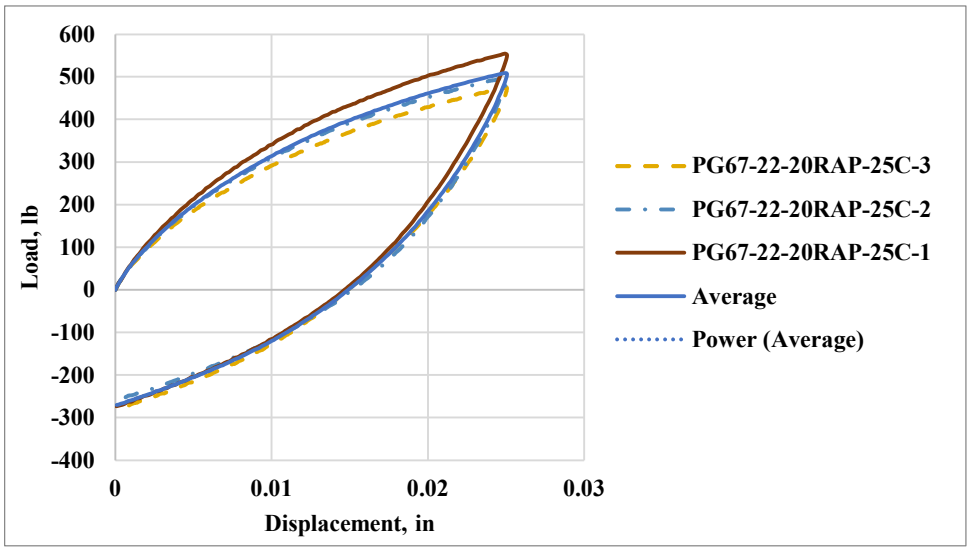

Figure B32. The first hysteresis loops of the OT specimens prepared with PG 67-22 + 20% RAP tested at room temperature.

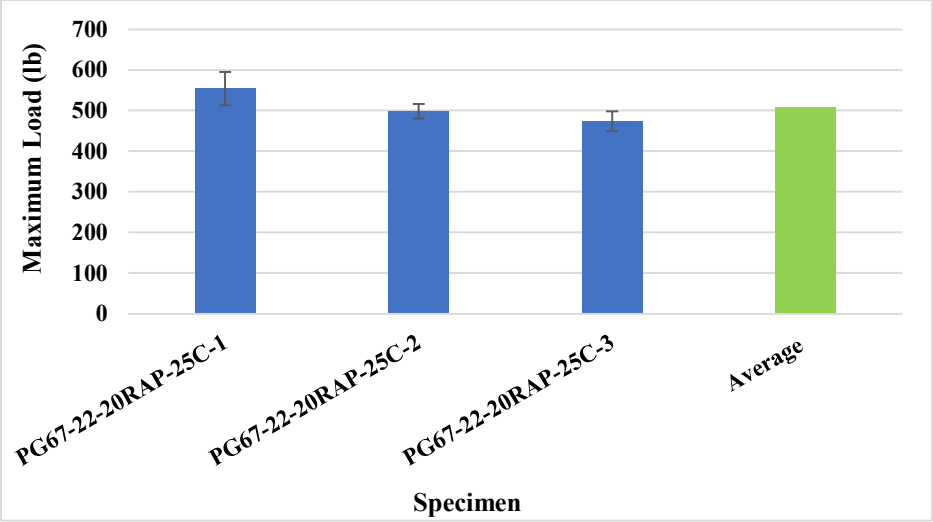

Figure B33. Maximum tensile load carried by OT specimens during the first loading cycle, prepared with PG 67-22 + 0% RAP and tested at low temperature.

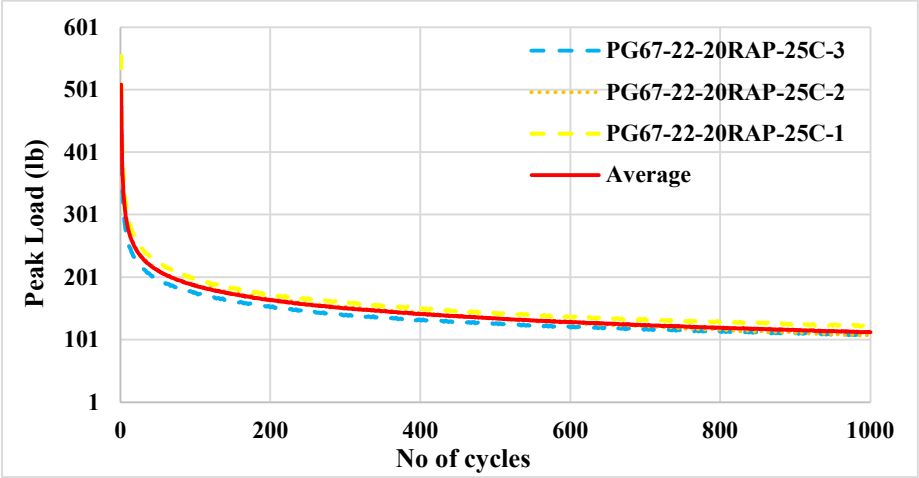

Figure B34. Reduction of crack driving force with respect to loading cycles for the OT specimens, prepared with PG 76-22 + 0% RAP and tested at low temperature.

To comparatively evaluate the performance of the replicates, the normalized load reduction curves for all replicates are superimposed. The variation of the normalized peak force with respect to loading cycles obtained for all the replicates and the average behavior is summarized in Figure B35. The abscissa is converted into a logarithmic scale. The acceptable limit (i.e., Normalized Peak Load vs No of cycles plot using CPR = 0.5) is also shown in Figure B35.

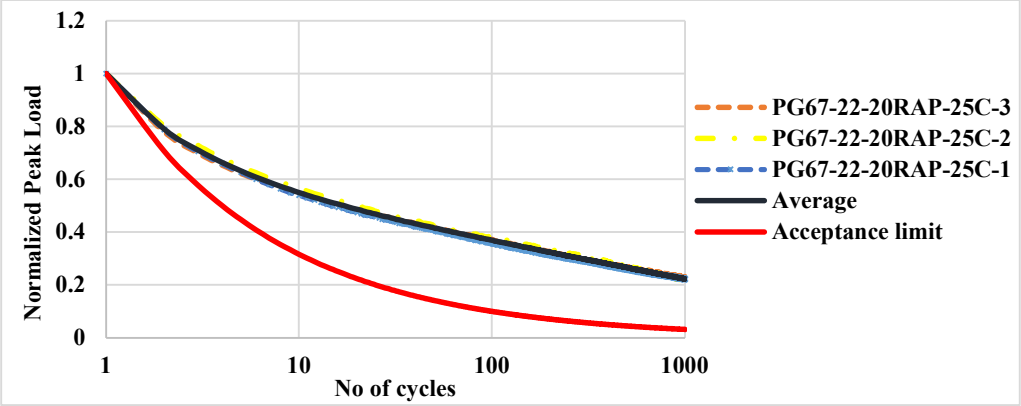

Figure B35. Normalized load reduction curves for all the replicates tested at low temperature.

From Figure B35 it can be observed that all the replicates showed similar normalized load reduction curves. The average load reduction curve is satisfactorily above the acceptance limit curve and therefore, shows good reflective cracking performance during the crack propagation phase.

B.8. Asphalt mixtures (PG 67-22 + 20% RAP) tested at low temperature (10°C)

Three replicates of OT specimens prepared with PG 67-22 asphalt binder and 20% RAP aggregates were tested in OT at low temperature (10°C) under one-phase loading at a maximum displacement of 0.025 in. (0.63 mm) until 93% peak tensile load reduction or 1000 cycles of loading. For this mixture type (PG 67-22 and 20% RAP) all the replicates failed before reaching 93% of the peak tensile load reduction. No specimens were able to withstand more than 300 loading cycles which means this mixture type did not satisfactory cracking performance during its service life.

All the specimens prepared with PG 67-22 and 20% RAP and tested in low-temperature exhibited similar load, displacement, and time histories as well the hysteresis behavior during the first loading cycle as shown in Figure B36 and Figure B37. It ensures the consistency of the raw data obtained from OT testing at room temperature. The maximum tensile load carried by each specimen, average maximum tensile load and standard deviation is presented in Figure B38. Additionally, the reduction of peak load (crack driving force) through the number of cycles is shown in Figure B39.

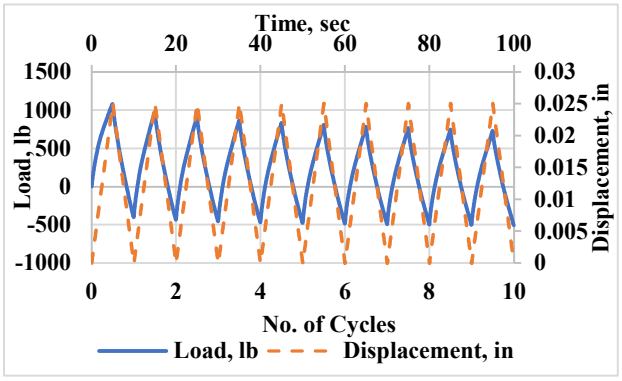

(a)

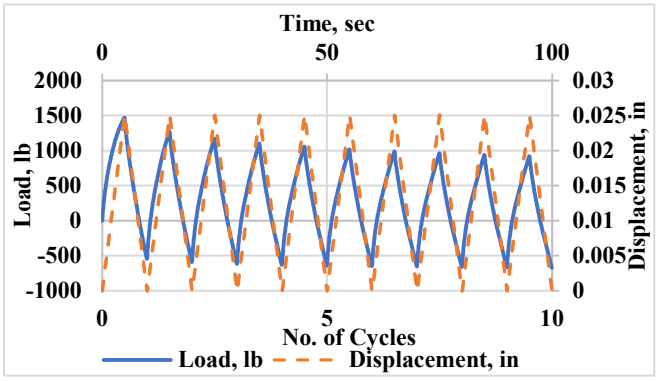

(b)

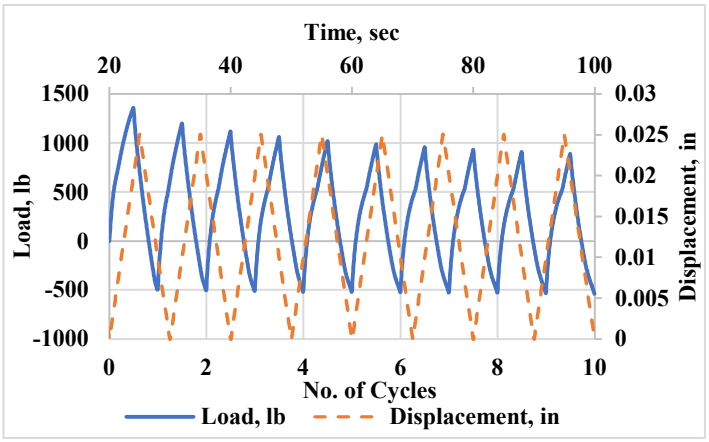

(c)

Figure B36. OT load, displacement, and time histories for (a) PG67-22-20RAP-10C-1, (b) PG67-22-20RAP-10C-2, and (c) PG67-22-20RAP-10C-3.

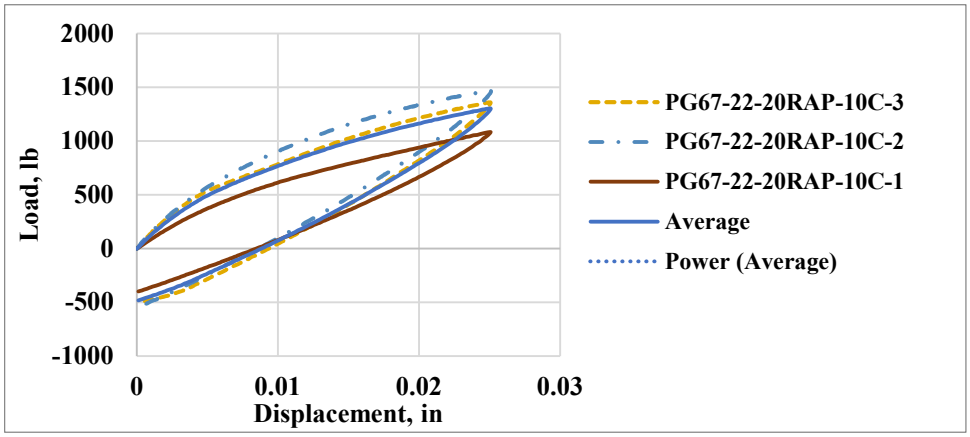

Figure B37. The first hysteresis loops of the OT specimens prepared with PG 67-22 + 20% RAP tested at room temperature.

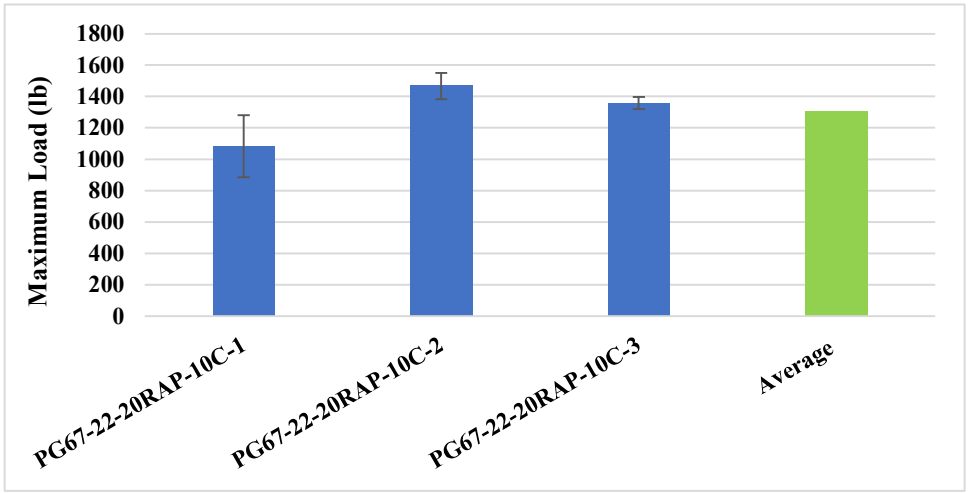

Figure B38. Maximum tensile load carried by OT specimens during the first loading cycle, prepared with PG 67-22 + 0% RAP and tested at low temperature.

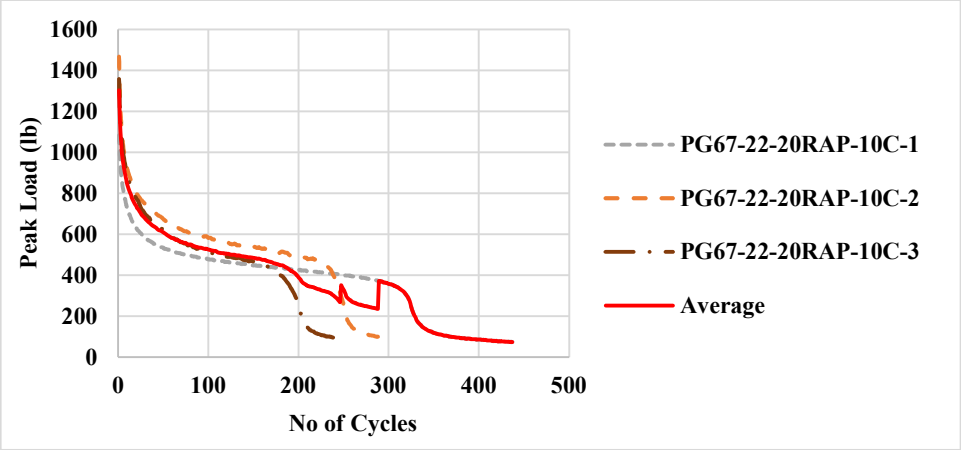

Figure B39. Reduction of crack driving force with respect to loading cycles for the OT specimens, prepared with PG 76-22 + 0% RAP and tested at low temperature.

To comparatively evaluate the performance of the replicates, the normalized load reduction curves for all replicates are superimposed. The variation of the normalized peak force with respect to loading cycles obtained for all the replicates and the average behavior is summarized in Figure B40. The abscissa is converted into a logarithmic scale. The acceptable limit (i.e., Normalized Peak Load vs No of cycles plot using CPR = 0.5) is also shown in Figure B40.

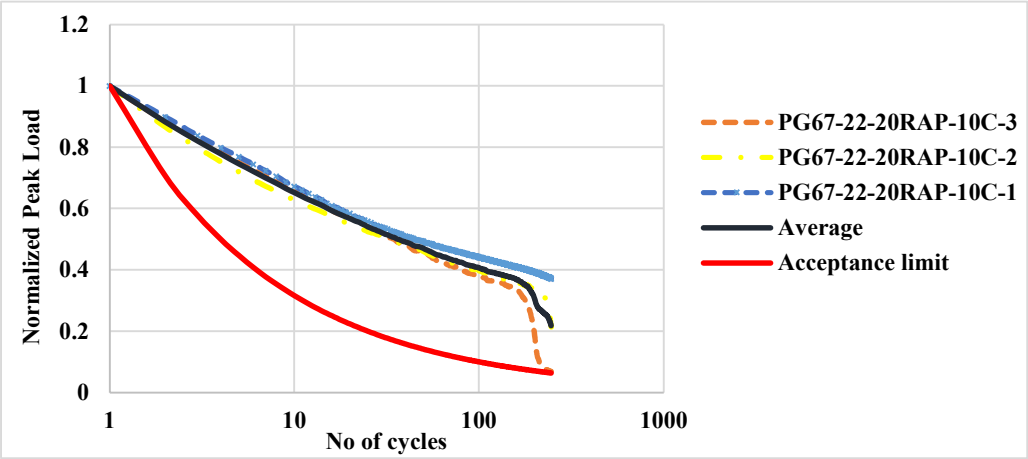

Figure B40. Normalized load reduction curves for all the replicates tested at low temperature.

From Figure B40 it can be observed that all the replicates showed similar normalized load reduction curves. Although, the average load reduction curve is above the acceptance limit curve until 100 cycles and all the specimens failed before reaching 300 cycles. Therefore, the average curve might go below the acceptance limit and might not perform good reflective cracking performance during the crack propagation phase.